Blade bulbous-bow concept application research using commercial CFD software

Mukhitdin Kakenov

Master Thesis

presented in partial fulfillment
of the requirements for the double degree:
“Advanced Master in Naval Architecture” conferred by University of Liege
"Master of Sciences in Applied Mechanics, specialization in Hydrodynamics, Energetics and Propulsion” conferred by Ecole Centrale de Nantes
developed at University of Genoa, Genoa
in the framework of the

“EMSHIP”
Erasmus Mundus Master Course
in “Integrated Advanced Ship Design”

EMJMD 159652 – Grant Agreement 2015-1687

Supervisor:
Prof.Dario Boote, University of Genoa, Genoa

Reviewer:

Genoa, February 2018

Declaration of Authorship

I, KAKENOV Mukhitdin
[please print name]

declare that this thesis and the work presented in it are my own and has been generated by me as the result of my own original research.

[title of thesis] Blade bulbous-bow concept application research using commercial CFD software

I confirm that:

1. This work was done wholly or mainly while in candidature for a research degree at this University;

2. Where any part of this thesis has previously been submitted for a degree or any other qualification at this University or any other institution, this has been clearly stated;

3. Where I have consulted the published work of others, this is always clearly attributed;

4. Where I have quoted from the work of others, the source is always given. With the exception of such quotations, this thesis is entirely my own work;

5. I have acknowledged all main sources of help;

6. Where the thesis is based on work done by myself jointly with others, I have made clear exactly what was done by others and what I have contributed myself;

7. Either none of this work has been published before submission, or parts of this work have been published as: [please list references below]:

8. I cede copyright of the thesis in favour of the University of Genova

Signed: KAKENOV Mukhitdin

Date: November, 2nd 2017

Contents

1. INTRODUCTION

From one port to another one, much faster as possible. Much cheaper as possible. Much more comfortable.

Bulbous bow's purposes are to fight against head wave impact and decrease drag from wave generating resistance. These two actions cover such important sections as financial costs (fuel consumption, hull maintenance cost), transportation time (seakeeping, ship's velocity), comfort for passengers and crew (vibration, wave shock impact).

Application of bulbous bow helps to significantly reduce all above listed costs, journey time and improve people's health condition onboard. Electronic equipment undergoes less shock and has less risk to be damaged due to wave impact on fore-part. Hull vibration levels may also be reduced by high values and frequencies.

But still, there is no limit to try to improve bulbous bow's performance further.

In this thesis the author will describe and provide the results from research made to find out about applicability of new concept of bulbous bow – blade bulbous bow – on a middle-size semi-displacement cruise yachts.

The new bow application already had obtained positive reviews in naval/maritime theme magazines. Here below some articles will be provided as side overview of existing vessels aiming such a bow.

2. OVERVIEW OF EXISTING VESSELS USING BLADE BULBOUS BOW

There are at least two yachts the thesis author would like to mention: first one is Ilumen 28M from Dominator shipyard and the second is Benetti's F-125 (see pictures on figures 2.1-2.7 for the Ilumen 28M and figures 2.8-2.10 for F-125). The sources the photos are taken from are [1] and [2] for the Ilumen 28M and [3] for the F-125.

2.1. Dominator Ilumen 28M

Fig.2.1.

Fig.2.2.

Reviewing the hulls of these ships, the author of thesis would like to tie your attention to the form of their bottoms. For the Ilumen 28M its bottom is close to pre-planning hull's one. The author does not have correct technical information about its draught depth (might be about 1,85 m [5]), but there are some assumptions made by himself that the key feature of Ilumen's hull is reducing the initial draught with during forwarding speed increasing: the wider than upper bow-part the blade bow's lower-forward edge used on this ship provides an initial moment causing a positive trim (on the stern), what is followed then by classical principles of the pre-planning hulls high-speed movement scheme: reducing the draught of the vessel with lowering the wetted surface (and, as a

result, the frictional drag). This vessel may develop its velocity from 23 knots up to 29 knots, the length on the waterline of the ship is 23.50 meters at half load [5]. The Froude number is about 1.515 – that should be beyond of the range of the usual pre-planning regime Froude number range [4], very good fact for the assumptions made. The ship page on the web-site of the Derani Yachts Co. Ltd. (https://www.derani-yachts.com/yachts/dominator-ilumen-28-metre/#) states that the ship able to have the maximal speed for 29 knots and 23 knots for cruising. Relating to the information collected the author would accept to consider the working speed as about 23 knots. And even in this case the Froude number still is calculated not lower than 1.4, what keeps the assumption of the pre-planning regime scheme for this yacht. On the maximal speed the ship may switch to planning regime, as the Froude number estimates as 1.91.

Fig.2.3. The length overall of the Ilumen 28M yacht is 28 meters. The draught of the ship is 1.85 meters (pictures from [5])

An approximate visual estimations of the relations between the ship dimensions on the figures 1-5 lets the author to suppose that the submerged part of the blade bulbous bow is not placed very deep under the free surface of the water, and the upper part of the bulbous bow has relatively small surface and very short connecting area between the rest fore-part of the hull and the edge of the “blade”, so, approximately, the submerged part may be reviewed as a separate hull, which faces the greatest part of incoming flow – this conclusion is made in connection to the forward movement behaviour of such a hull, described above.

Fig.2.4. Low-scale testing model for towing tank. [8][13]

Fig.2.5. Low-scale testing model for towing tank. [8][13]

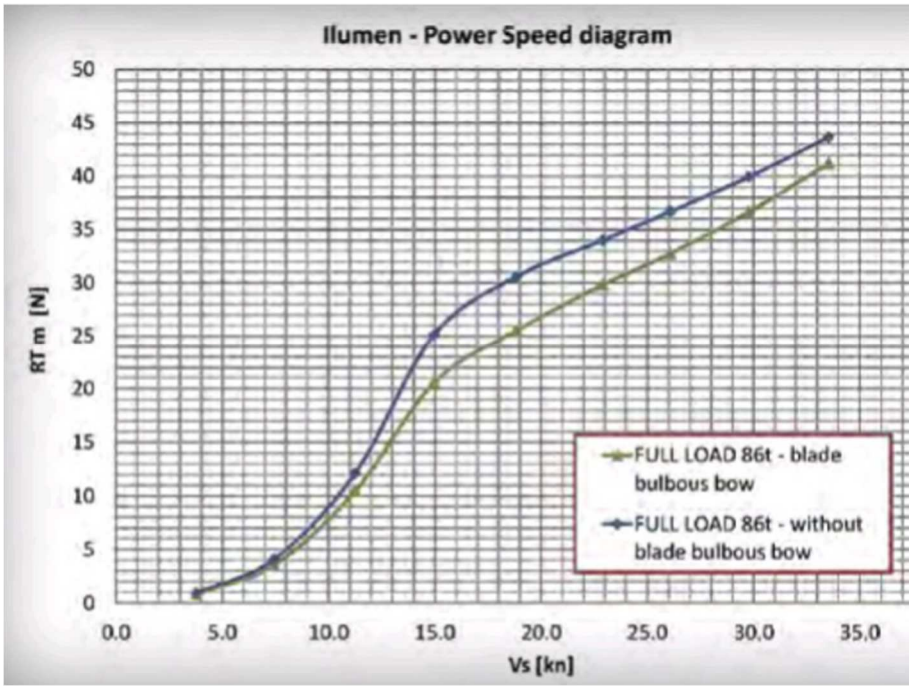

Fig.2.6. Comparison between use of convenient and blade bow (F-125). [8][13] RT – total resistance, Vs – velocity.

Fig.2.6

Fig.2.7.

2.2. Benetti F-125

Now about the Benetti's F-125. According to the technical information available for public use [10], [12]:
Length waterline – 31.0 meters,
Maximum beam – 8.23 meters,
Half load draught – 2.01 meters,
High-speed range – 17.5-22 knots.

See pictures on figures 2.8-2.10.

Fig.2.8.

Fig.2.9.

Fig.2.10. The author had edited the copy of the original picture in order to show the featured outline of the blade bow.

Like for the Ilumen 28M, the draught of the F-125 is not very deep relatively its board height. As you can notice on the figures 2.8-2.10, the blade bow's sharp edges are continued along the ship's length, so that there is again the case of a "hull on a hull" mentioned already for the first reviewed ship. This part of the hull (from the keel up to the level of the upper surface of the blade bow). The author supposes the same ship motions behaviour on higher speeds almost like it was written above for the Ilumen. The speeds are lower, but still the Froude number is high enough to guess about the sinkage decrease during forward directing velocity value elevation. The fore part of the ship around stem post is inclined for very sharp angle. The blade bow part is as long as it would be for a convenient (bulbous) one. Perhaps, there is no much need for the bow to provide a usual work to crush an incoming wave in front of the stem post – due to relatively small draught – since the free surface does not much cover the upper surface of the bow, so the wetted part of the hull works like a separate hull; mostly, no need to observe it as a hull with a blade bow as an attached device, in the cases when the ship goes in still water.

3. PROBLEM TO SOLVE

Main objective: check potential benefits from application of the blade bulbous bow concept in case of a 60-meters long luxury cruise yacht (design and production by Sanlorenzo Shipyard in La Spezia, Italy). Compare to the same yacht with the old bulbous bow. Justify the advantages in performance of the blade bulbous bow in comparison with the initial (convenient) one.

Yacht general arrangements:
Length between perpendiculars – 54.2 m
Length on waterline – 62.3 m
Breadth on waterline – 12.6 m
Draught – 3.3 m

It is important to note that its hull is far to have any features as previously observed here pre-planning hulls have. The yacht represents by itself a fully-displacement ship with convex shape outlines – see figures 3.1-3.3.

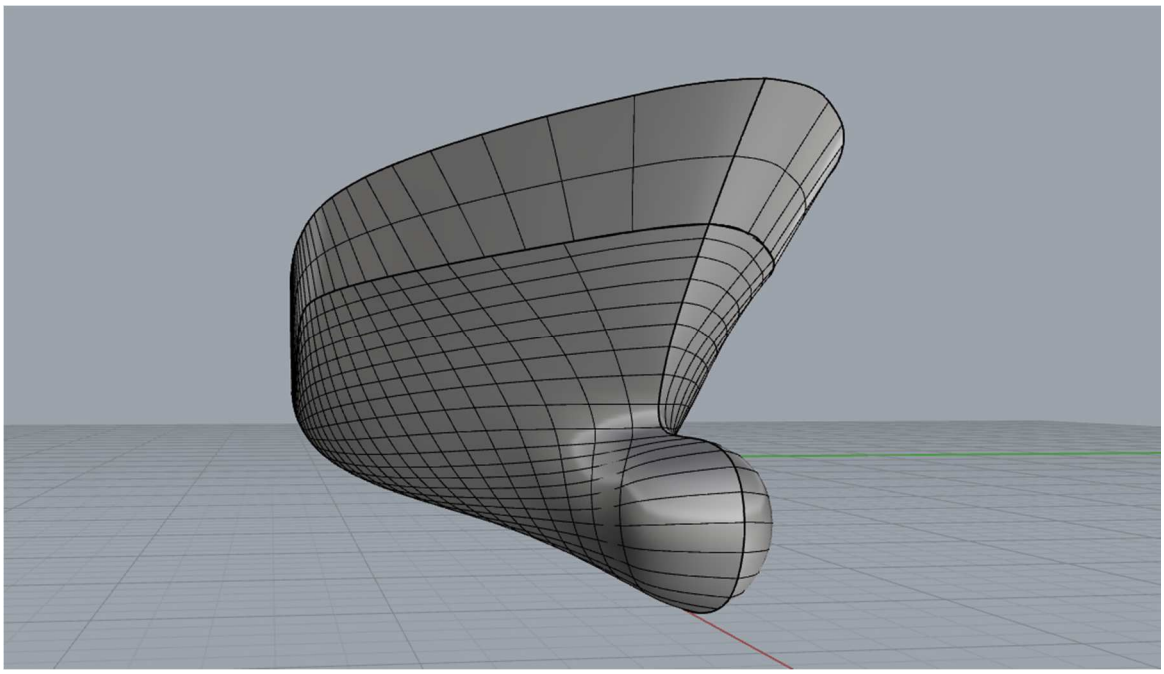

Fig.3.1. The subject of interest

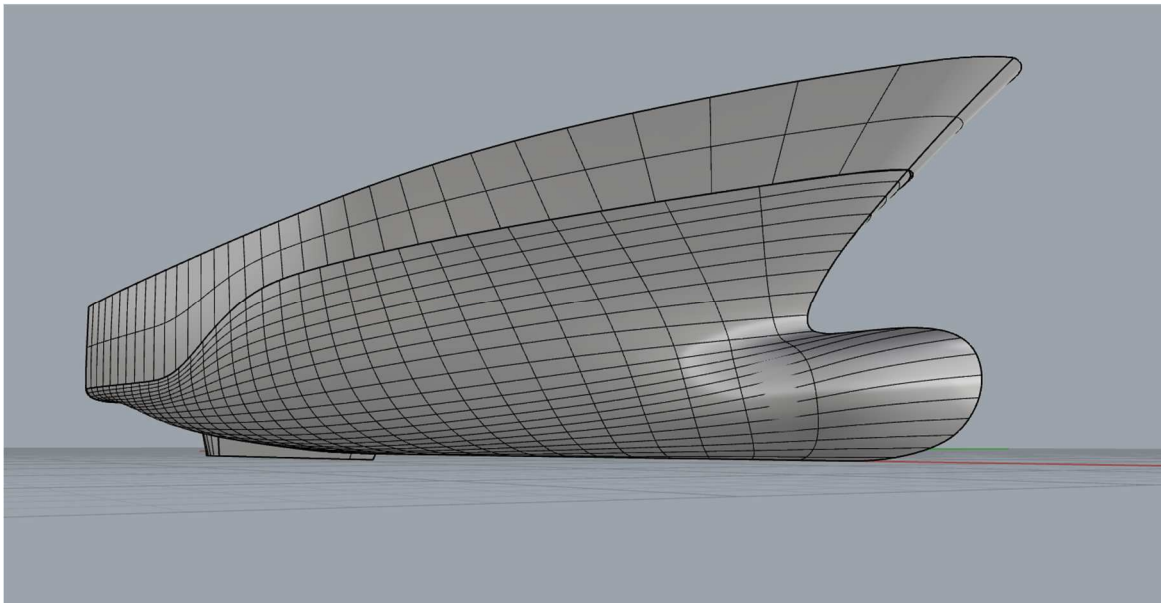

Fig.3.2. The subject of interest

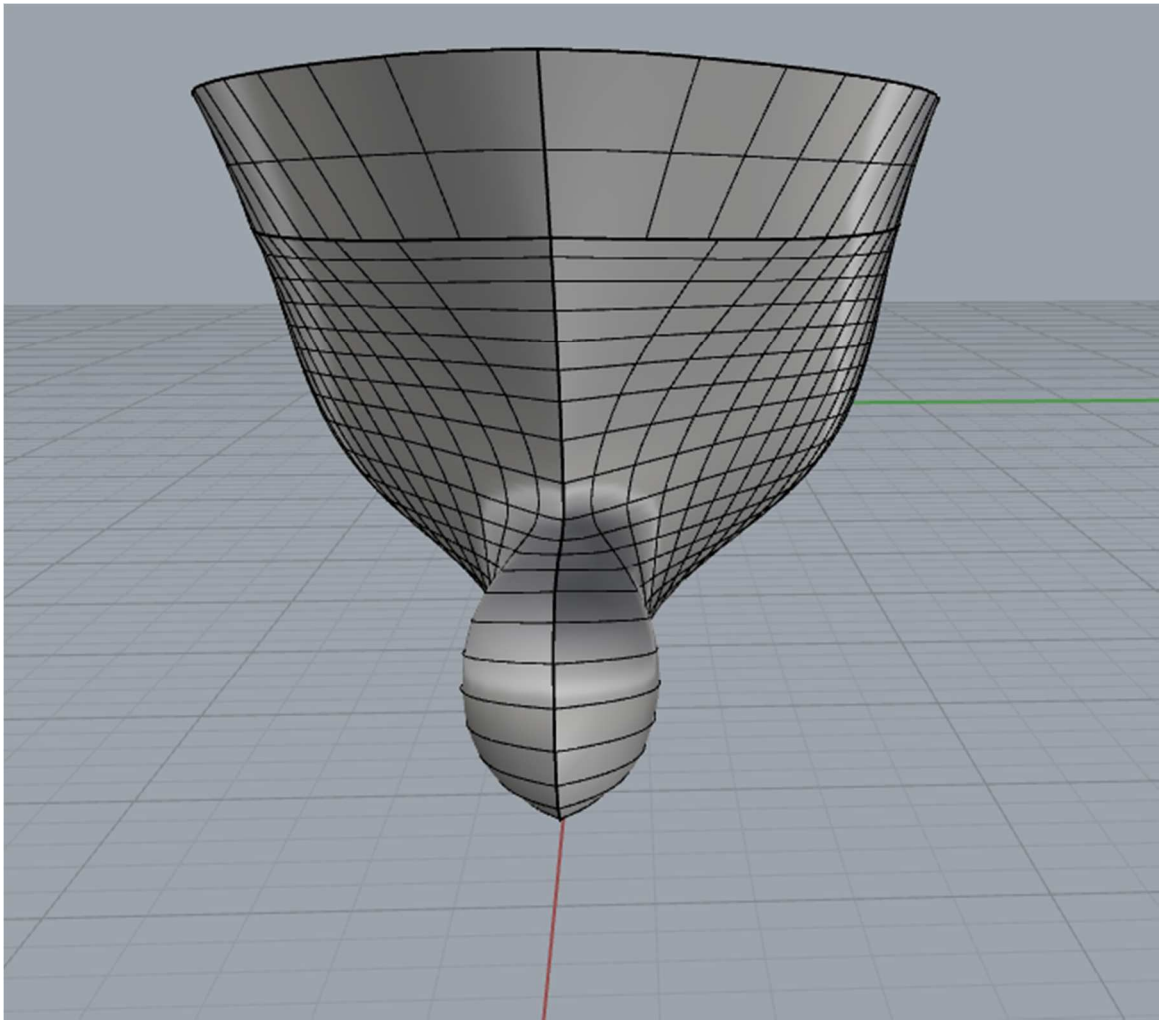

Fig.3.3. The subject of interest

4. MODELLING THE PHYSICS. THEORY PART.

Physical model used: multi-phase flow, turbulence k-ε model, incompressible flow, isothermal flow – keeping constant density of each phase.

Chosen solvers:

- Implicit unsteady
- 6-dof solver
- VOF model
- Segregated volume flux based flow
- Volume fraction
- Realizable k-epsilon turbulence two-layer model
- RANS

Navier-Stokes equation:

$\mathrm{div}\, \upsilon = 0$ – incompressible flow,

$$p\frac{\partial\vec{\vartheta}}{\partial t} + \rho\,\overrightarrow{\overrightarrow{grad}\vec{\vartheta}}\cdot\vec{\vartheta} = \rho\vec{g} - \overrightarrow{grad}p - \frac{\mu}{3}\overrightarrow{grad}\left(div\vec{\vartheta}\right) + \mu\vec{\Delta}\vec{\vartheta}, \qquad (1)$$

$\nu = \frac{\mu}{\rho}$ – kinematic viscosity,
ϑ – velocity of flow,
μ – dynamic viscosity,
p – pressure,
ρ – density

$\frac{\mu}{3}\overrightarrow{grad}\left(div\vec{\vartheta}\right) = 0$, since we consider an incompressible flow.

For free surface simulation the Volume of Fluid approach is usually used in such a CFD simulation of a rigid body motions in multi-phase.
"Volume of Fluid (VOF) is a simple multiphase model. It is suited to simulating flows of several immiscible fluids on numerical grids capable of resolving the interface between the phases of the mixture.
In such cases, there is no need for extra modeling of inter-phase interaction, and the model assumption that all phases share velocity, pressure, and temperature fields become a discretization error."
"…The VOF Waves model is used to simulate surface gravity waves on the interface between a light fluid and a heavy fluid. This model is typically used with the 6-DOF Motion model for marine applications." [11]

Reynolds averaged Navier-Stokes equations:

$$\frac{\partial(\rho U_i)}{\partial t} + \frac{\partial(\rho U_i U_j)}{\partial x_j} = -\frac{\partial P}{\partial x_i} + \frac{\partial}{\partial x_j}\left[\mu\left(\frac{\partial U_i}{\partial x_j} + \frac{\partial U_j}{\partial x_j}\right)\right] - \frac{\partial}{\partial x_j}(\rho\overline{u_i' u_j'}) + f_i \quad (2)$$

$$\frac{\partial U_i}{\partial x_i} = 0 \qquad (3)$$

$$\frac{\partial c}{\partial t} + \frac{\partial U_j}{\partial x_j} = 0 \qquad (4)$$

c – volume fraction, defined by ratio V_{air}/V_{total}, where V_{total} is total volume of a computational cell volume, V_{air} is volume of air in V_{total}; volume of water is obviously maybe calculated by $V_{total} - V_{air} = 1 - c$;
the total density of a cell in multi-phase condition is formulated as $\rho = \rho_{air}\, c + \rho_{water}\,(1 - c)$, dynamic density $\mu = \mu_{air}\, c + \mu_{water}\,(1 - c)$.

On the figure 4.1 below there is an illustration of different grids to compare: the left grid (a) is too large to cache small air bubbles, whilst the grid (b) shown on the right has more chances to capture volumetric difference (or V_{air}/V_{total} ratio) of air and water presence in a cell more accurate, more precise. This is a useful note about practical need to perform the global meshing operation with grid refinements option. Phase 1 is showing water phase, and phase 2 is shown for air.

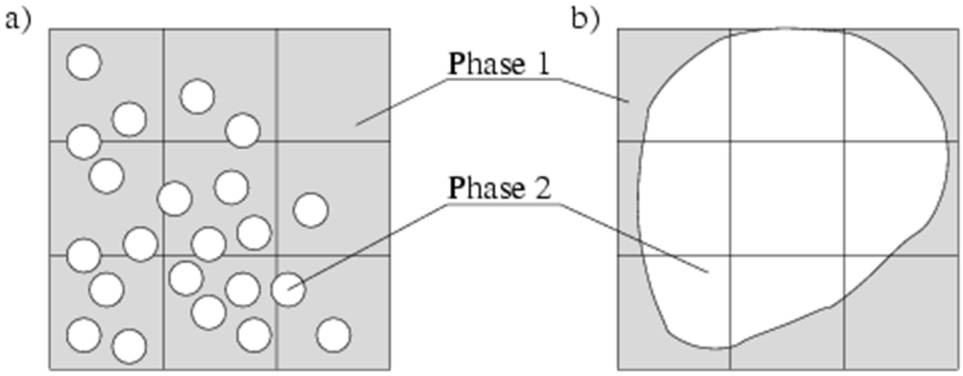

Fig.4.1. [13]

"The two-layer approach, first suggested by Rodi, is an alternative to the low-Reynolds number approach that allows the K-Epsilon model to be applied in the viscous sublayer. In this approach, the computation is divided into two layers. In the layer next to the wall, the turbulent dissipation rate **ε** and the turbulent viscosity $\boldsymbol{\mu_t}$ are specified as functions of wall distance. The values of **ε** specified in the near-wall layer are blended smoothly with the values computed from solving the transport equation far from the wall. The equation for the turbulent kinetic energy is solved in the entire flow. This explicit specification of **ε** and $\boldsymbol{\mu_t}$ is arguably no less empirical than the damping function approach, and the results are often as good or better. In STAR-CCM+, the two-layer formulations work with either low-Reynolds number type meshes $y^+ \sim 1$ or wall-function type meshes $y^+ > 30$." [11]
The volume controls for the blade bow aiming hull remains the same in order to simulate the same quality of local streams as for the case with the previous, initial, bow.

The motions of the yacht hull are calculated by 6 Degrees of Freedom (6-DOF).
The moments of inertia and the centre of mass remains the same as for the initial hull, as well as for mass of the ship.

Eulerian Multiphase model was applied to numerically describe any appeared air-water dispersion resulted from interaction between hull and water – resulting due to wave-making hit in bow part and other turbulence producing issues.
From a general description of multiphase [11]: "Multiphase flow is a term which refers to the flow and interaction of several phases within the same system where distinct

interfaces exist between the phases. The term ‘phase’ usually refers to the thermodynamic state of the matter: solid, liquid, or gas.

In modelling terms, a phase is defined in broader terms, and can be defined as a quantity of matter within a system that has its own physical properties to distinguish it from other phases within the system. For example:
- Liquids of different density
- Bubbles of different size
- Particles of different shape

Multiphase flows are different from multi-component flows. In multi-component flows, the different species are mixed at the molecular level. These species have the same convection velocity. In multiphase flows, the different phases are mixed at the macroscopic scale. These phases have different convection velocity. Many flows are multiphase multi-component flows.
Multiphase flows can be classified into two categories:
- Dispersed flows, such as bubbly, droplet, and particle flows
- Stratified flows, such as free surface flows, or annular film flow in pipes.

A phase is considered dispersed if it occupies disconnected regions of space—otherwise it is continuous.”

k-ε model is applicable in cases to model turbulence near wall of a solid object in a flow. The turbulence behaviour is modelled by Wolfstein’s scheme (fig.4.2).

Wolfstein Model

The one-equation model of Wolfstein [98] is as follows:

$$l_\varepsilon = c_l y\left[1 - \exp\left(-\frac{\mathrm{Re}_y}{A_\varepsilon}\right)\right]$$

$$A_\varepsilon = 2c_l$$

$$c_l = \kappa C_\mu^{-3/4}$$

where $C_\mu = 0.09$ and $\kappa = 0.42$.

The turbulent viscosity is:

$$\frac{\mu_t}{\mu} = \mathrm{Re}_y C_\mu^{1/4}\kappa\left[1 - \exp\left(-\frac{\mathrm{Re}_y}{A_\mu}\right)\right]$$

where $A_\mu = 70$.

Fig.4.2. Wolfstein’s proposed k-ε turbulence model, [11]. ε – turbulent dissipation rate, l_ε – turbulent lenght, y, Re_y – wall-distance-based turbulent Reynolds number, A_ε - , μ – dynamic viscousity, μ_t – turbulent viscousity, C_μ and κ are constants

5. WAY TO SOLVE THE PROBLEM

It is an actions scheme presented below on a Scheme 1 below.

Scheme 1. Algorithm of the research work to be done on the stage of the thesis.

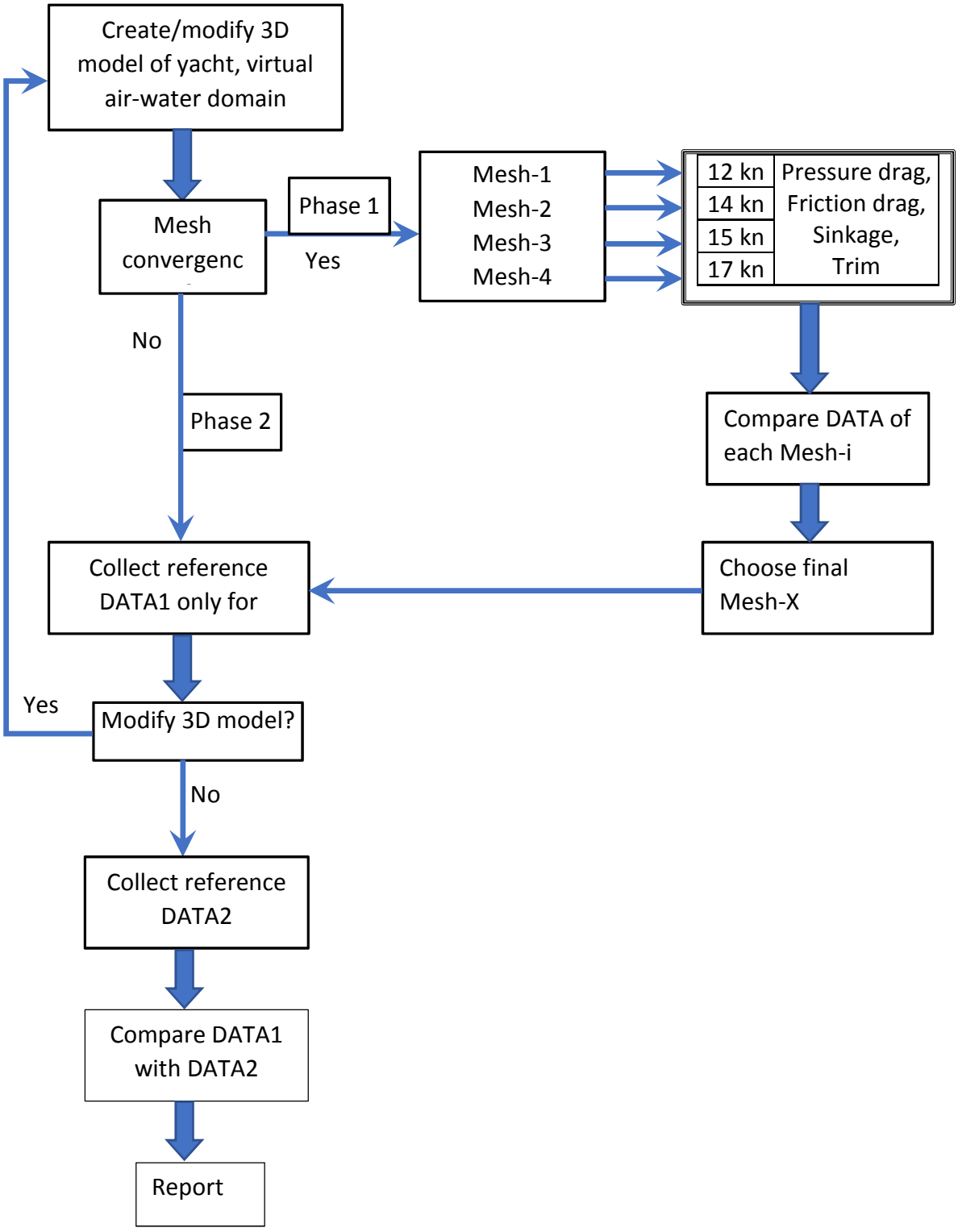

I. Collect reference data of motions, forces and moments of the yacht hull with the old bow for different velocities.
II. Test new bow in the same conditions.
III. Compare both data collected, make conclusion.

Notes about the new bow construction: the shape of blade bow was sketched and made by those blade bulbous bows presented on magazines photos, no special drafts were used; the new bow has to be limited by the main dimensions (length, breadth, height) of the old one. Main shape features of this kind of bow were accepted are: flat horizontal plane on top of the bow, transversal profile flows from U-shaped into V-shaped sharpening on the forward continuing keel line. However, transverse section may also be shaped as an inequilateral rhomb. The next important feature should be mentioned, due to difficulties of connection the triangle shape of the blade bulbous bow with the yacht hull (and any other one, as visual appearance shows so) the hull part between the blade bow and the hull became wider than in case with the old convenient bow. The tests will show how much higher will be the pressure (and friction) drag of the new model of yacht. See figures 5.1-5.5 (taken from the articles [8-9]).

Fig.5.1. “Dominator Ilumen 28M”

Fig.5.2. Built by Fincantieri. [8]


Fig.5.3. Benetti F-125 [8]

Fig.5.4. Benetti Vivace 125 (F-125), photo by [6].

Fig.5.5. Benetti F-125 [8]

5.1. Comparison of popular methods

Towing tank and computational fluid dynamics software are two obvious tools always mentioned firstly. Since there is no any hull made similar to the yacht is being overviewed here, it's not possible to use the prototype approach.

Thus, the first two ways mentioned above were chosen to be compared before the author can decide which one is more appropriate. From here, there are some main questions to be clarified for both of them:

1) How is it expensive?
2) Is the length of a tank enough to perform robust tests of a scaled model?

3) What is the biggest scale may be used in chosen tank until the standard conditions of towing tank tests (to avoid the walls and scale effect) will be overstepped?
4) How long will it take to provide such a test in the chosen tank with the chosen model scale? Including standard preparations and test process - overall.
5) What percentage of errors may occur during processing experimental and numerical tests and which approach usually shows less measurements deviations over the full-scale tests? By other words, which tool shows better convergence with the same measurements for real ship?

Towing tank tests requires much less financial expenses than numerical one.
But in case of the model size may be used, the numerical approach for sure has an advantage here, since there is almost no any size limit for an object which needs to be analysed, whilst enough CPU power and RAM were provided for it.

5.2. Chosen method - CFD

The commercial CFD software STAR-CCM+ had been chosen to simulate yacht movements on different speeds and then obtain the measurements of forces and moments acting on the ship, recording sinkage and trim behaviour.

The standard way of simulation setting was used: deep and wide virtual “towing tank” to avoid wall effects and have more available space to apply fine enough mesh in air-water domain around the yacht hull for modelling fluid behaviour as more realistic as possible, in order to reduce the calculation error.

All technical requirements of experimental equipment needed was defined as for a computer with 20 cores with CPU power minimum 1.7 GHz each, at least 12 GB RAM memory and space on hard drive about 2 GB for each simulation file (total number of simulations had been done during research work was 22 sets, including mesh convergence study, reference data collection and the same data refreshing by launching the yacht with the new bow mounted on virtual model).

3D model of the initial yacht hull and the modified one were made by using the commercial CAD software Rhinoceros. Meshing operations were performed by STAR-CCM+’s inner meshing tool.

The model was tested in the STAR-CCM+ as full-scale, avoiding possible mistakes from rescaling the results obtained in case of using smaller hull.

6. MESH CONVERGENCE STUDY

Comparison was made by shear and pressure drag of the yacht hull depending on the number of cells used for a solution. Each drag diagram curve had been resulted by points from each speed given by 14, 15, 17 knots.

Since number of cells directly dependent from a base size chosen in STAR-CCM+, author also notes different base size values in the same comparing table as alternative reference value instead of number of cells. This had been done to show the relation between all given dimensions (virtual air-water domain, ship's general arrangements, volumetric refinements done) – in order to study a practical approach to current commercial software when dealing with the same subject of interest as a middle-speed vessel in still water conditions. The Base size is a value which is taken as reference one, all main volumetric and surface mesh refinements are taken by percentage from this value. Whilst base size is being varied the percentage of each mesh control remains the same. In the program this value is set in reference to specific area covered around the ship, and defined by volumetric refinements.

Table 1

Number of cells = 891486; Base size = 10 m	Velocity, kn	Shear drag, kN	Pressure drag, kN	Sinkage, m	Trim, deg
	14	19.76657115	26.63347473	-0.176262845	0.494623313
	15	22.74049515	31.94867126	-0.219005168	0.528570385
	17	29.21494457	55.07470809	-0.291786416	0.6319012

Table 2

Number of cells = 1673806; Base size = 7.5 m	Velocity, kn	Shear drag, kN	Pressure drag, kN	Sinkage, m	Trim, deg
	14	19.88839339	25.50340452	-0.175948402	0.487821608
	15	22.71141888	30.60855957	-0.216470852	0.519347939
	17	29.3228924	54.75375905	-0.293865647	0.602759934

Table 3

Number of cells = 2989818; Base size = 6 m	Velocity, kn	Shear drag, kN	Pressure drag, kN	Sinkage, m	Trim, deg
	14	19.88163236	24.44349585	-0.173079991	0.49611262
	15	22.81391047	30.11767118	-0.214673105	0.529019871
	17	29.40883949	54.13670687	-0.292880558	0.598633927

According the results had been obtained, the most suitable number of cells will be for 1.7 million (mln) cells. Comparing modelling for 1.7 mln cells with 3 mln cells modelling, the wall time to calculate 1.7 mln cells was approximately for 15 hours less.

Take a look on the figures 6.1-6.4. Comparison between frictional resistance, pressure drag, trim an sinkage are presented on those pictures, in order to visually evaluate which mesh grid fits another with the best match.

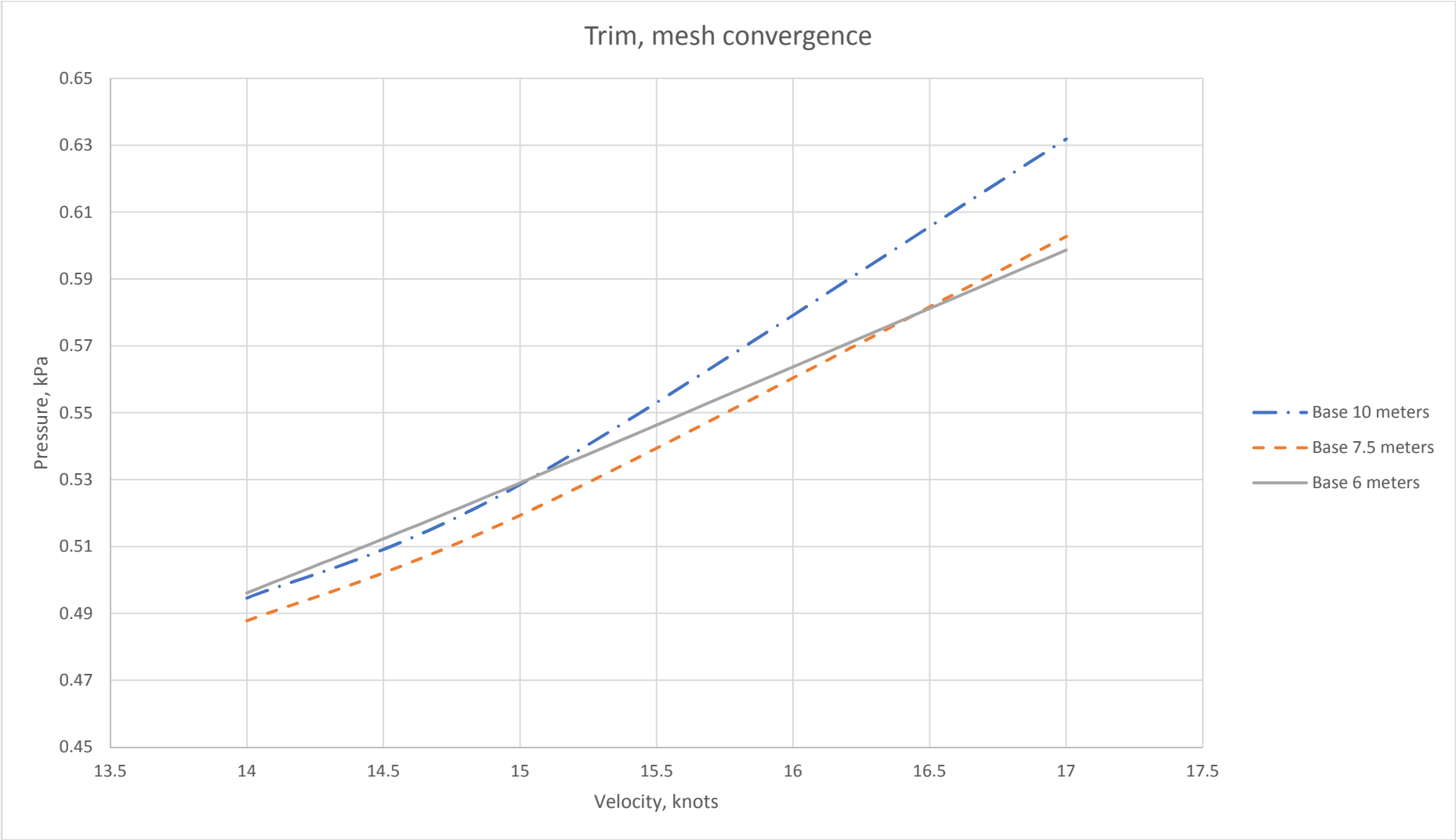
Trim, mesh convergence
Pressure, kPa
0.65
0.63
0.61
0.59
0.57
0.55
0.53
0.51
0.49
0.47
0.45
13.5
14
14.5
15
15.5
16
16.5
17
17.5
Velocity, knots
Base 10 meters
Base 7.5 meters
Base 6 meters

Fig.6.1.

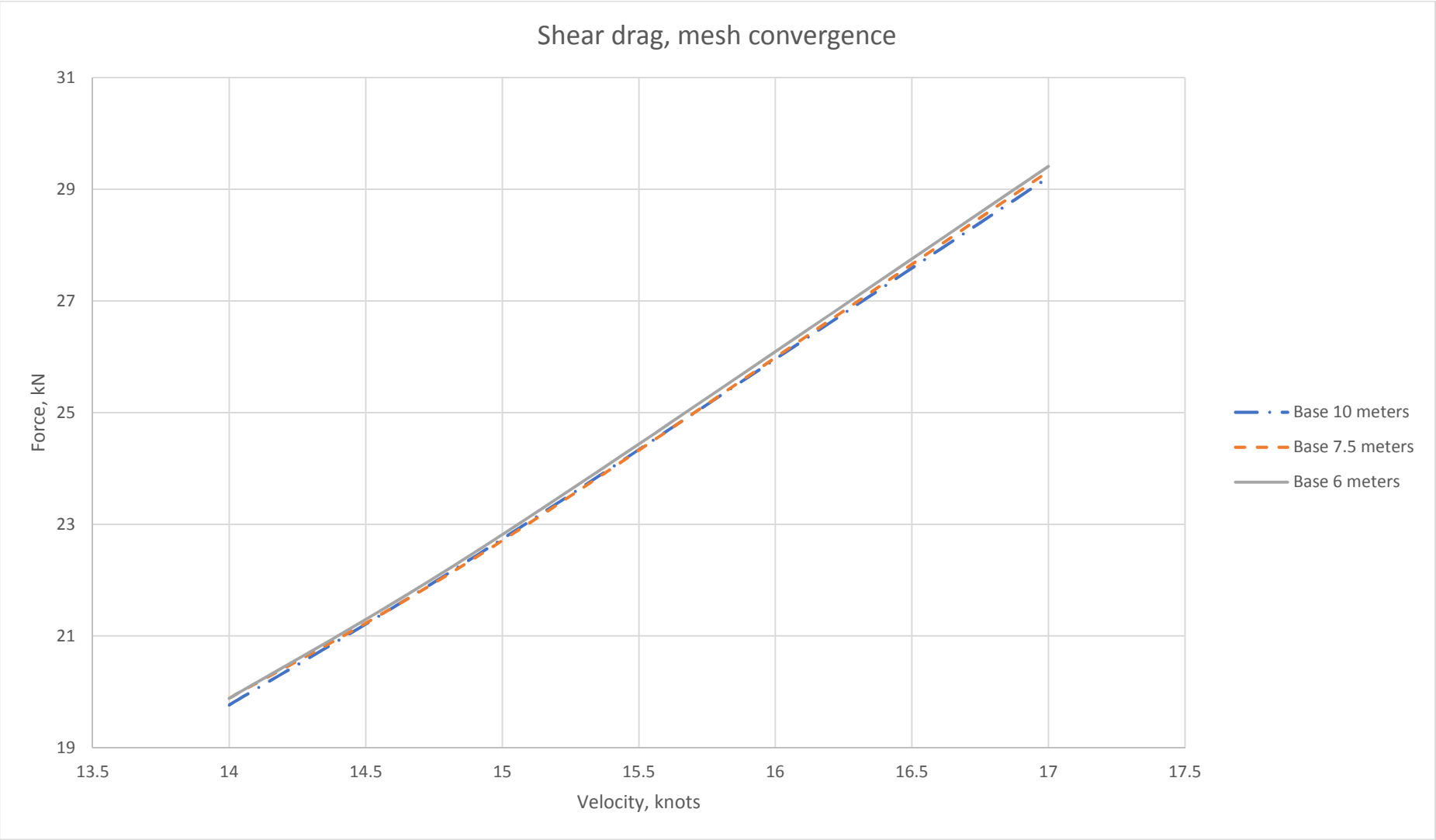
Shear drag, mesh convergence
31
29
27
25
23
21
19
Force, kN
13.5
14
14.5
15
15.5
16
16.5
17
17.5
Velocity, knots
Base 10 meters
Base 7.5 meters
Base 6 meters

Fig.6.2.

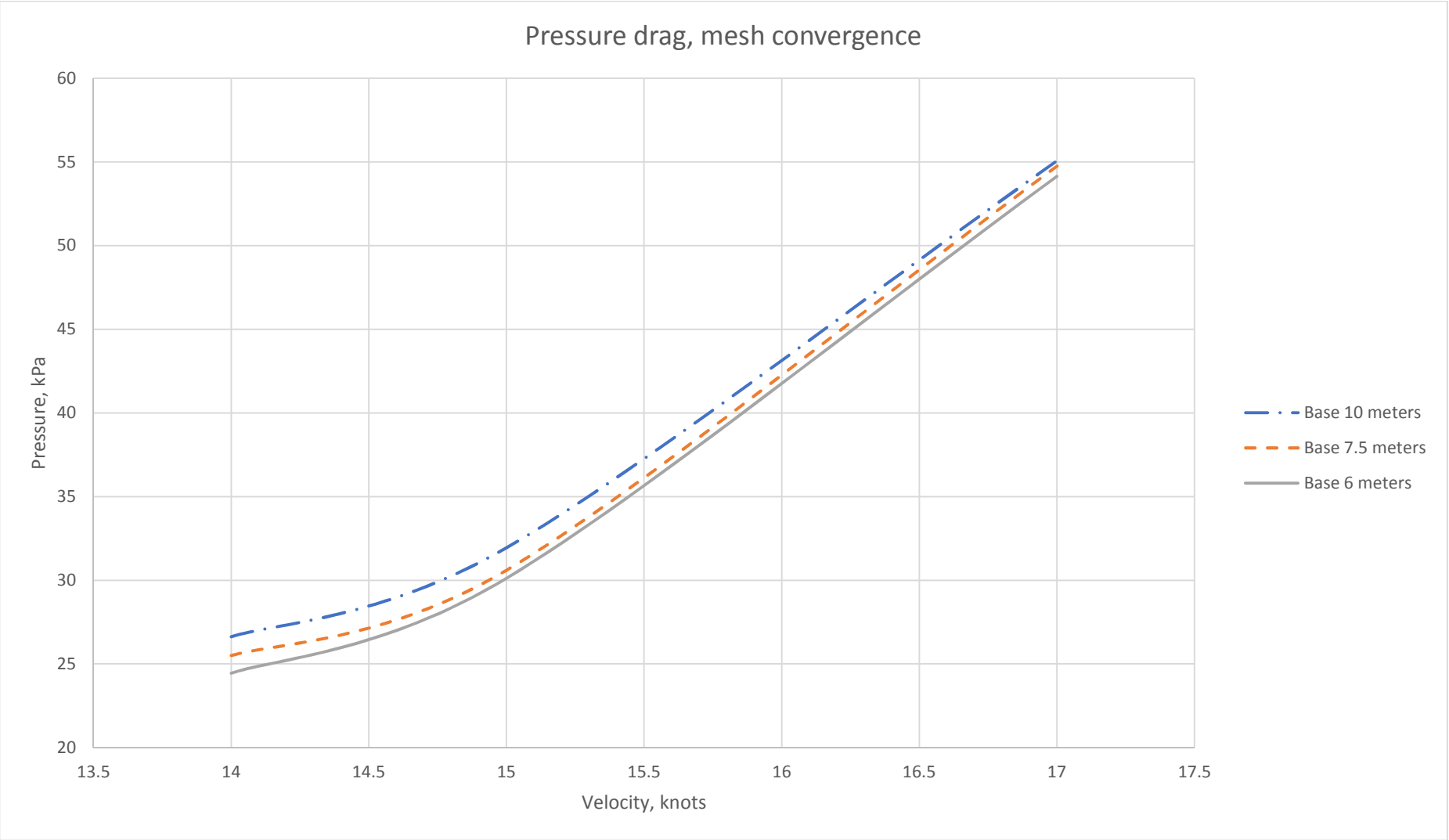
Pressure drag, mesh convergence
Pressure, kPa
60
55
50
45
40
35
30
25
20
13.5
14
14.5
15
15.5
16
16.5
17
17.5
Velocity, knots
Base 10 meters
Base 7.5 meters
Base 6 meters

Fig.6.3.


Sinkage, mesh convergence
-0.15
-0.17
-0.19
-0.21
-0.23
-0.25
-0.27
-0.29
-0.31
Cantimeters
13.5
14
14.5
15
15.5
16
16.5
17
17.5
Velocity, knots
Base 10 meters
Base 7.5 meters
Base 6 meters

Fig.6.4.

7. TEST LAUNCHES

Results values presented are not rounded in order to show that comparison will be made below uses detailed information to catch even small differences.
Test models have initial similar physical and volume/surface meshing conditions. As it was mentioned above, there are only three main velocities are interesting to obtain ship's behavior for.

Each simulation set spent about 35 hours of wall time – by our real time. At the end of each set sinkage and trim diagrams had sinusoidal-like deviations by ±0.1° for trim and ±0.05 meters (or 5 cm) for sinkage, some very small deviations for pressure drag and shear drag signals during 65-90 seconds of modelled physical time. For this case it was decided to take the average values for the final report.

7.1. Initial bow aimed yacht

On the figures 7.1.1.-7.1.6 below, you can see the side view of the imitation of free surface behavior near the yacht's hull. The initial bow seems to be functioning normally, reducing the wave-creating forces. Stagnation pressure zone on the bulb's front surface is mostly the only interesting place here since the pressure drag is the one of only two forces we have under observation. The center of gravity is placed approximately on the middle of the hull (it is shown by a green dot on the hull, on the red-colored YX axis vector).

Tables contain main information collected during all tests.

Table 4

Number of cells:	Velocity, kn	Shear drag, kN	Pressure drag, kPa	Sinkage, m	Trim, deg
1673806	14	19.88839339	25.50340452	-0.175948402	0.487821608
Base size 7.5 m	15	22.71141888	30.60855957	-0.216470852	0.519347939
	17	29.3228924	54.75375905	-0.293865647	0.602759934

The subject of interest. Bulbous bow.

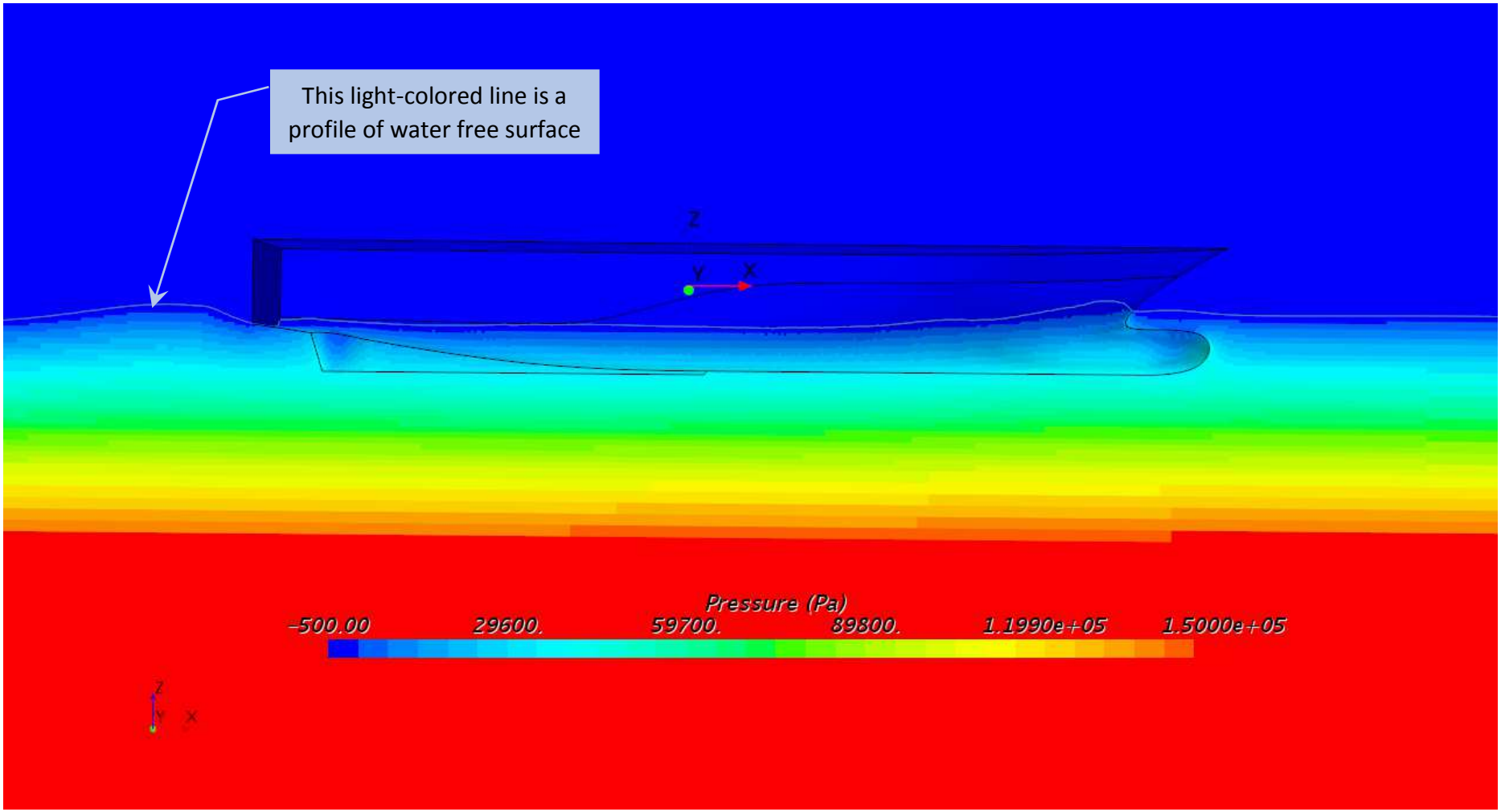

Fig.7.1.1. 14 knots side view

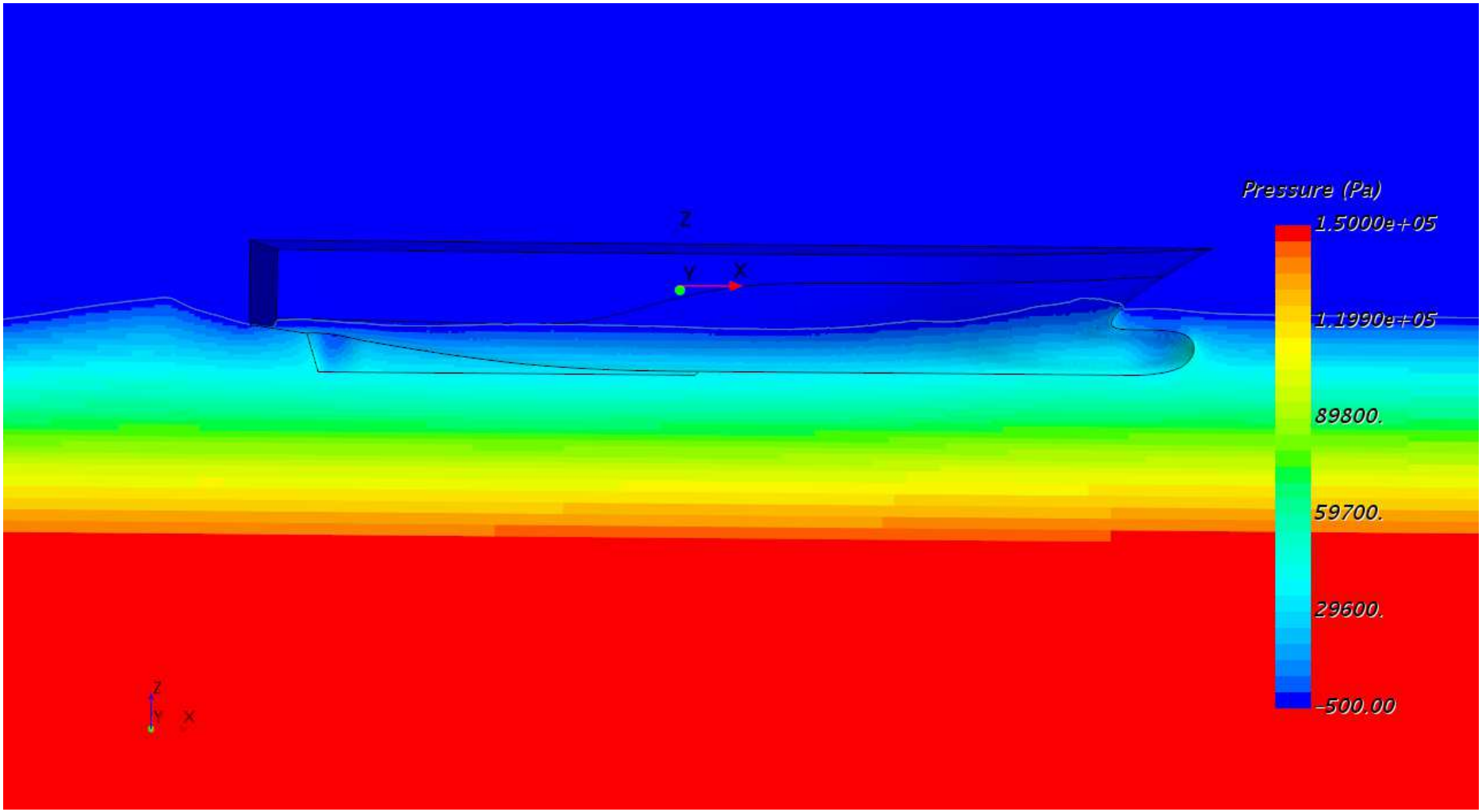

Fig.7.1.2. 15 knots side view

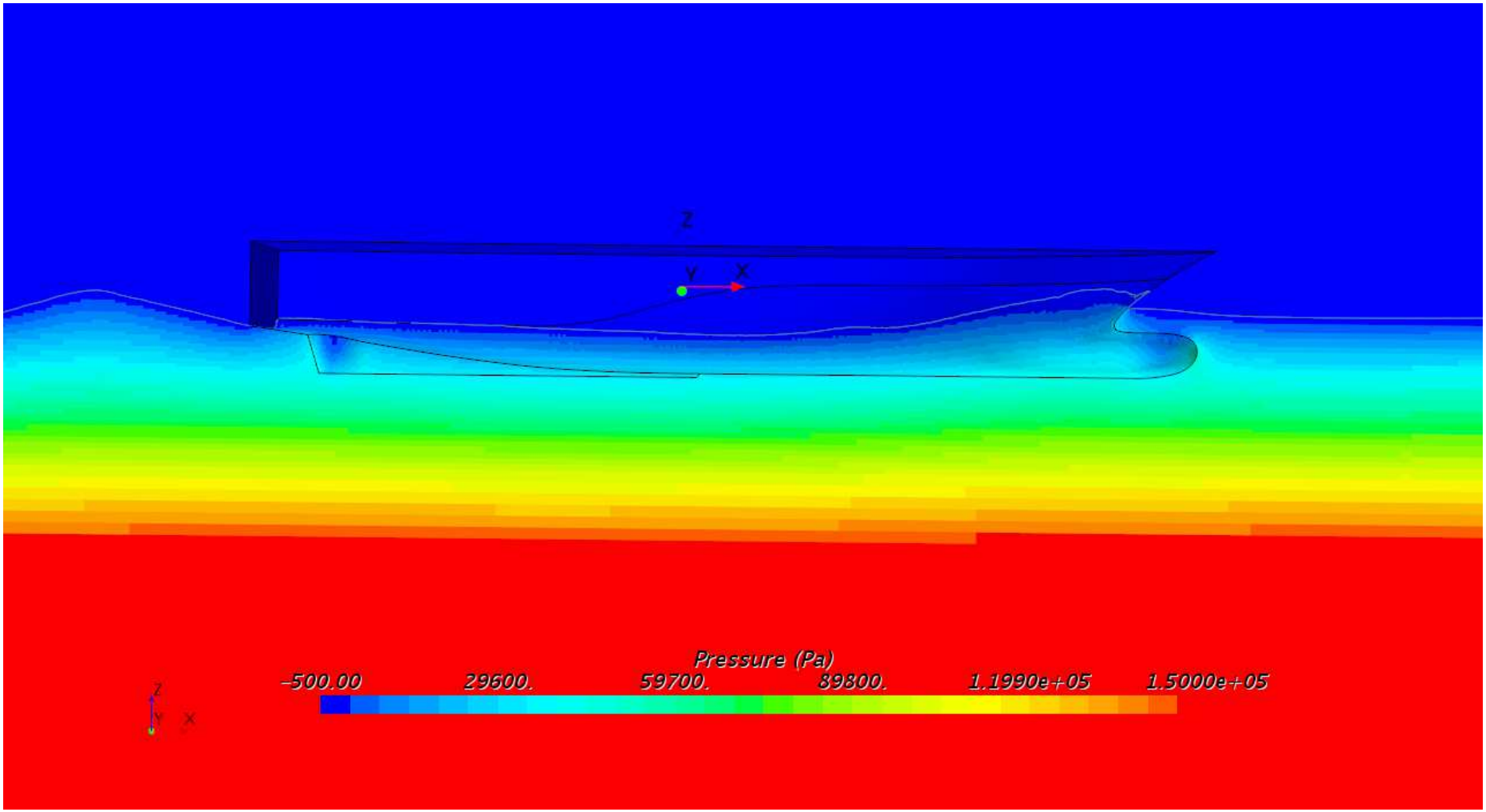

Fig.7.1.3. 17 knots side view

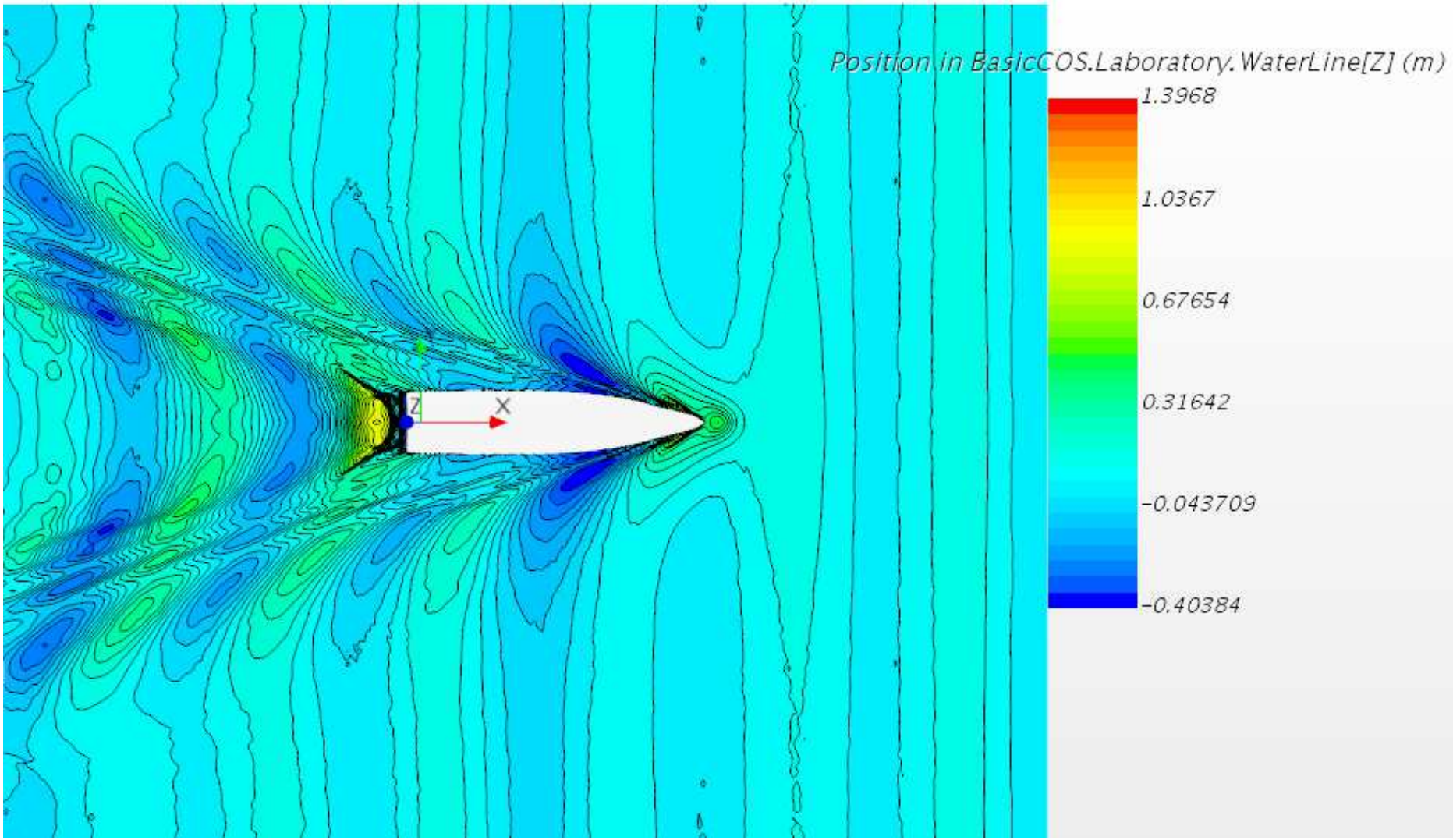

Fig.7.1.4. 14 knots top view

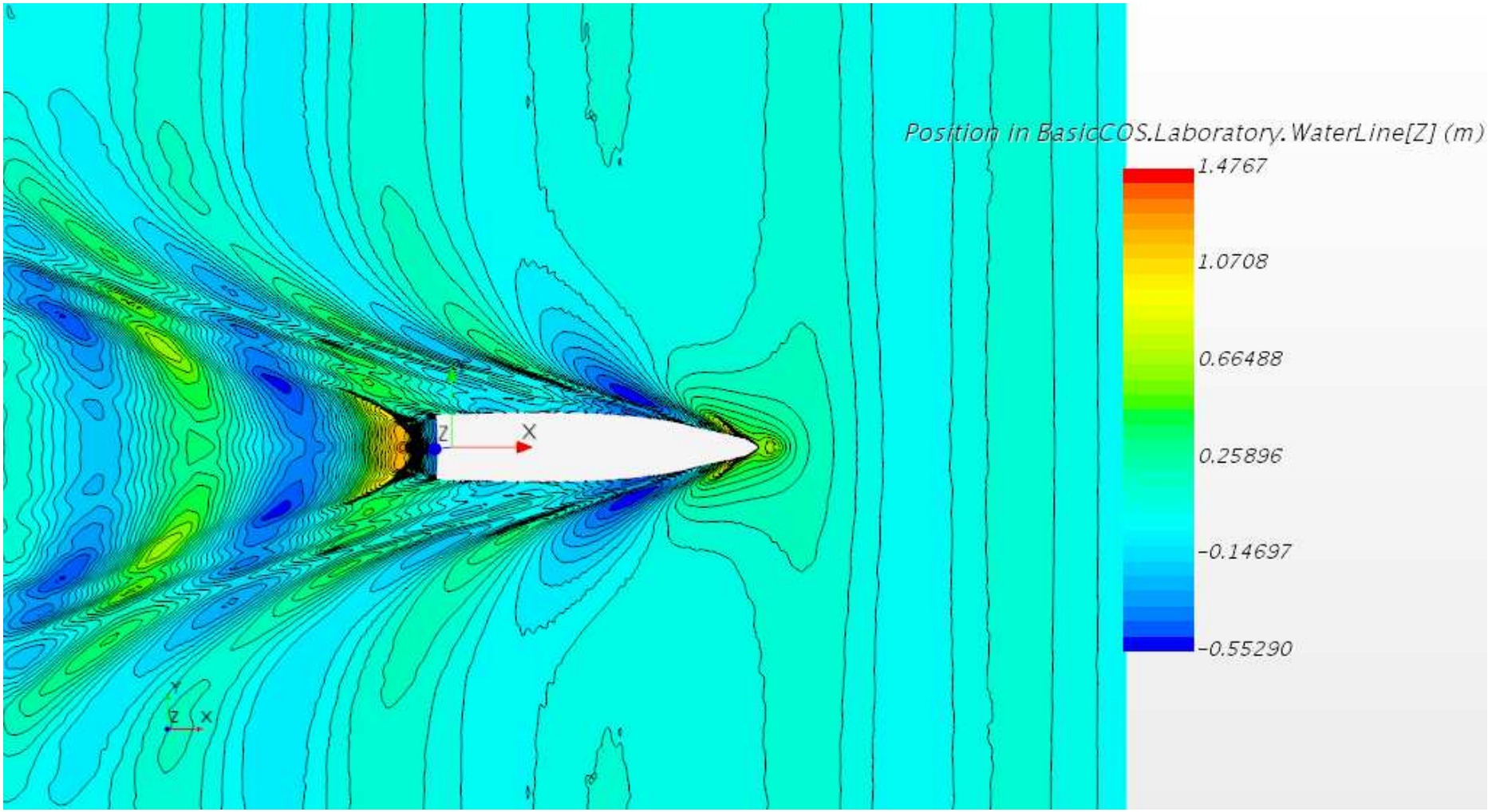

Fig.7.1.5. 15 knots top view

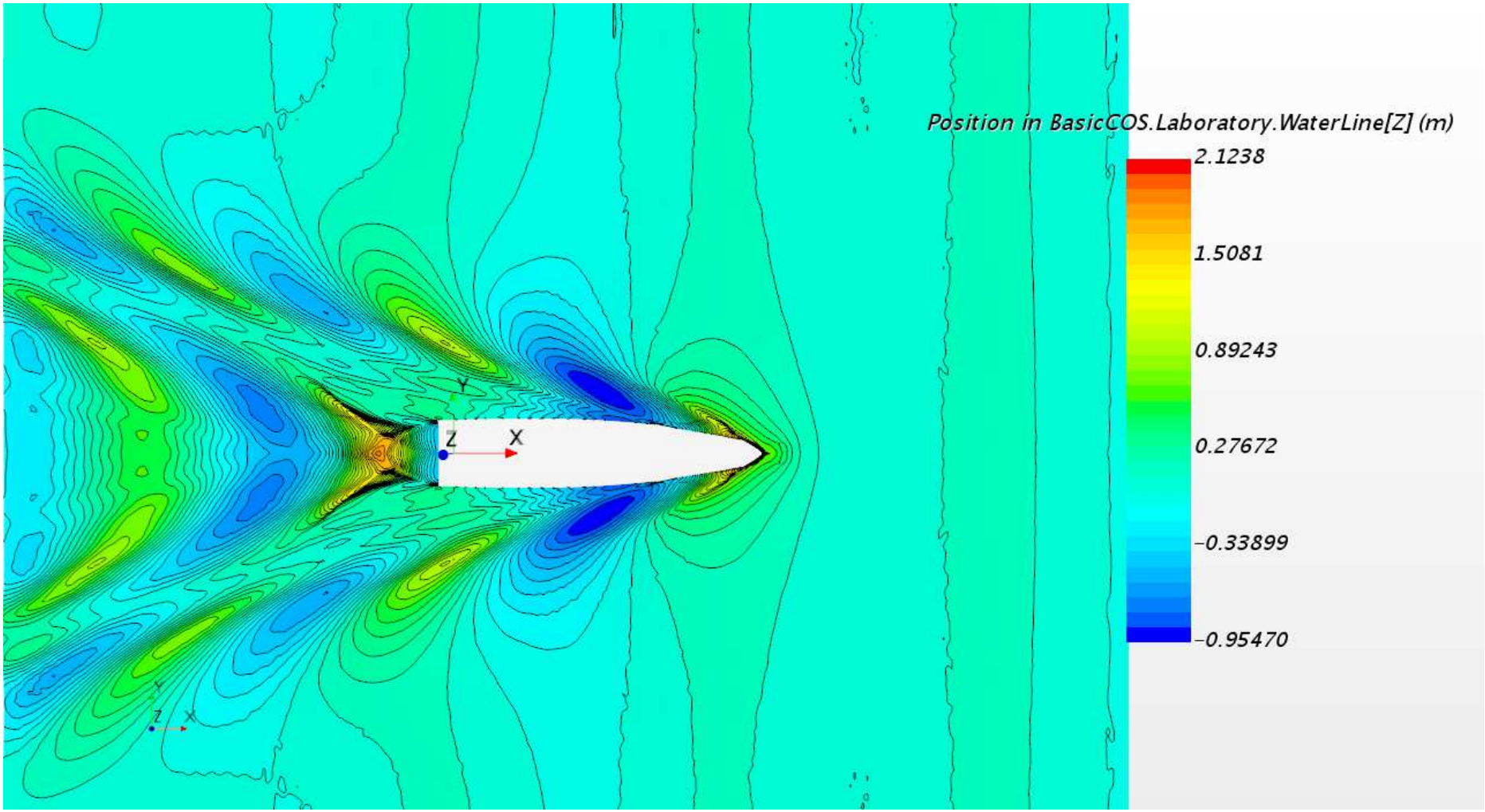

Fig.7.1.6. 17 knots top view

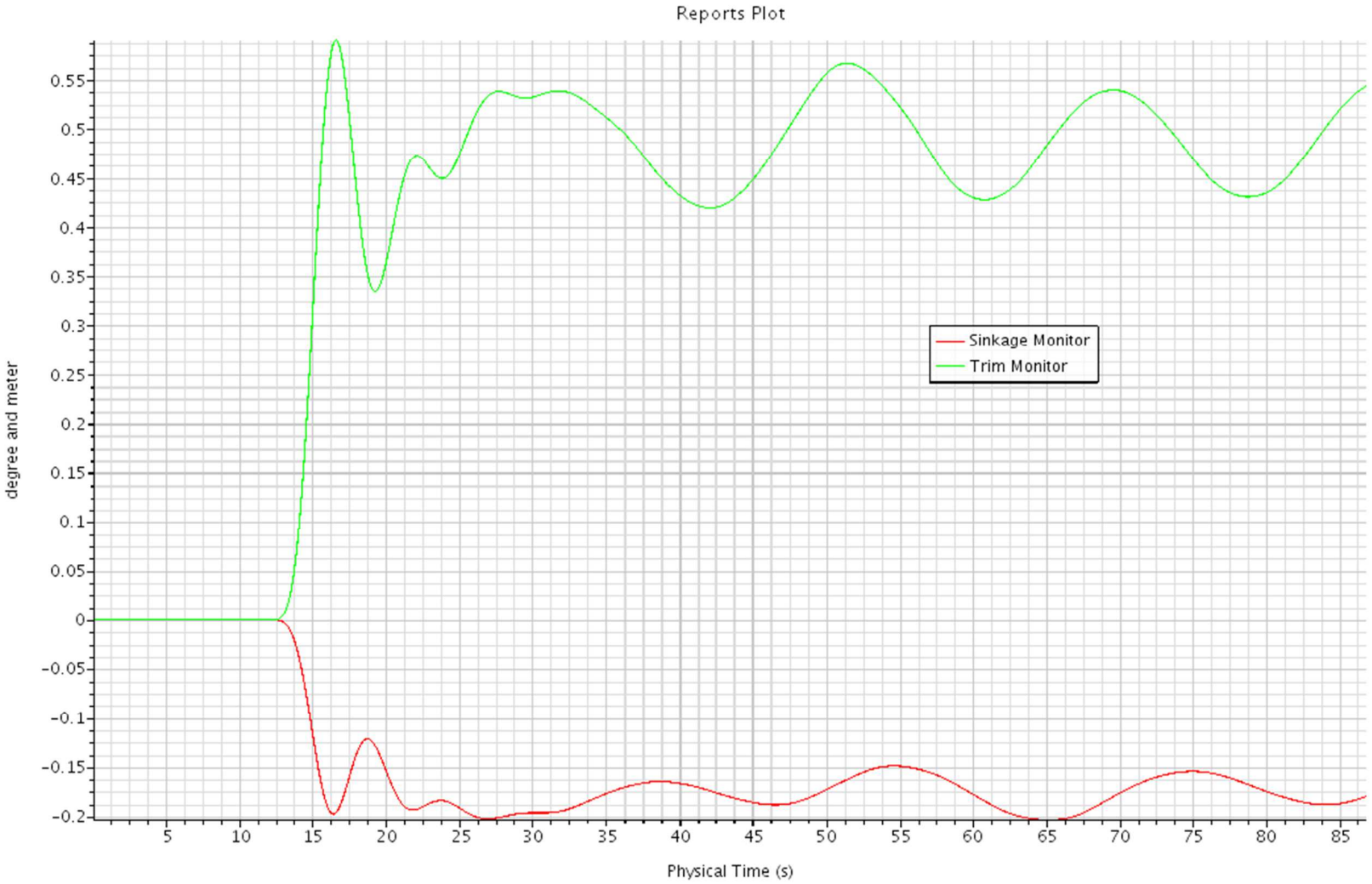

Fig.7.1.7. Motions, 14 knots

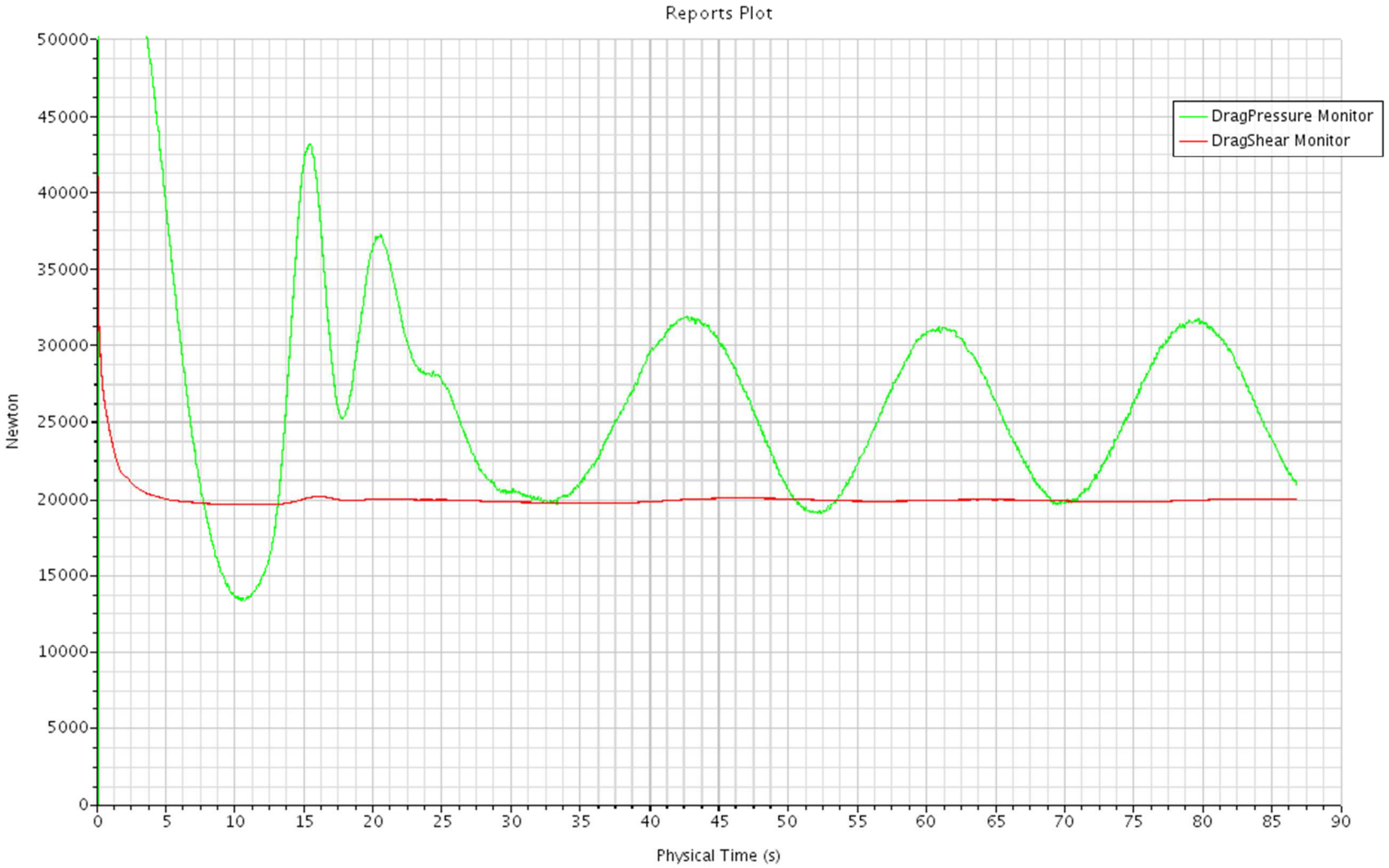

Fig.7.1.8. Resistance plot, frictional drag and pressure drag, 14 knots

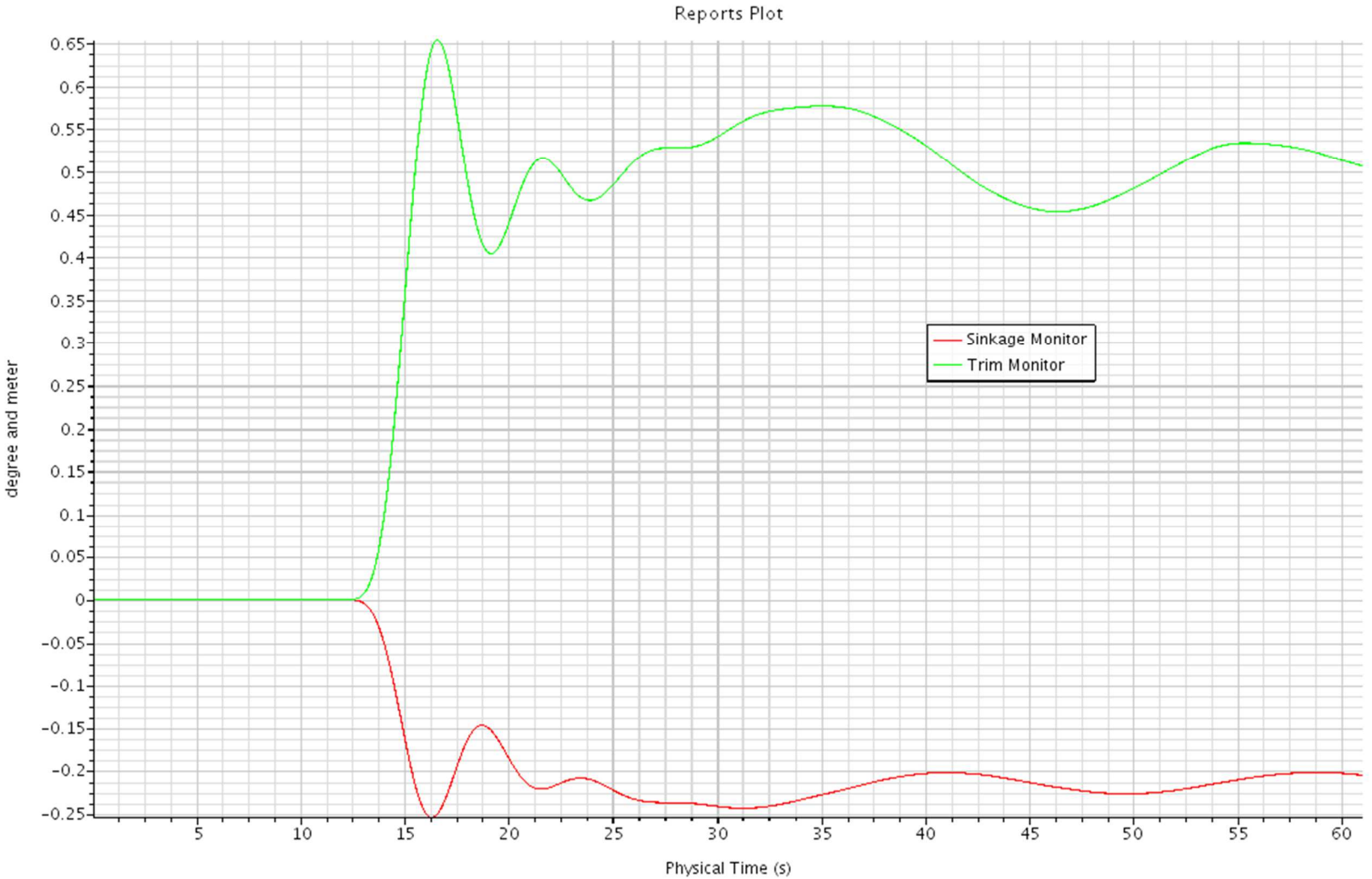

Fig.7.1.9. Motions, 15 knots

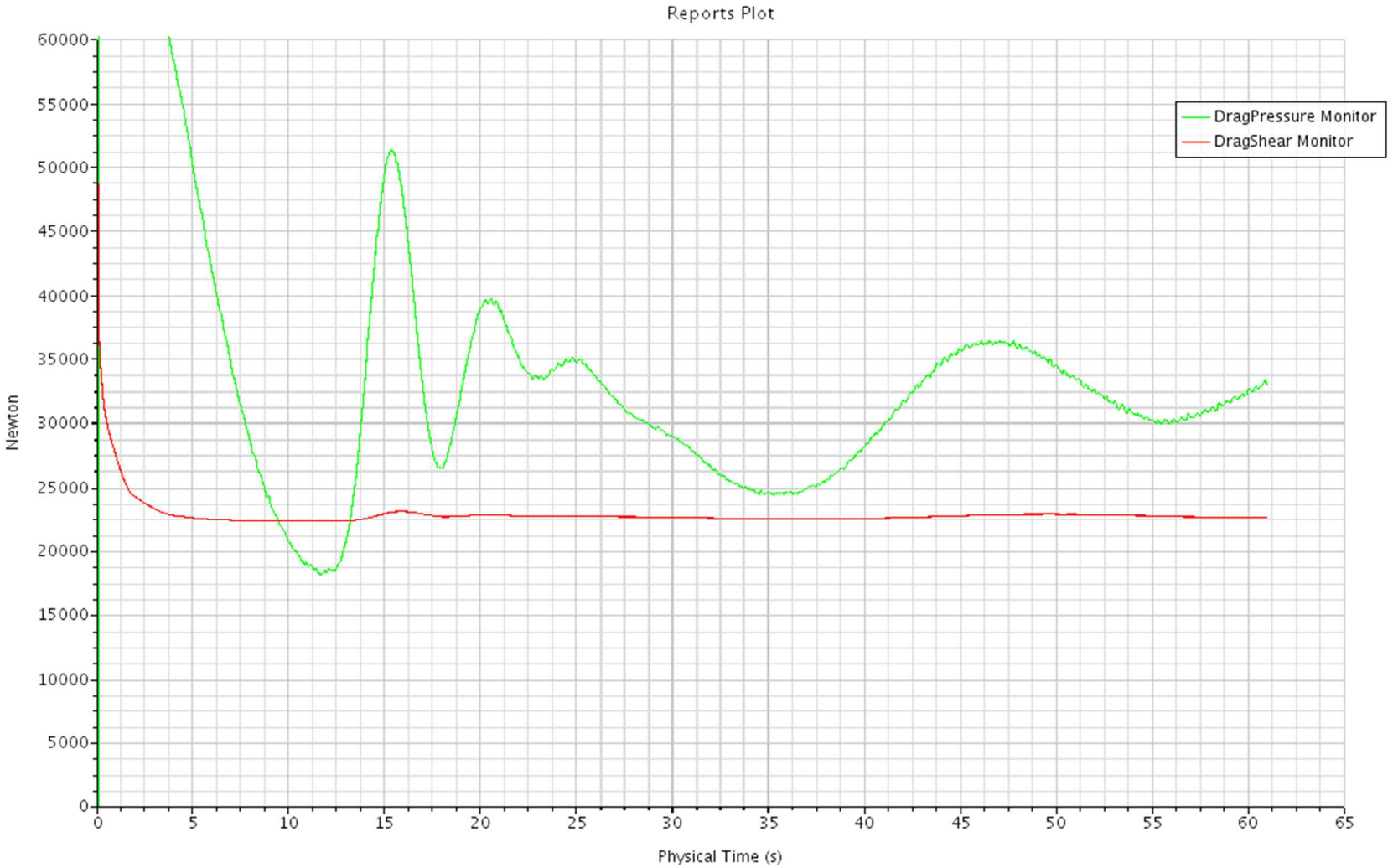

Fig.7.1.10. Resistance plot, frictional drag and pressure drag, 15 knots

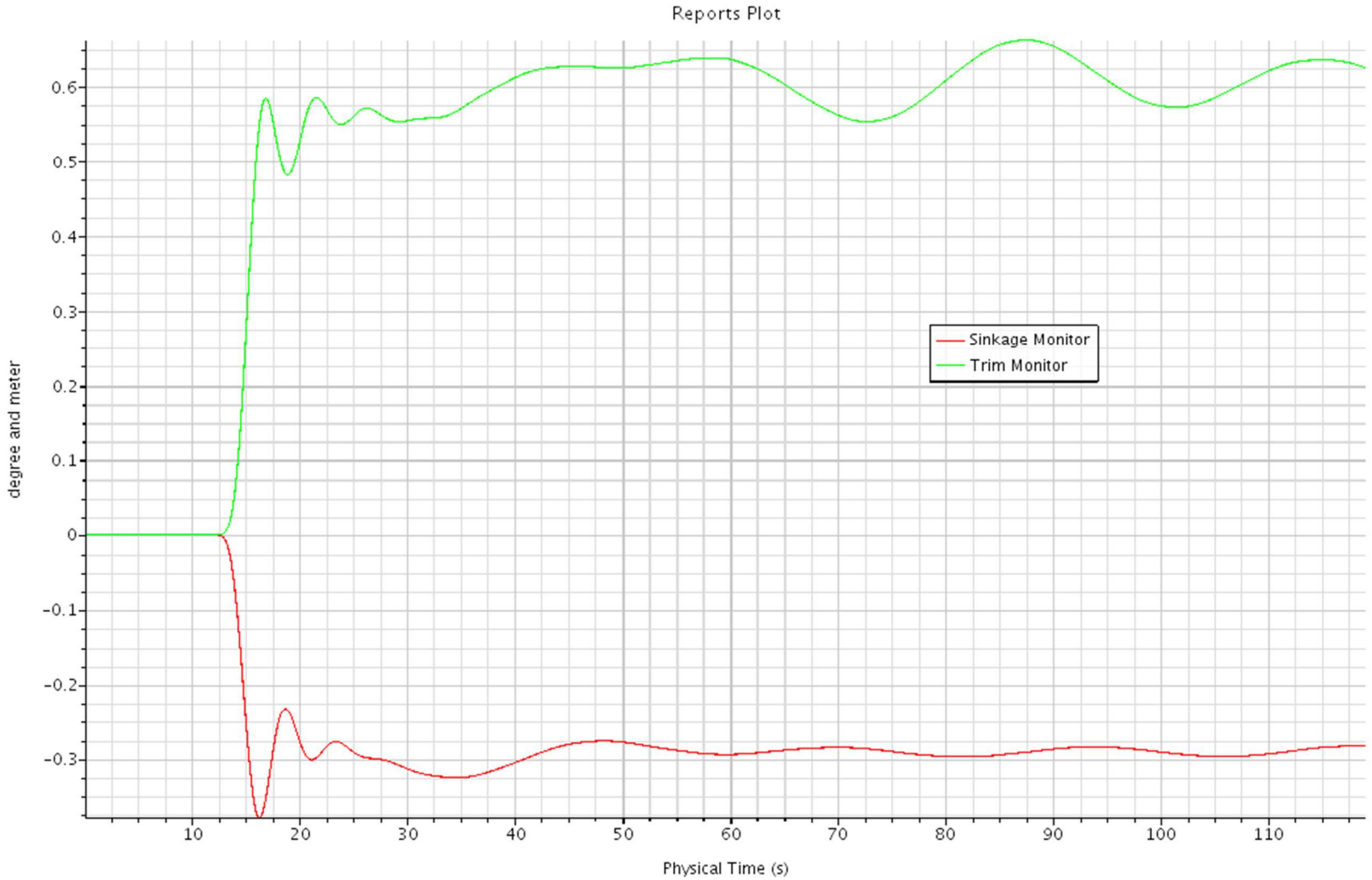

Fig.7.1.11. Motions, 17 knots

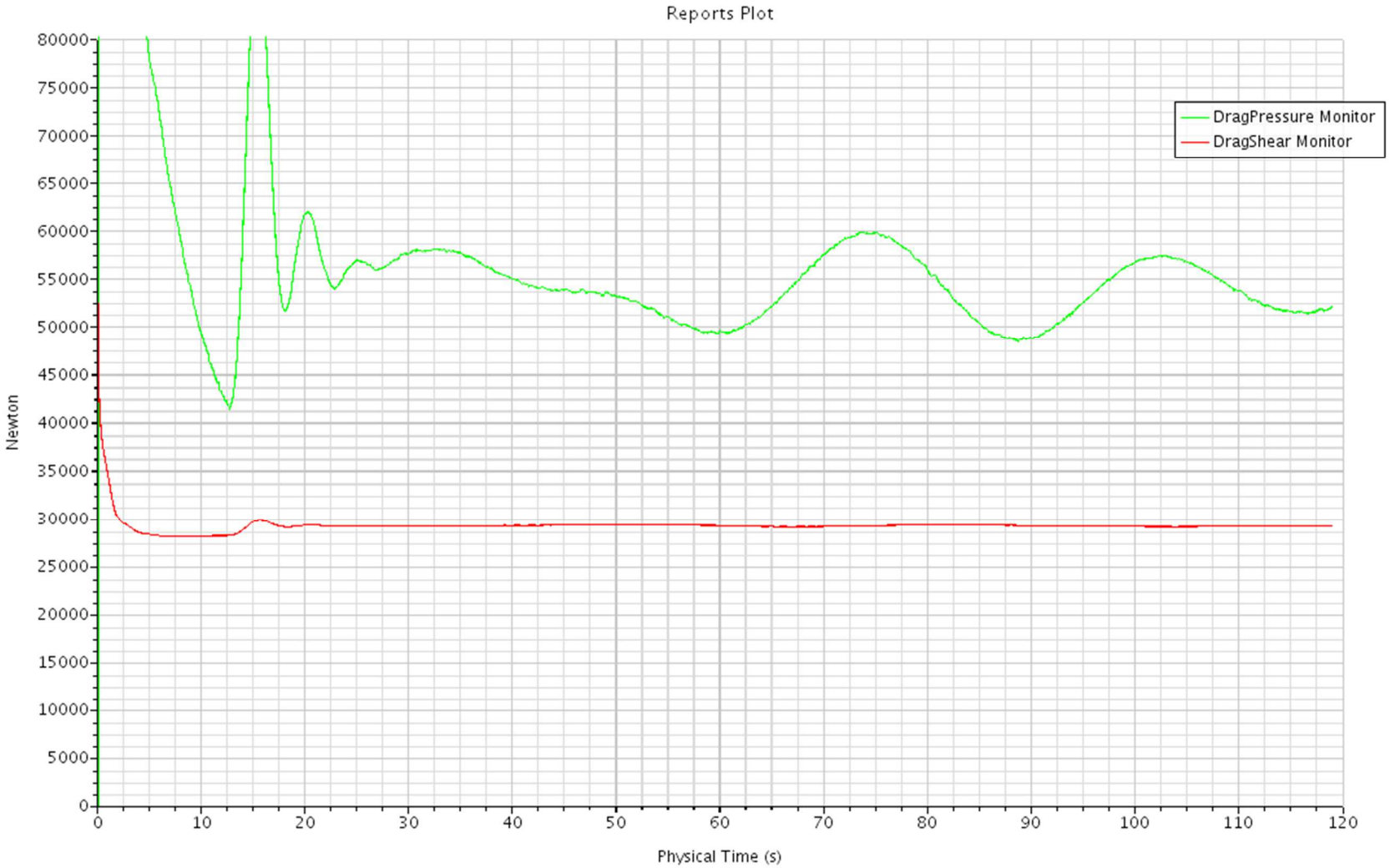

Fig.7.1.12. Resistance plot, frictional drag and pressure drag, 17 knots

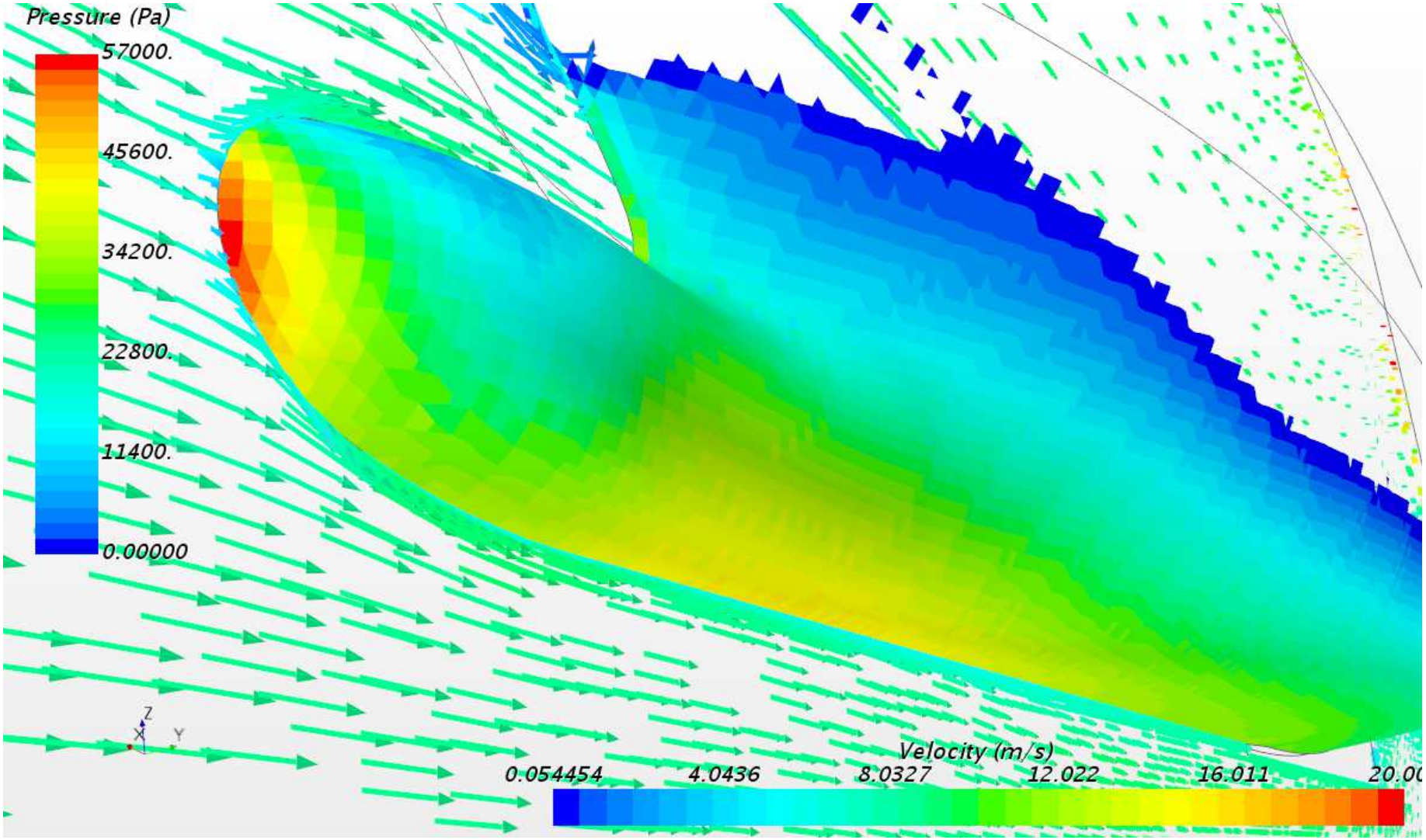

Fig.7.1.13. Pressure and velocity vector scene, 17 knots

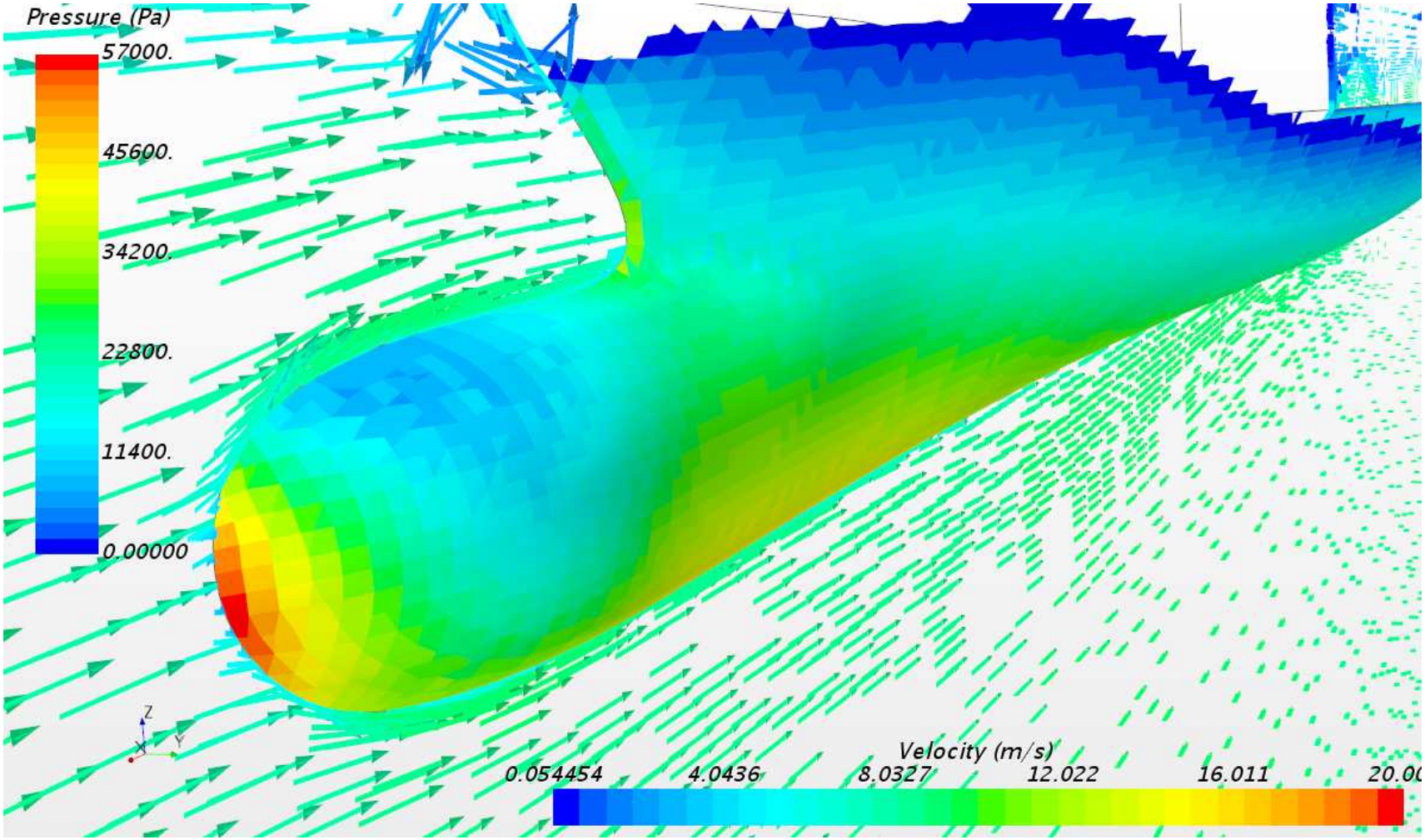

Fig.7.1.14. Pressure and velocity vector scene, 17 knots. The highest value of dynamic pressure is applied on the front part of the bulb almost horizontally, it may be assumed. As a result, we have a positive moment causing the positive trim, since the center of gravity is found higher from the presupposed line of the dynamic pressure caused force acts on.

7.2. Blade bow, 1st variant

This bow has been created using the magazines publications about the existing mounted blades.

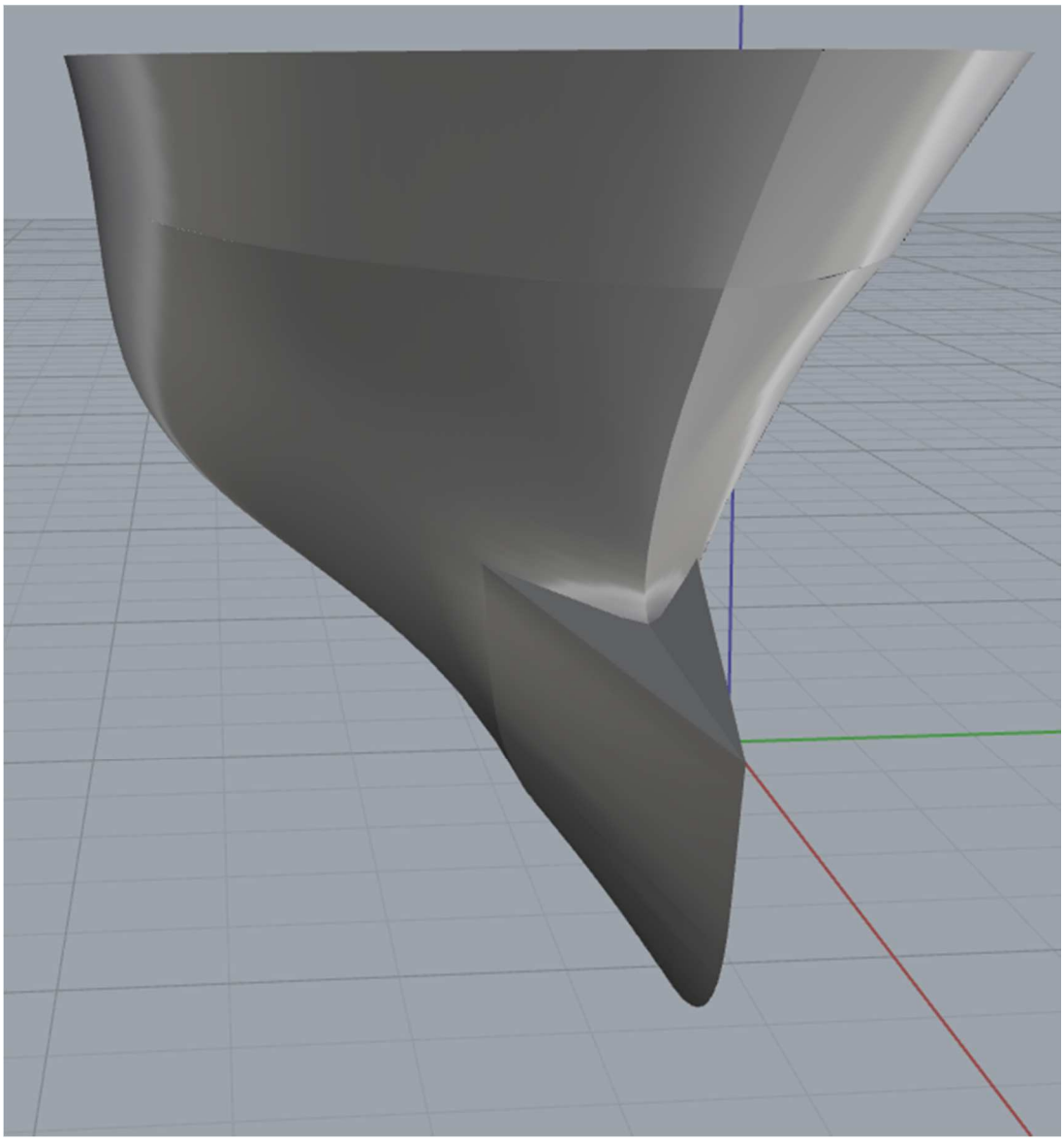

Fig.7.2.1. The halves of the top surface of the blade has some not straight angle between them looking up.

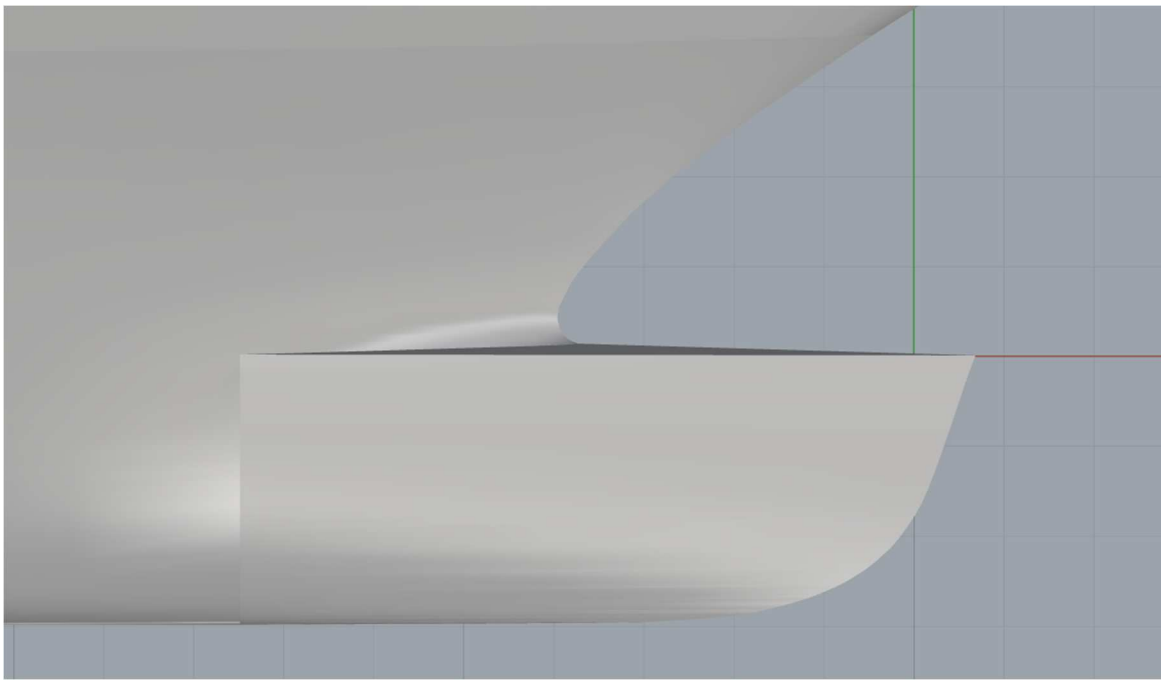

Fig.7.2.2. Note the profile of the new bow. Neglecting some minor render errors, it, however, reminds first fast boat hulls which found out for the advantages of dynamic pressure appear in the fore-part of the bottom. The profile of the top edge is almost horizontal line.

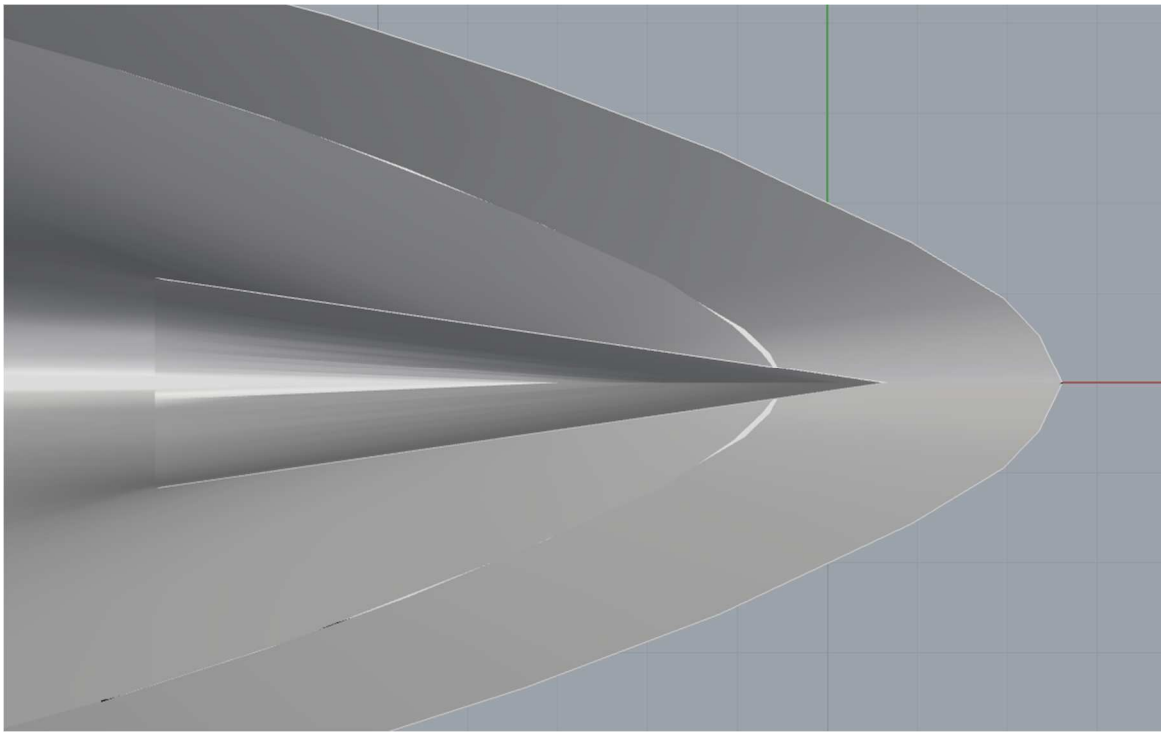

Fig.7.2.3. The sharp front of the blade bow is supposed to easily penetrate through water domain

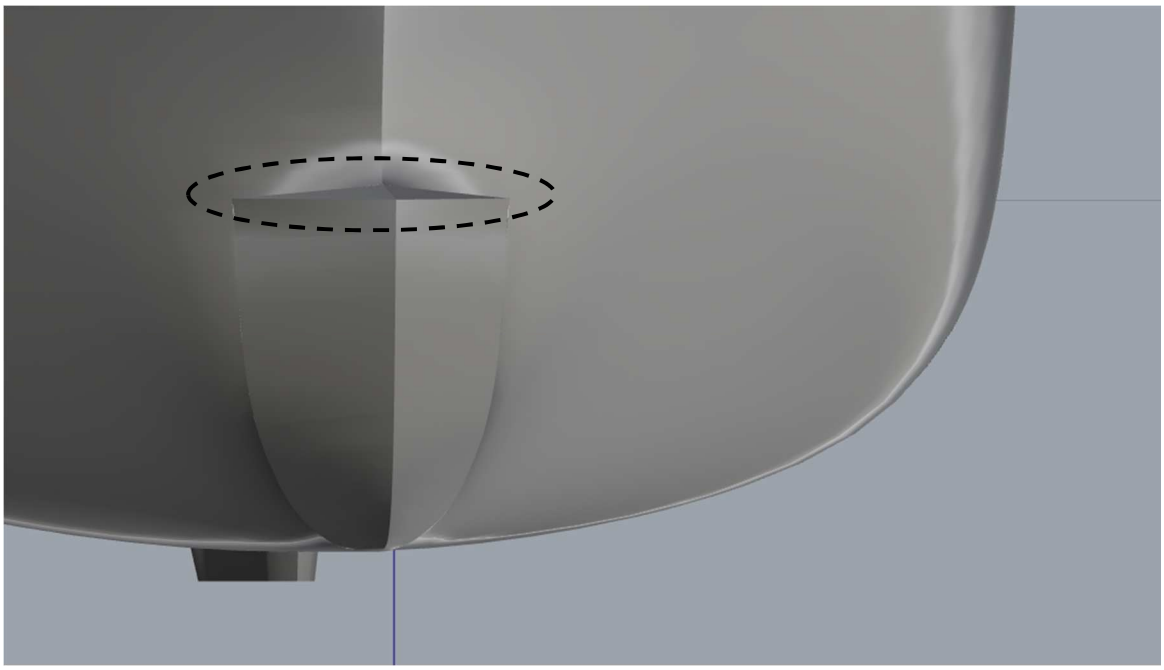

Fig.7.2.4. Here you may notice the angle between two halves of the blade's top surface

Table 5

Number of cells:	Velocity, kn	Shear drag, kN	Pressure drag, kPa	Sinkage, m	Trim, deg
1649612	14	20.09391647	32.58250392	-0.244054297	0.8841737
Base size 7.5 m	15	23.10868299	38.8515669	-0.286090606	0.909170396
	17	29.70691572	65.29461566	-0.3547204	1.03442323

Tests of the 1st variant of the blade bow concept showed higher values of the pressure drag, whilst the friction drag was not much increased – refer to table 6 below.

Table 6

1st BLADE BOW TO INITIAL BULBOUS BOW, %				
Velocity, kn	Shear drag, kN	Pressure drag, kPa	Sinkage, m	Trim, deg
14	101.03	127.76	138.71	181.25
15	101.75	126.93	132.16	175.06
17	101.31	119.25	120.71	171.61

The trim values show that additional positive (on the bow) moment has appeared. The center of gravity of the ship situates high enough above the bow, and the scene showing the local pressure on a wetted surface of the yacht gives an idea, that the dynamic pressure load was concentrated on the lower-front part of the bow (figure 7.2.5):

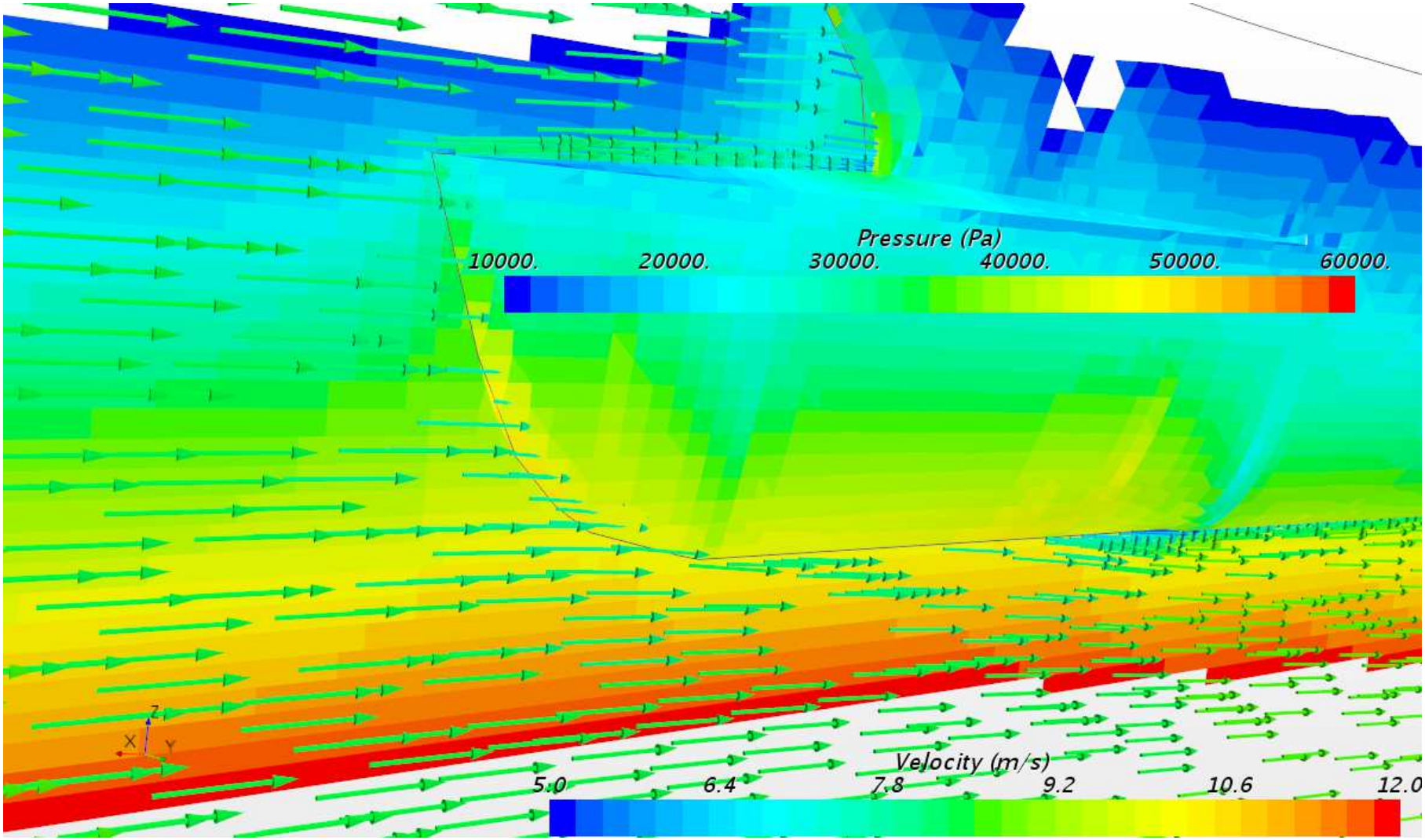

Fig.7.2.5. All colored area except vectors refers to “Pressure” color bar. The color of velocity vectors explains by the “Velocity” color bar for observed velocity range.

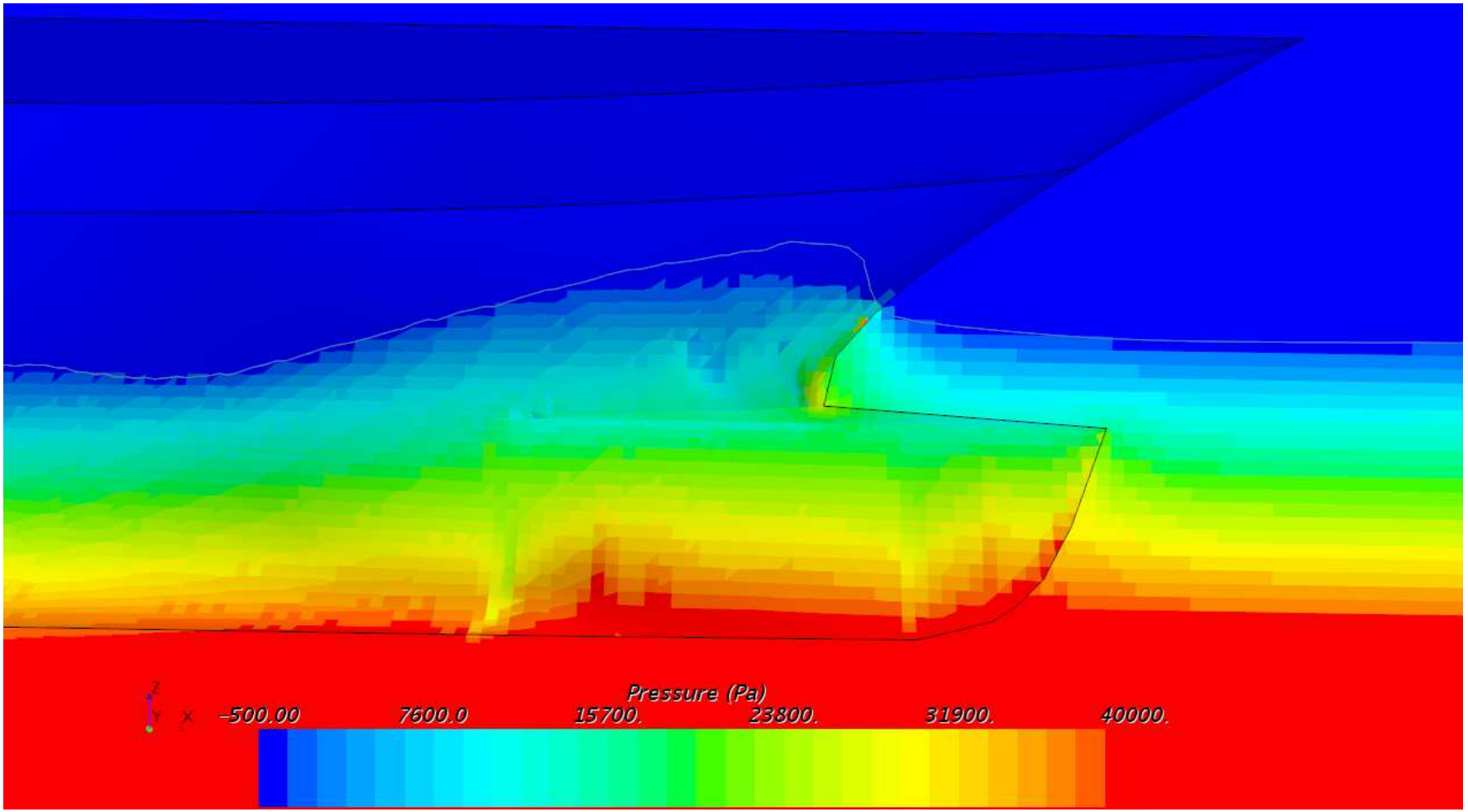

Fig.7.2.6. 14 knots. The trim already has been changed positively, so the top edge's profile looks now more inclined than it was presented on the figure 7.2.2.

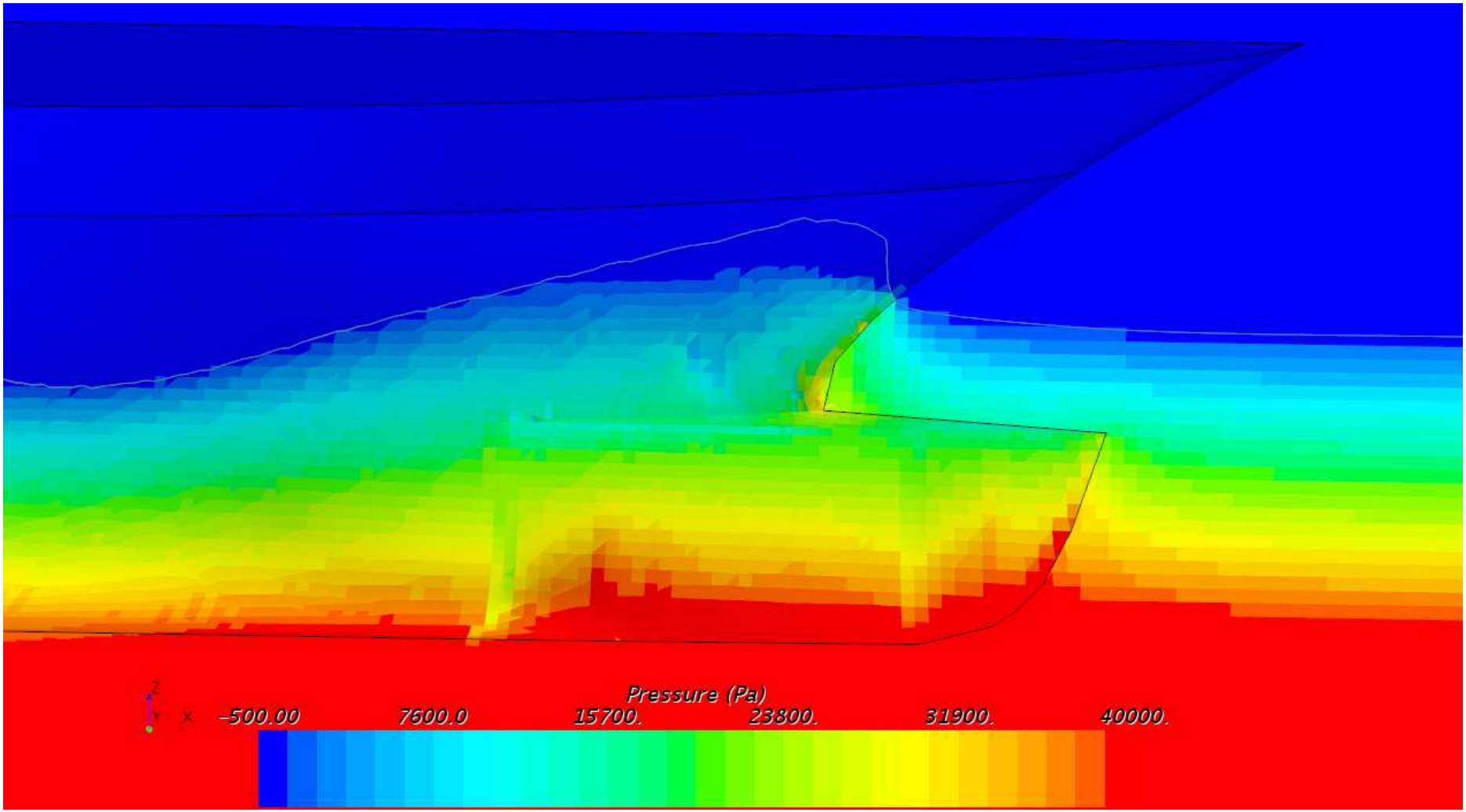

Fig.7.2.7. 15 knots

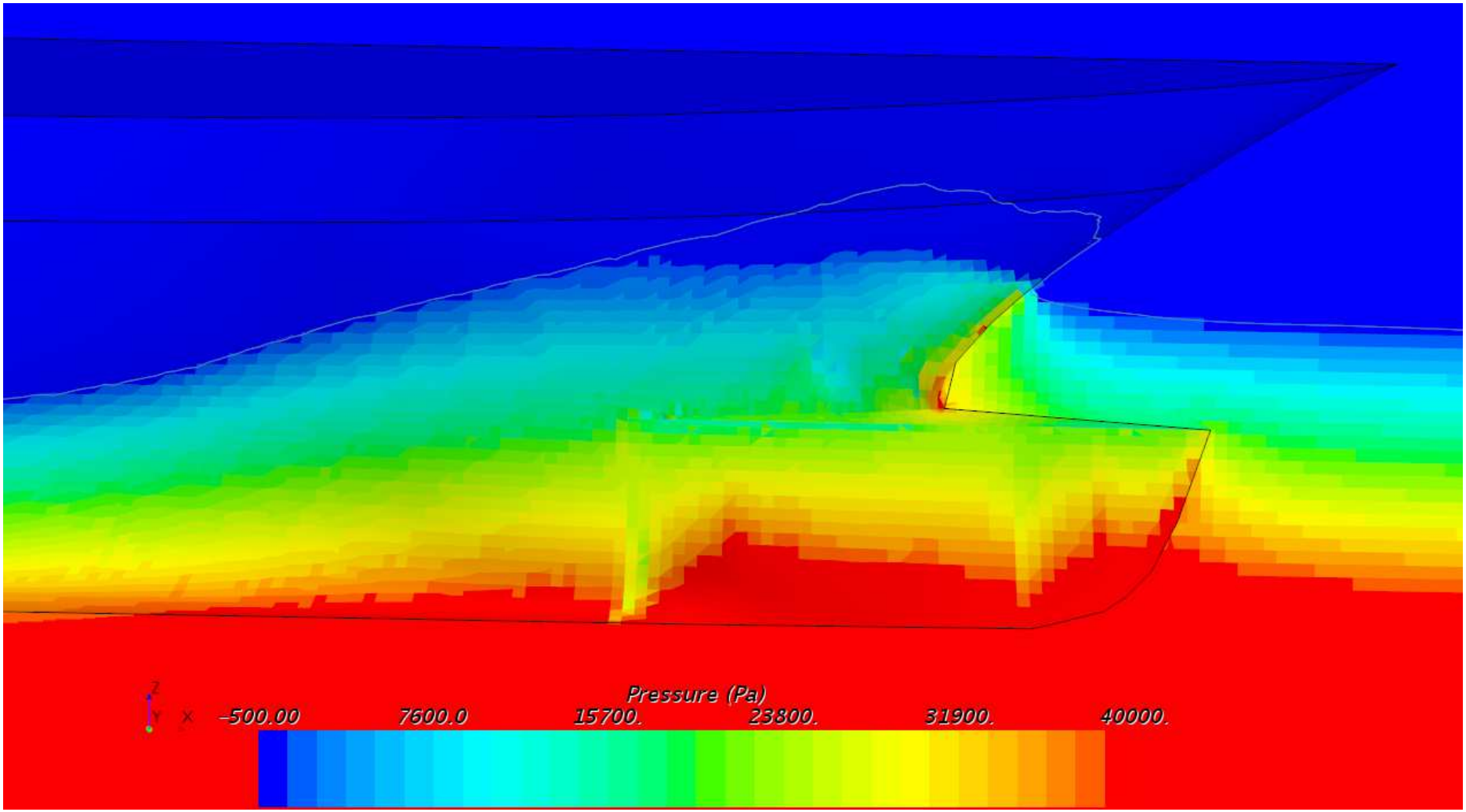

Fig.7.2.8. 17 knots

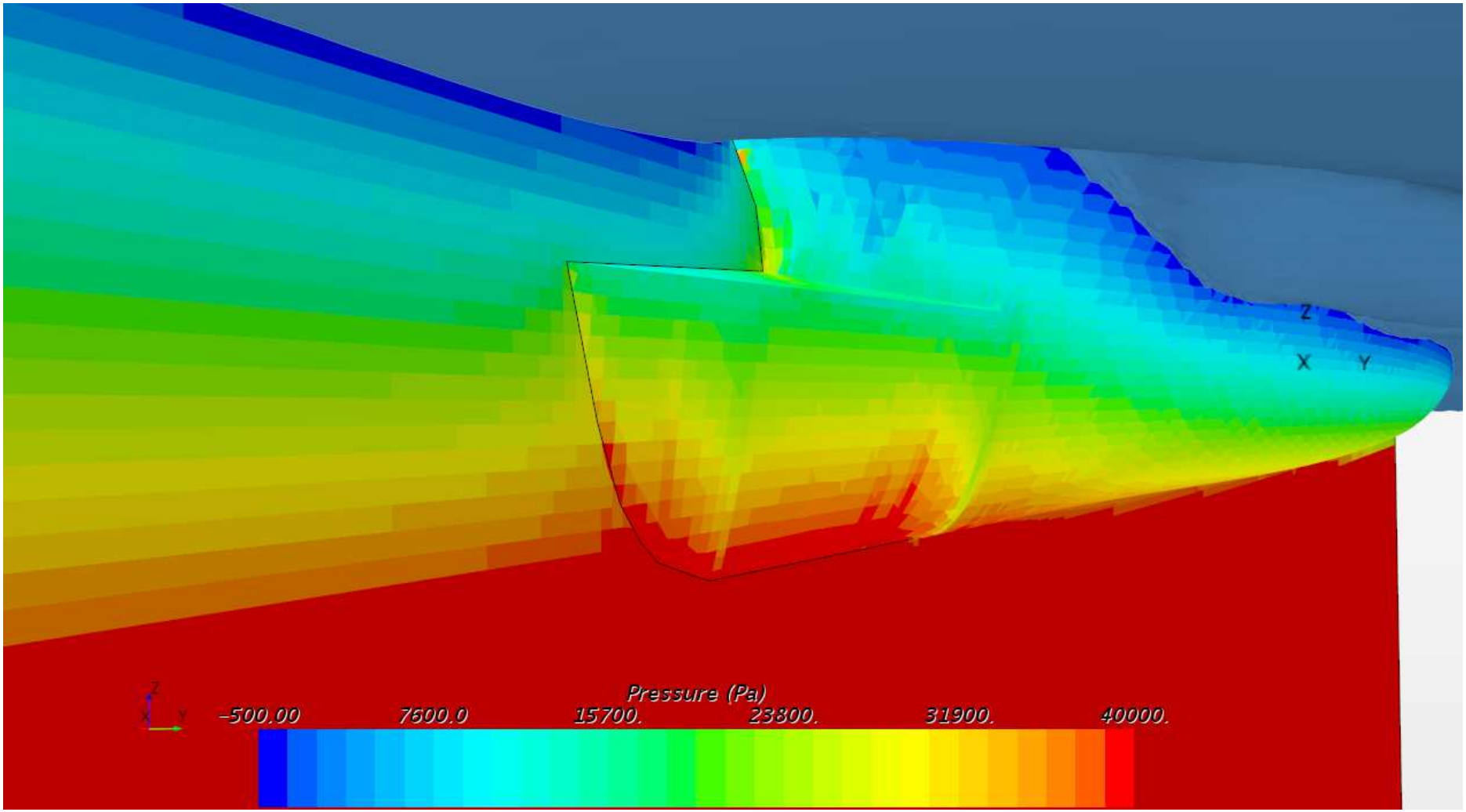

Fig.7.2.9. Bow part, 14 knots

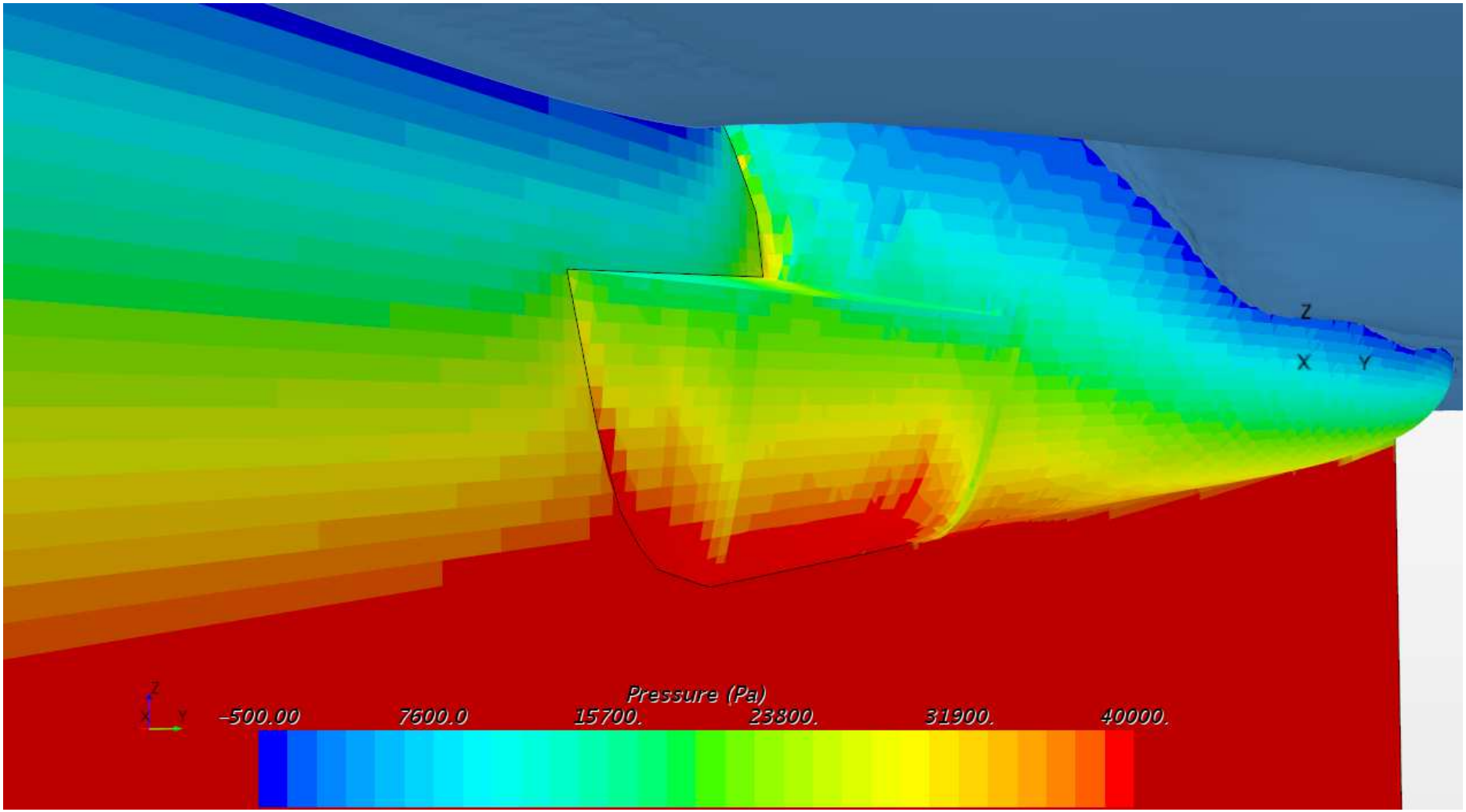

Fig.7.2.10. Bow part, 15 knots

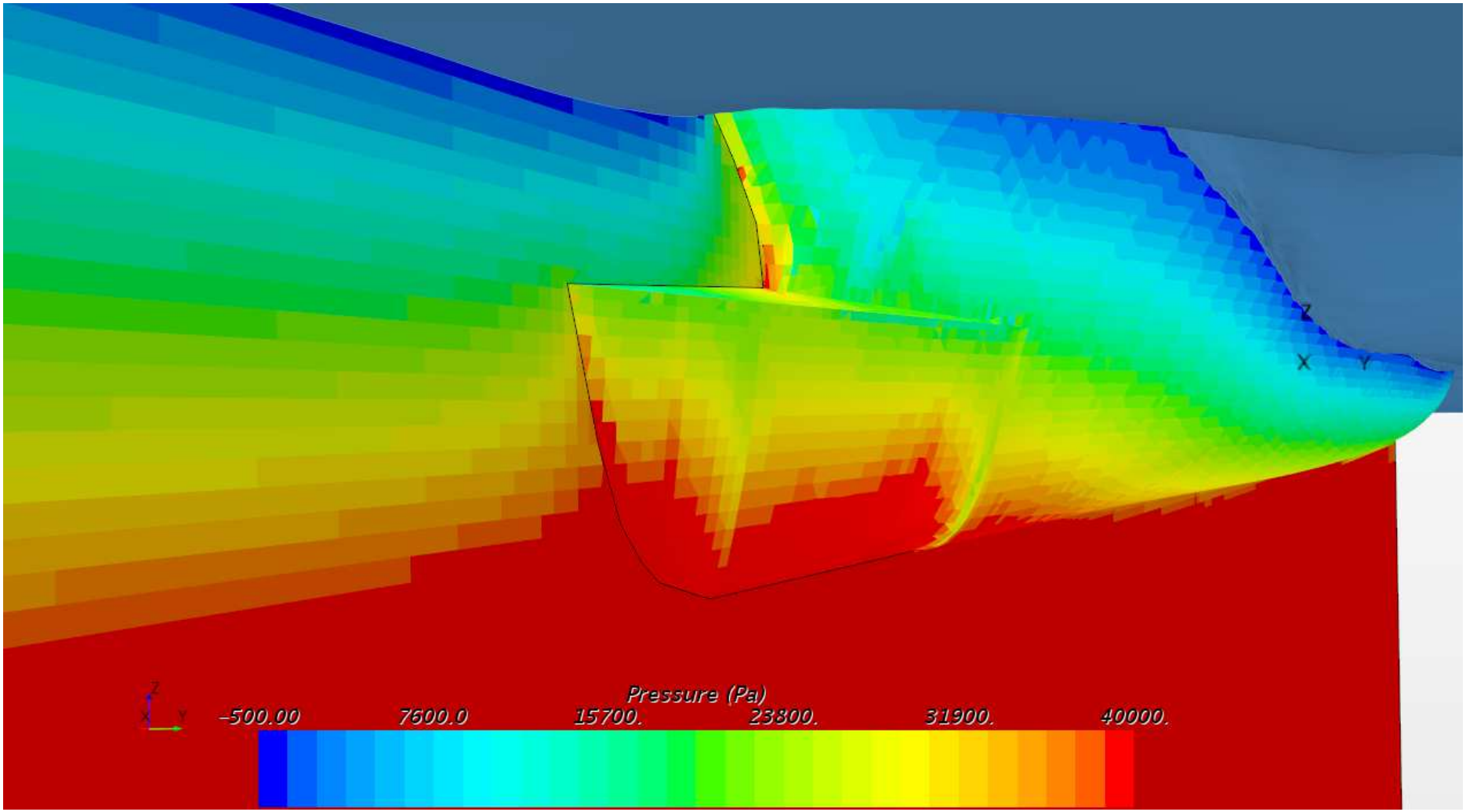

Fig.7.2.11. Bow part, 17 knots

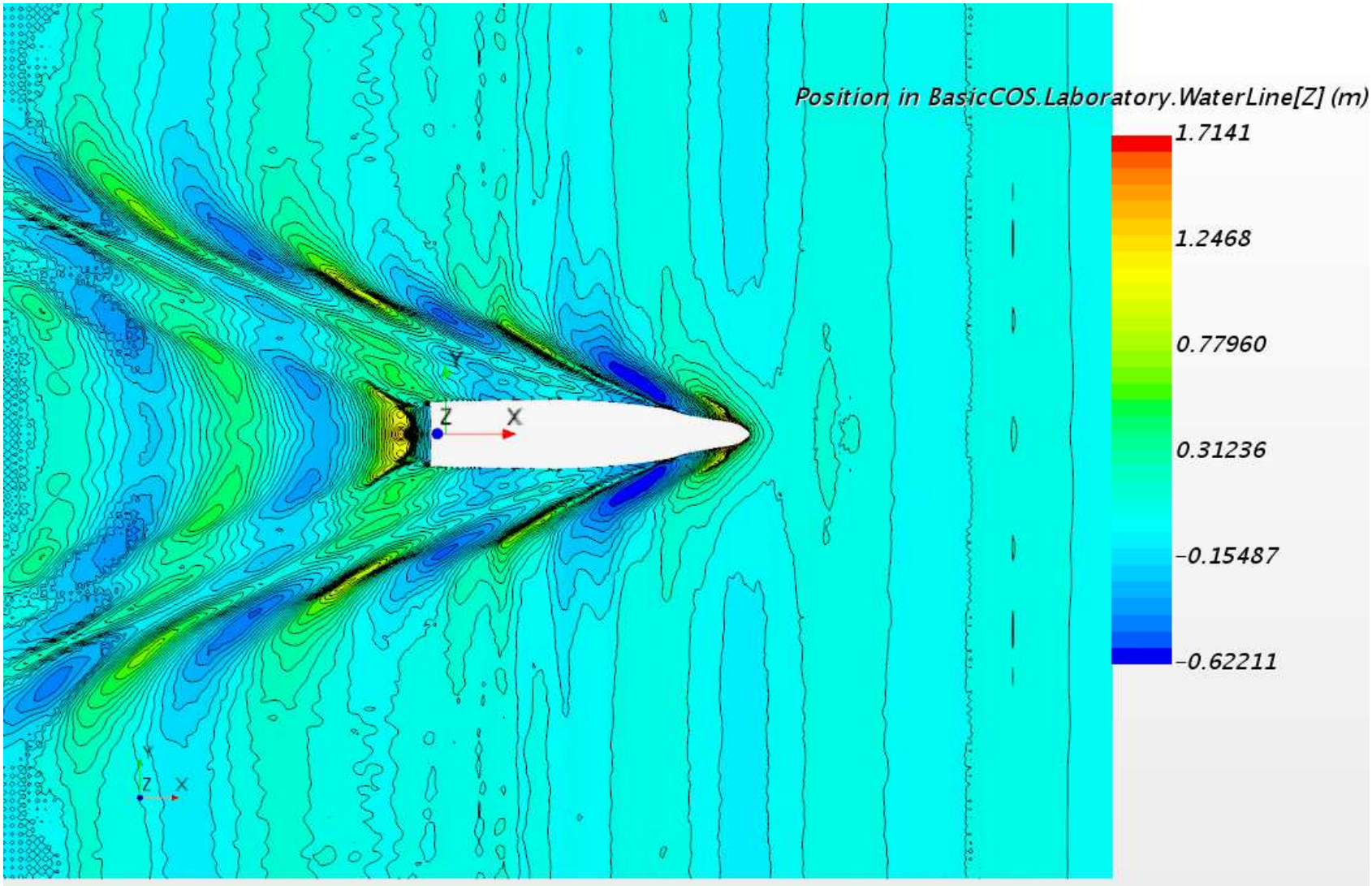

Fig.7.2.12. 14 knots

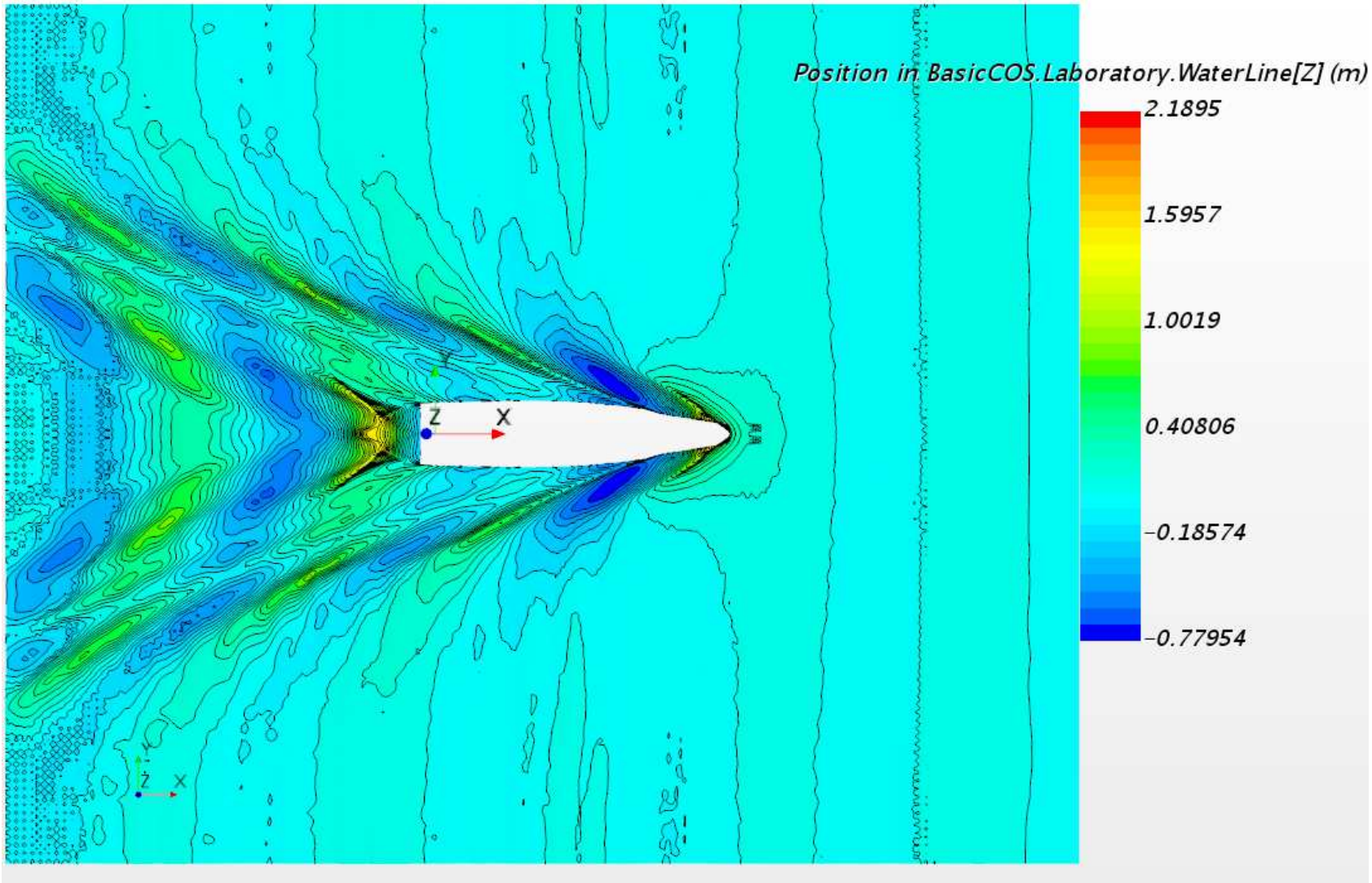

Fig.7.2.13. 15 knots

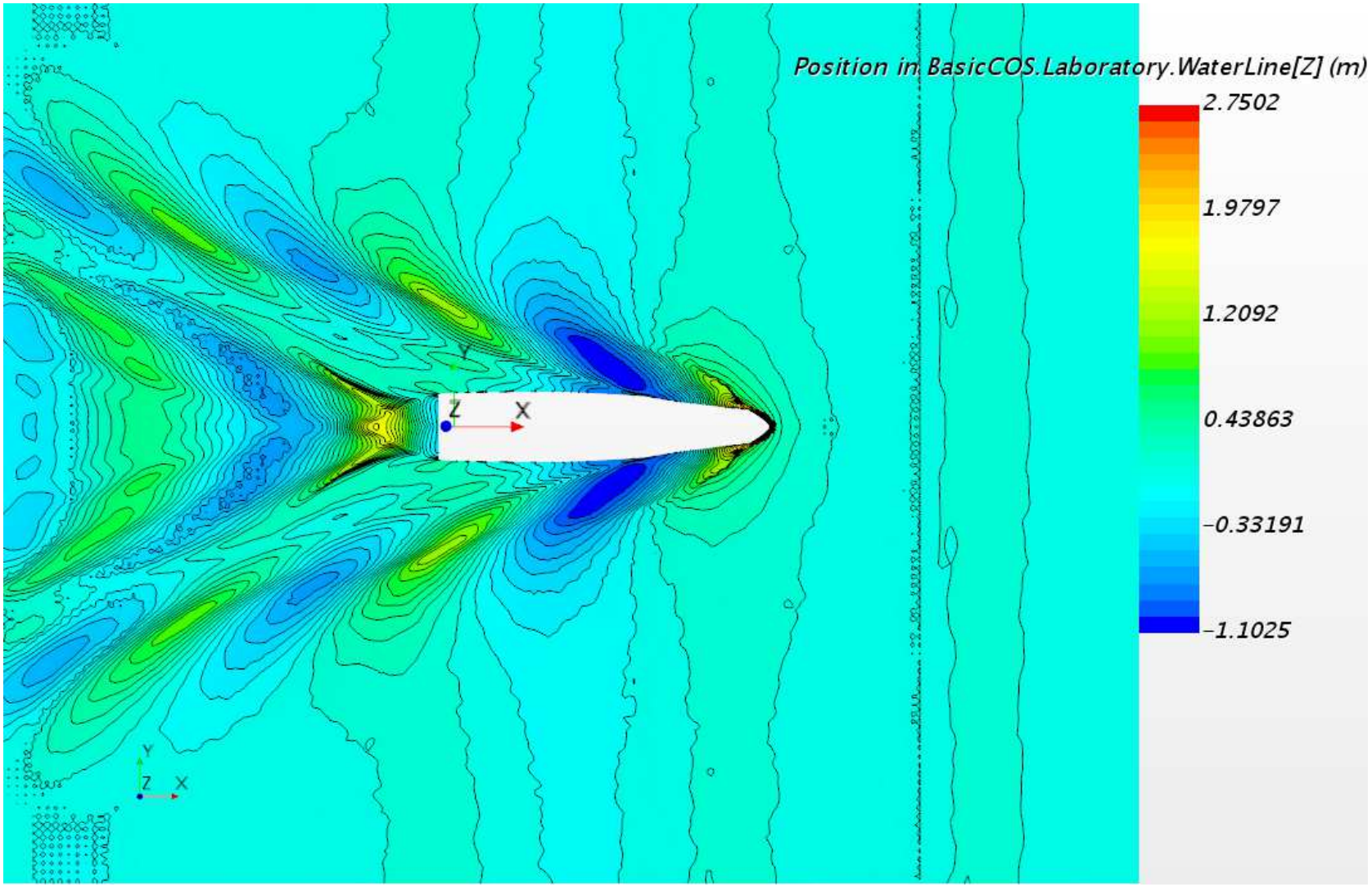

Fig.7.2.14. 17 knots

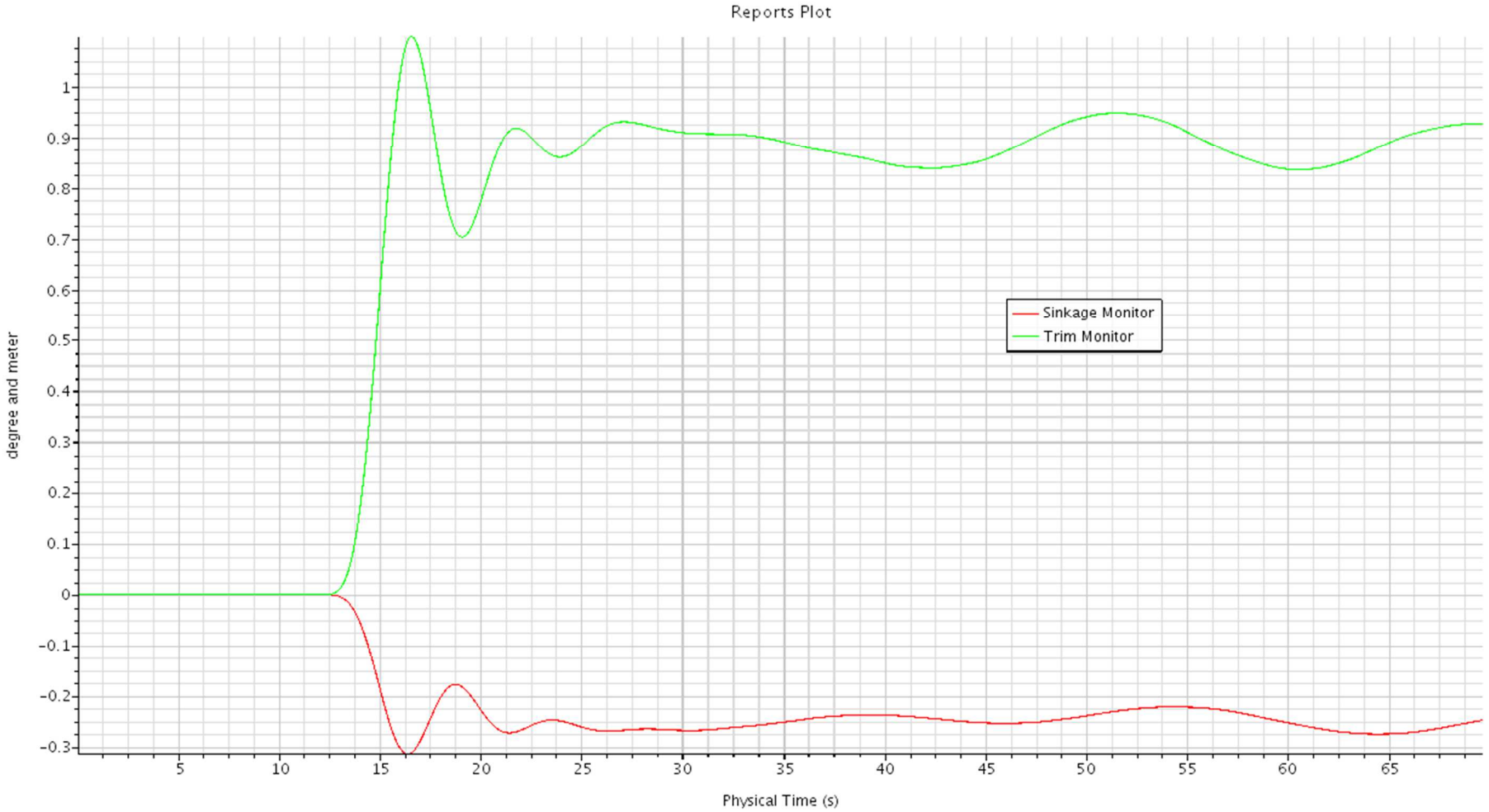

Fig.7.2.15. Motion plot, 14 knots

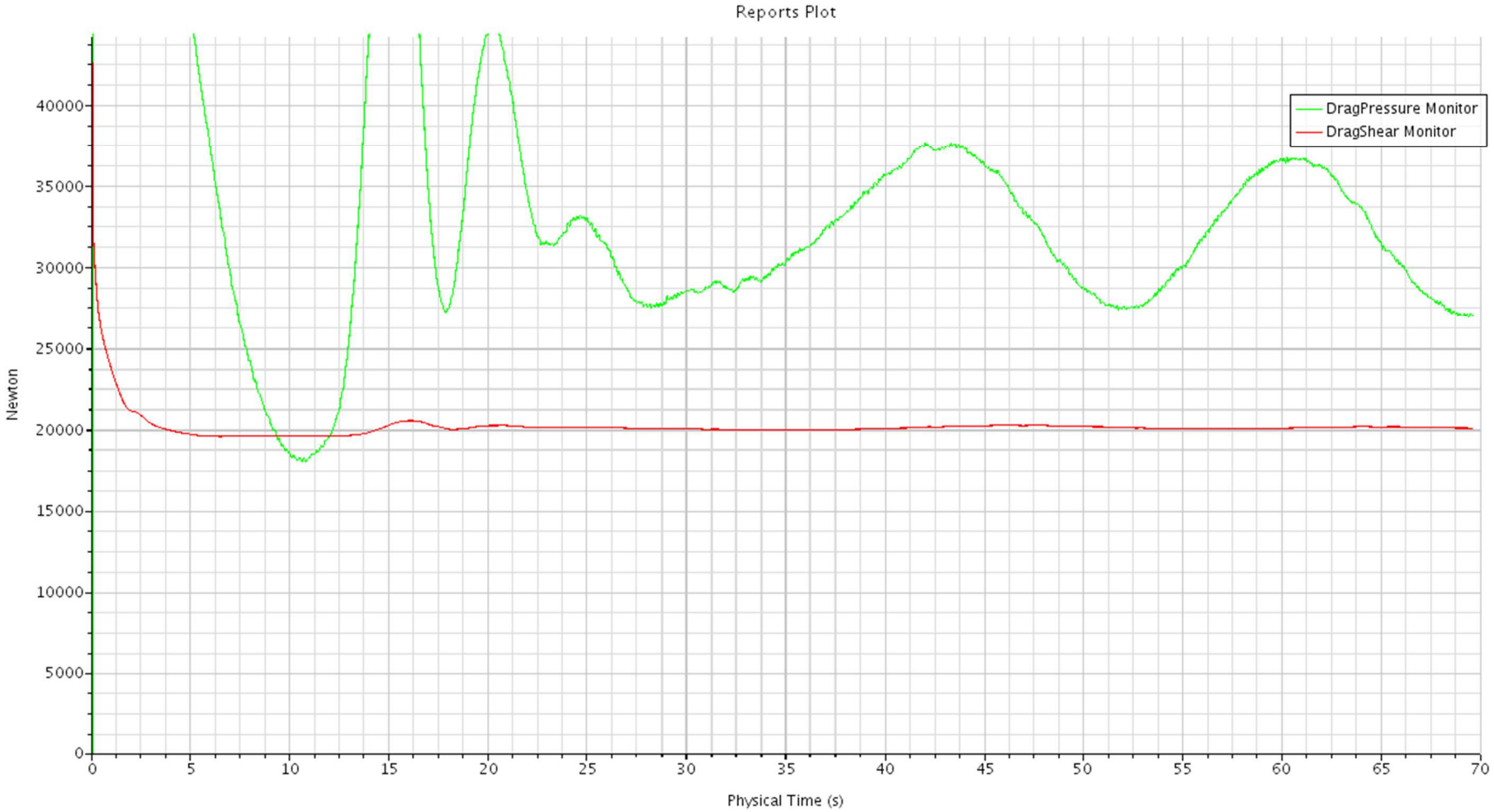

Fig.7.2.16. Resistance plot, frictional drag and pressure drag, 14 knots

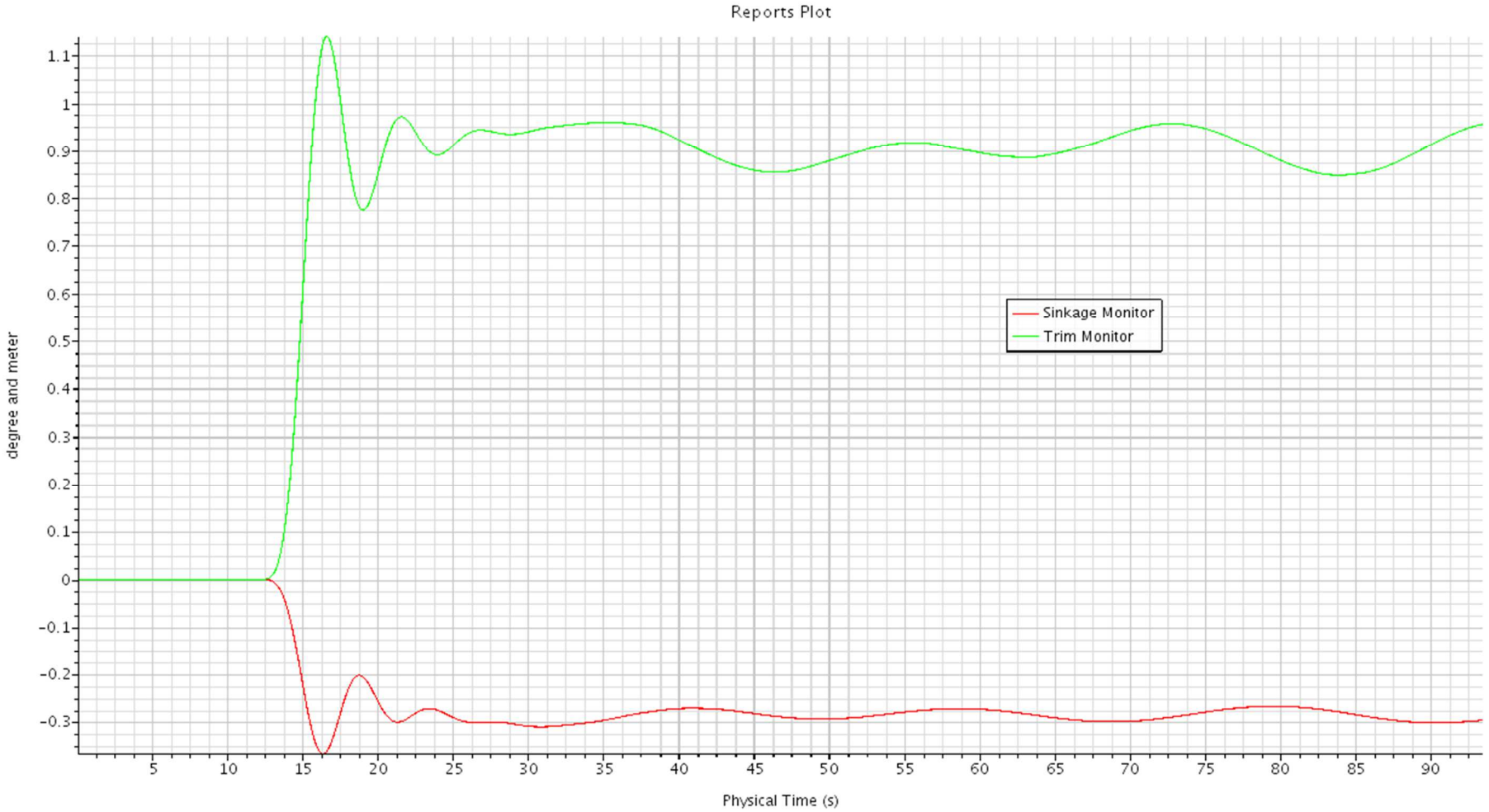

Fig.7.2.17. Motion plot, 15 knots

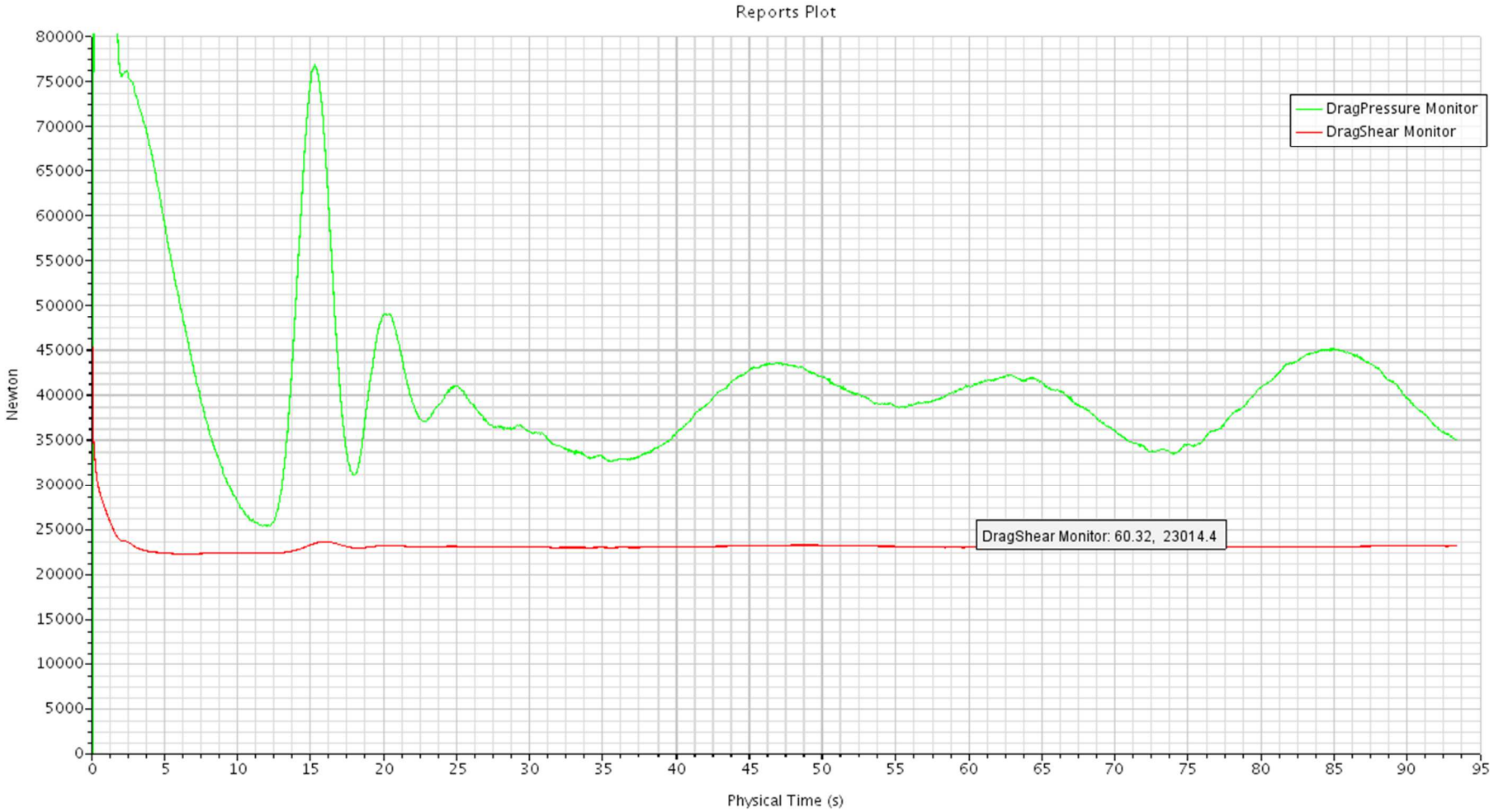

Fig.7.2.18. Resistance plot, frictional drag and pressure drag, 15 knots

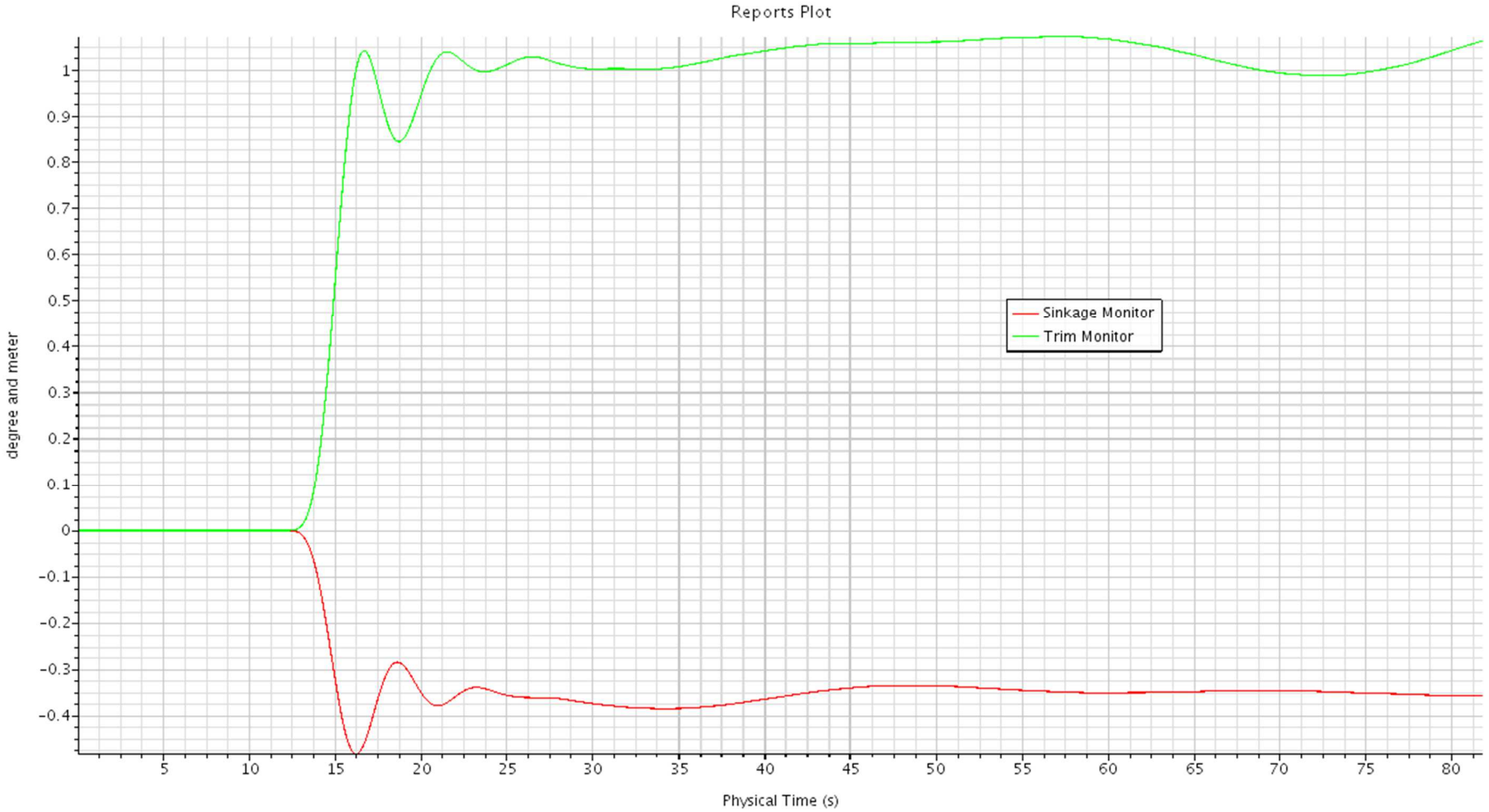

Fig.7.2.19. Motion plot, 17 knots

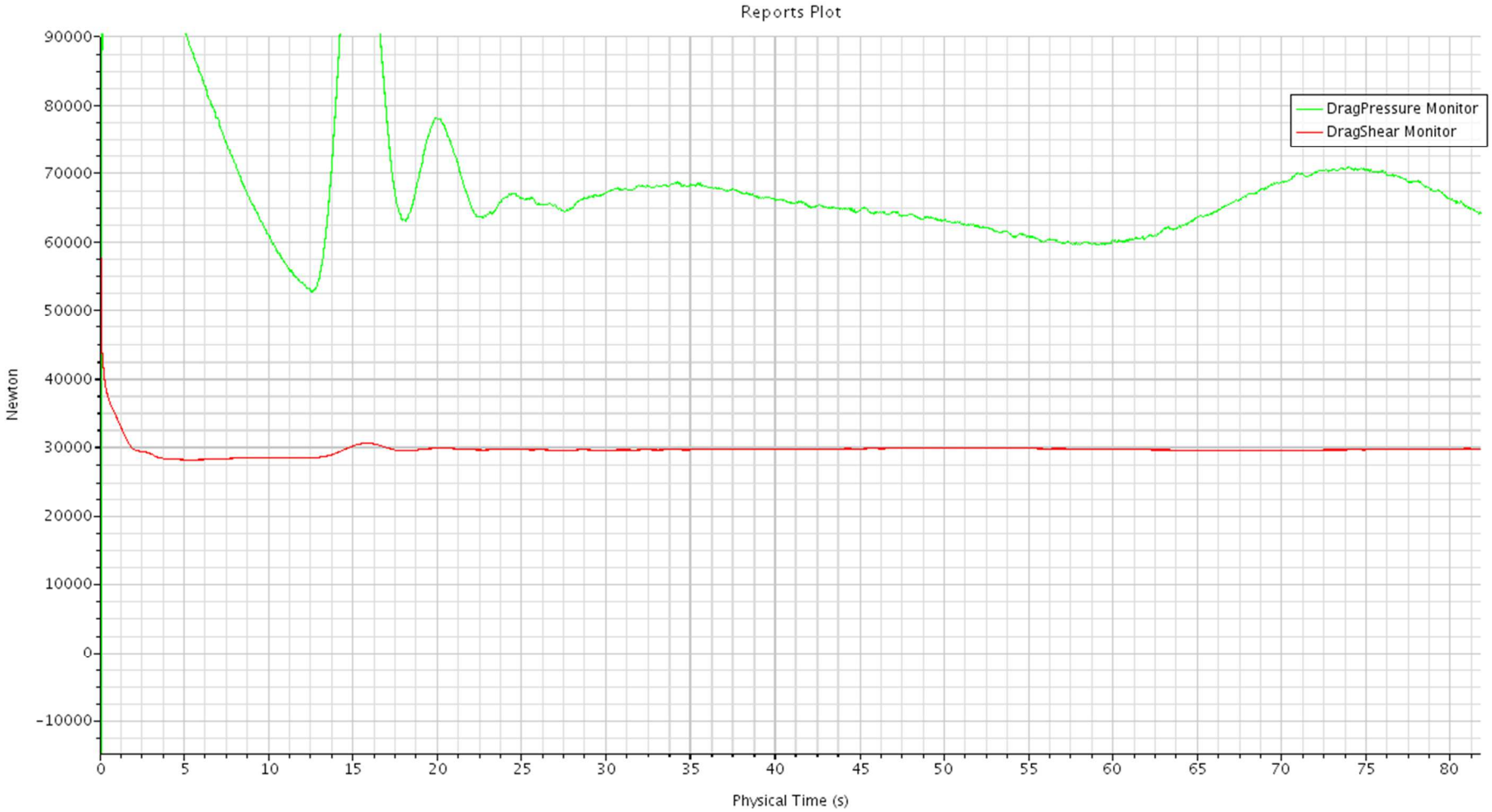

Fig.7.2.20. Resistance plot, frictional drag and pressure drag, 17 knots

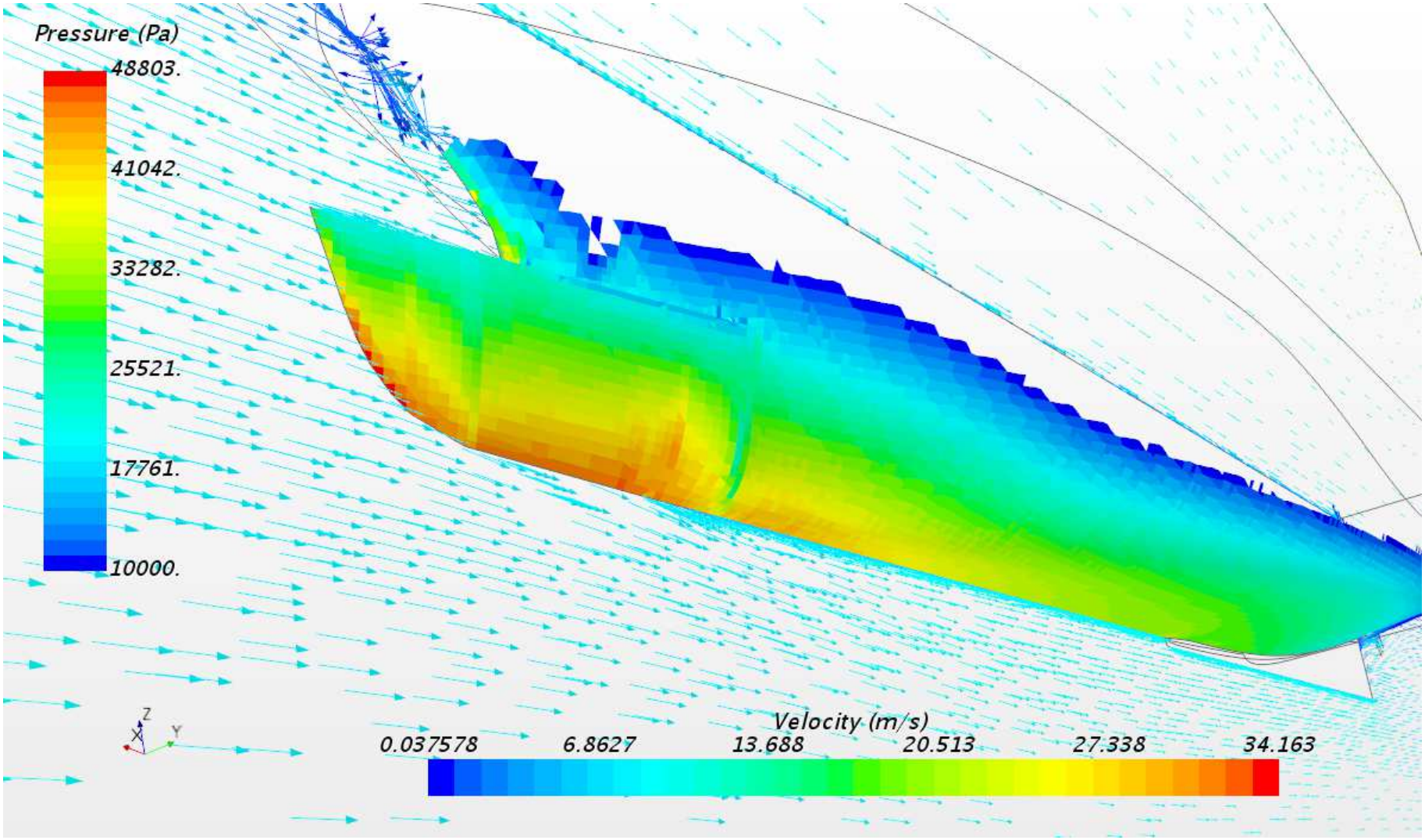

Fig.7.2.21. Pressure and velocity vector scene, 17 knots

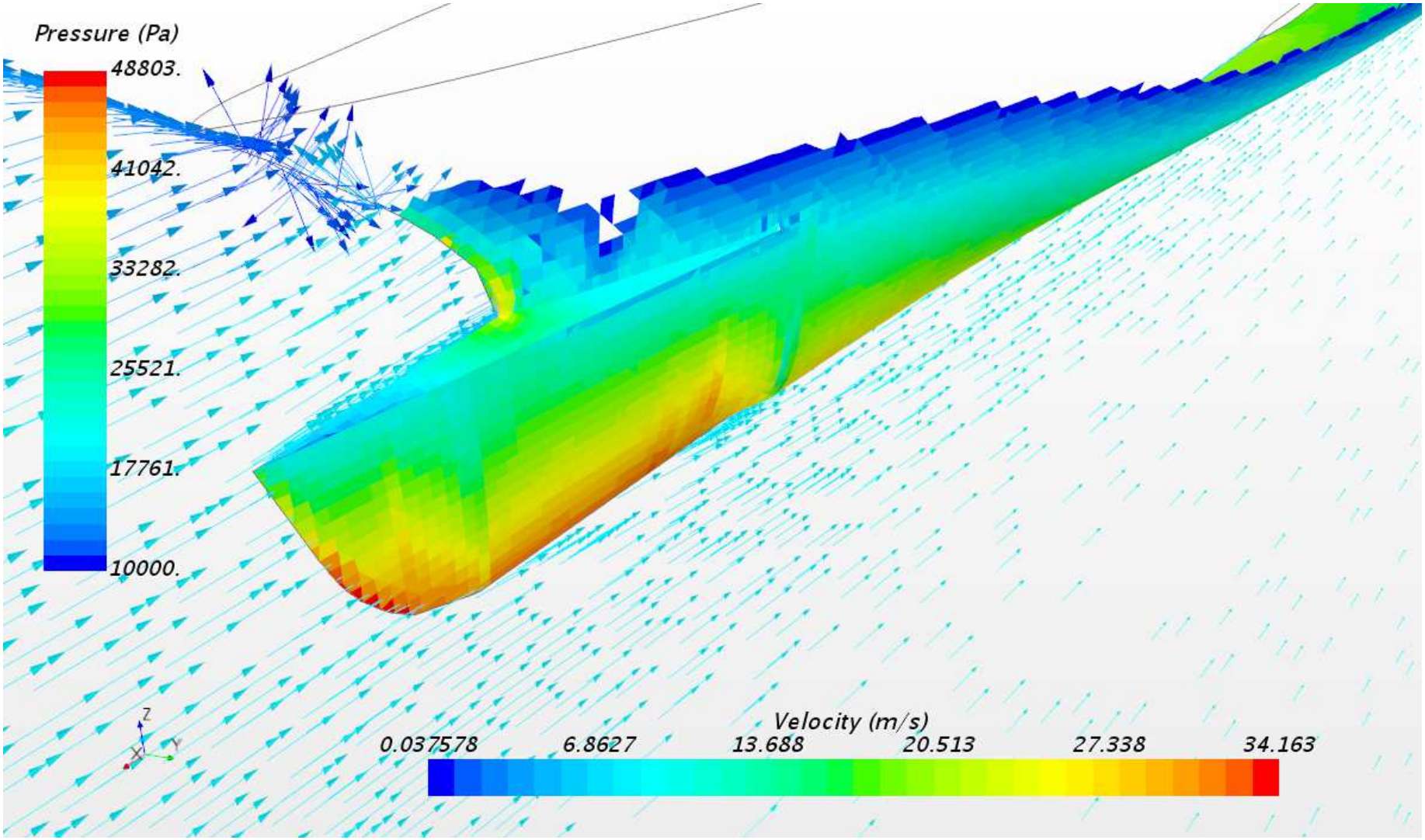

Fig.7.2.22. Pressure and velocity vector scene, 17 knots

7.3. Blade bow, 2nd variant

The next variant of the blade bow has bigger top angle and lower placed vertex (figures 7.3.1-7.3.3):

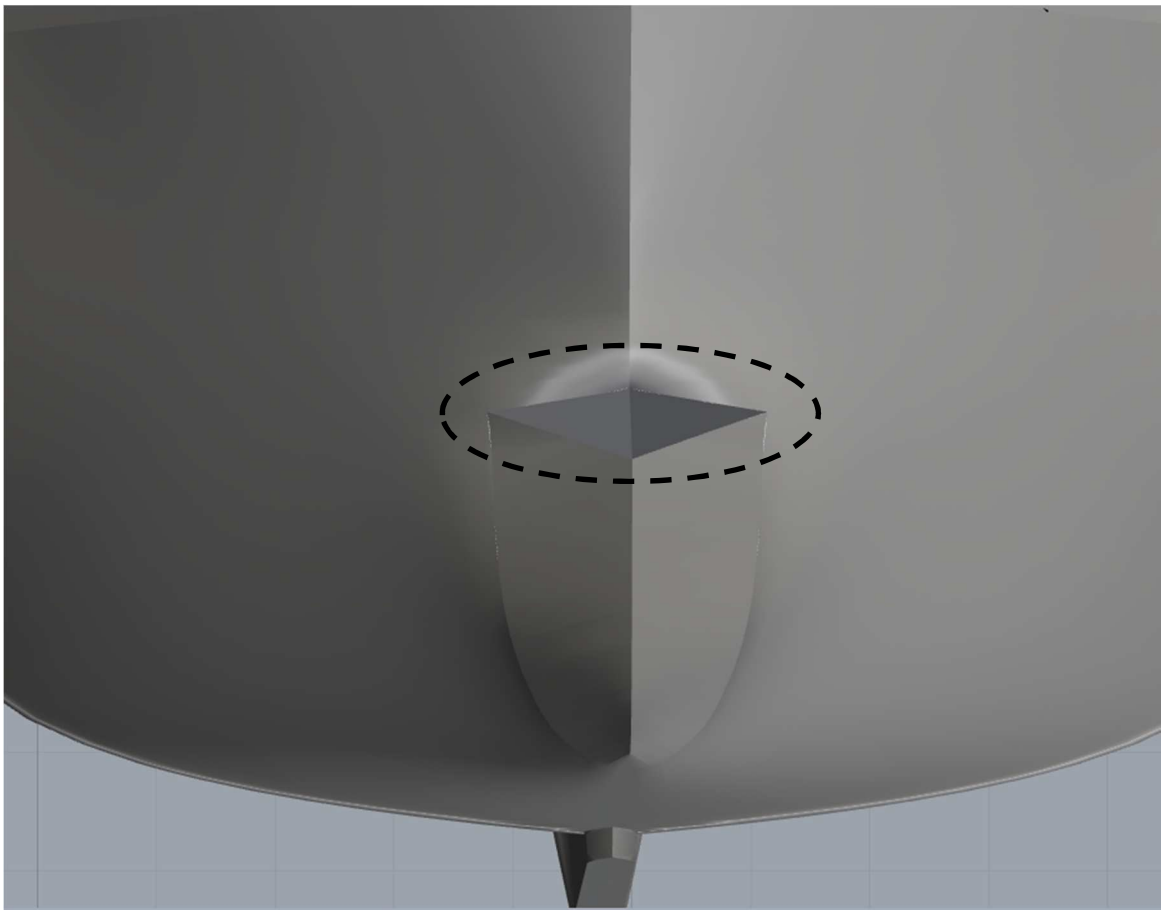

Fig.7.3.1

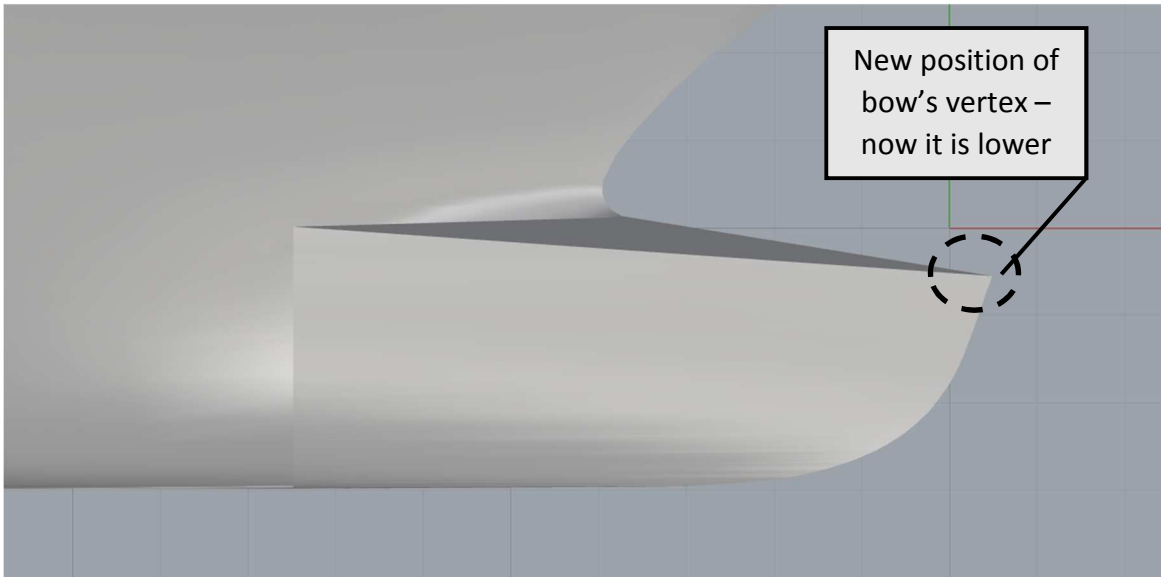

Fig.7.3.1. Now the top edge profile has about 9.5 degrees from horizontal plane. Will the top surface concentrate more dynamic pressure?

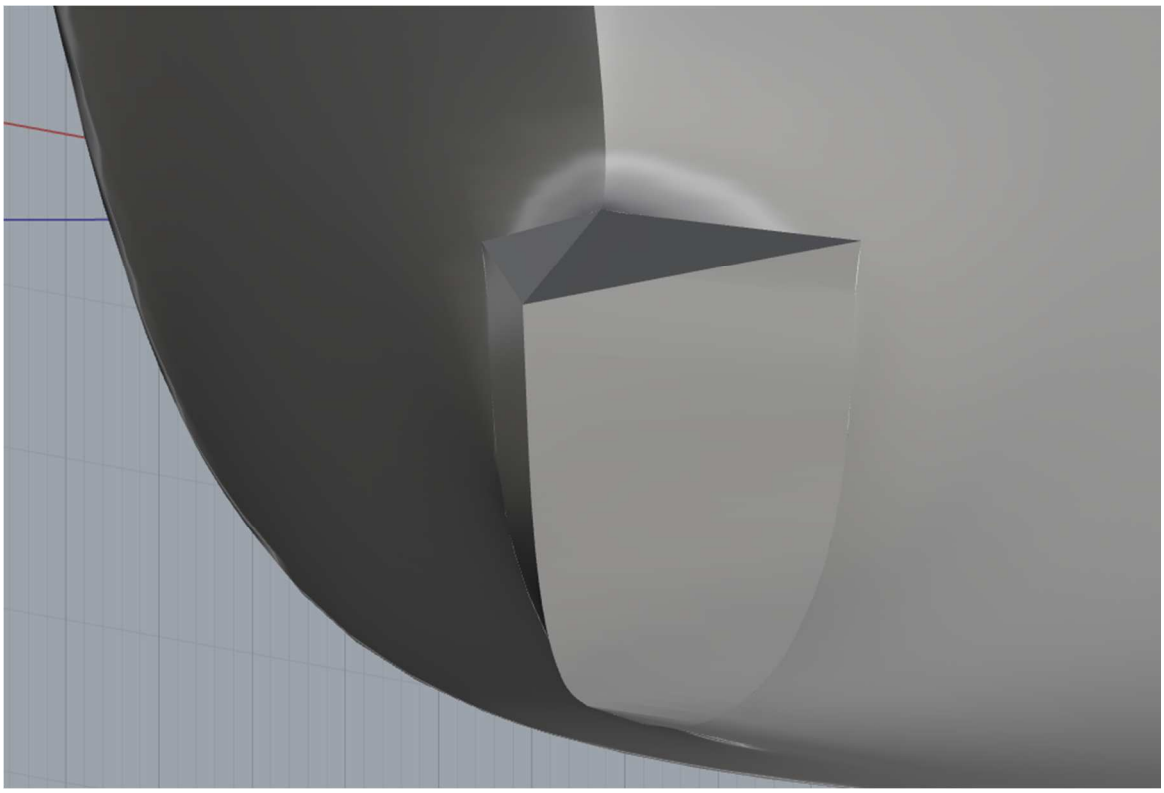

Fig.7.3.2.

The working speeds were chosen only for 15 and 17 knots, because lack of available time. However, these speeds are more interesting for us now because of considering them as often in yacht's cruising range.

Table 7

Number of cells:	Velocity, kn	Shear drag, kN	Pressure drag, kPa	Sinkage, m	Trim, deg
1636962	14	---	---	---	---
Base size 7.5 m	15	22.80722	38.24284	-0.27947	0.873208
	17	29.12652	63.72949	-0.34743	1.002303

Table 8

2nd BLADE BOW TO INITIAL BULBOUS BOW, %				
Velocity, kn	Shear drag, kN	Pressure drag, kPa	Sinkage, m	Trim, deg
14	---	---	---	---
15	100.42	124.94	129.10	168.14
17	99.33	116.39	118.23	166.29

Comparing the tables 6 and 8, it could be noted that the second variant of the “blade” has better performance than the first one. The shear drag values in this case are almost the same with the results for the initial bow. Pressure drag on 17 knots also less. Trim and sinkage differ from the results for the first “blade” being closer to the motions when aiming the initial bulb. The trim angle and sinkage had been reduced.

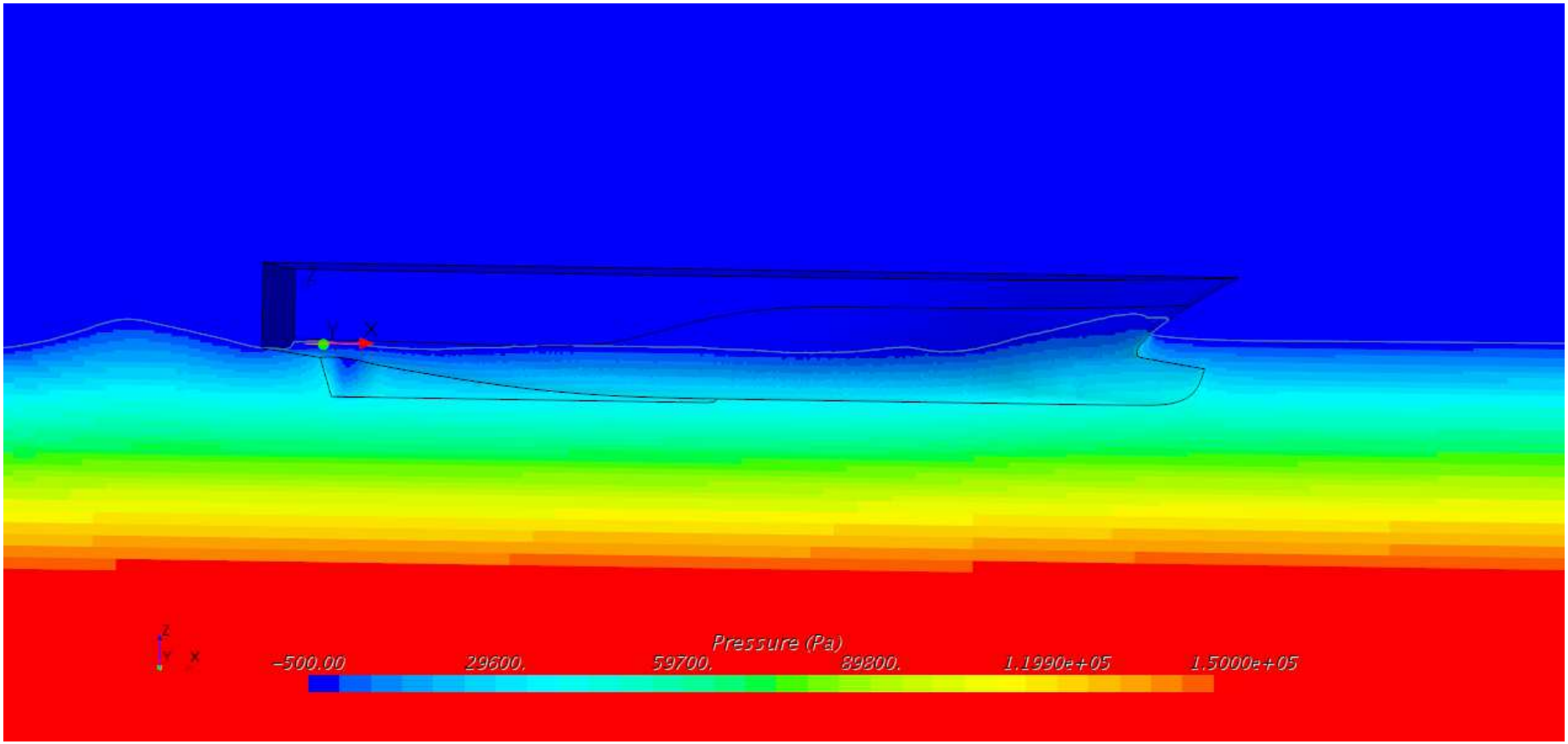

Fig.7.3.3. 15 knots

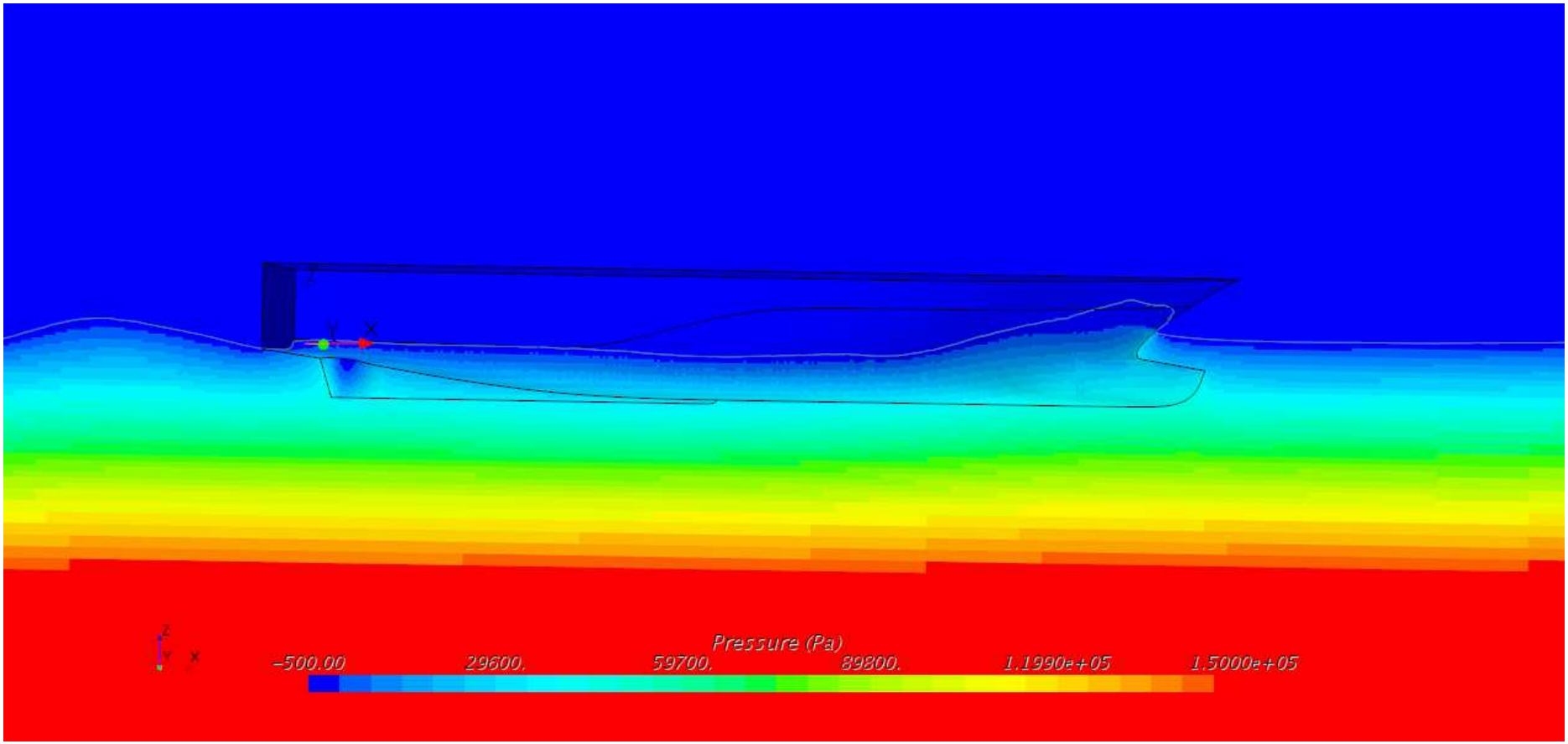

Fig.7.3.4. 17 knots

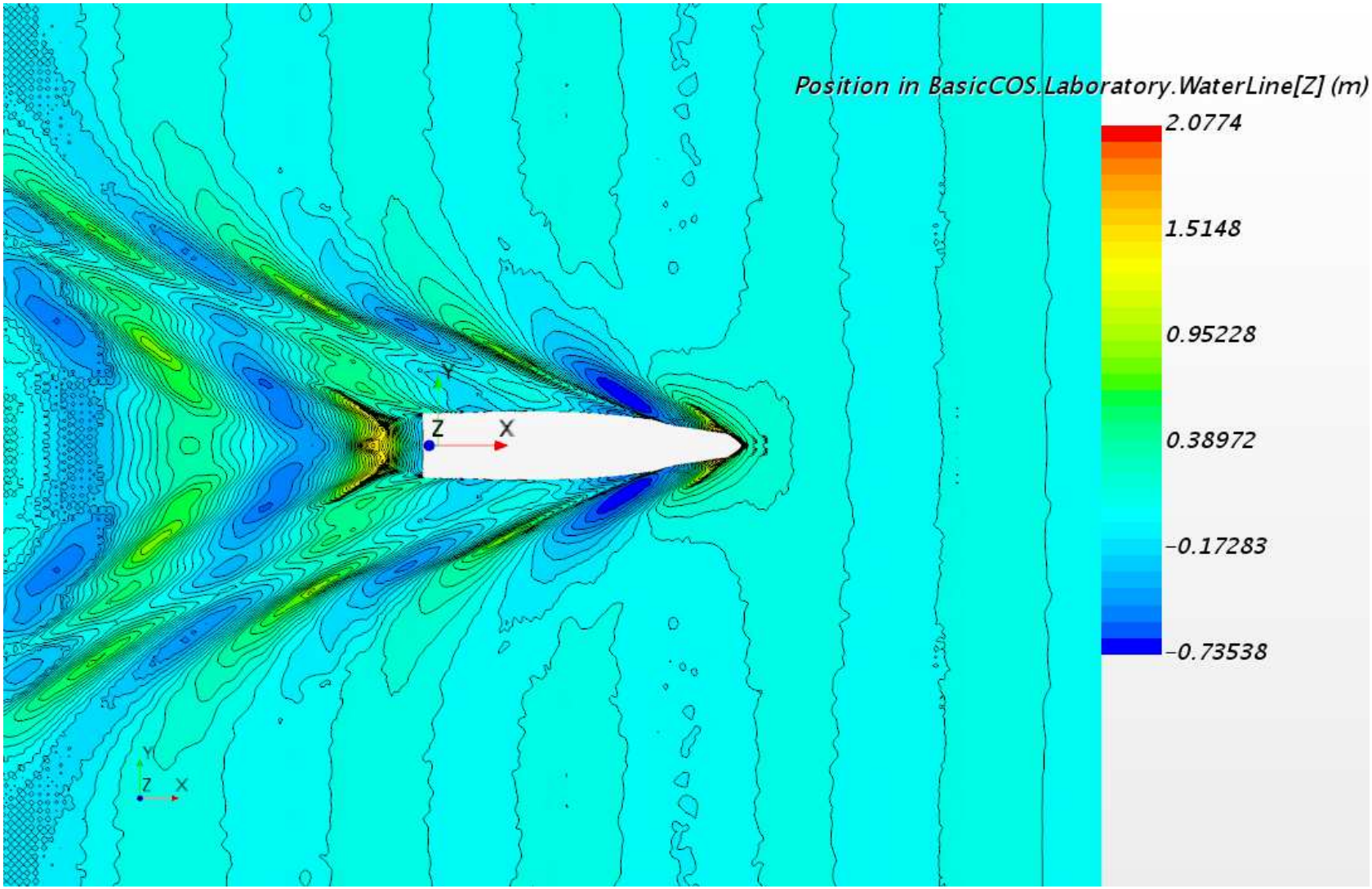

Fig.7.3.5. 15 knots

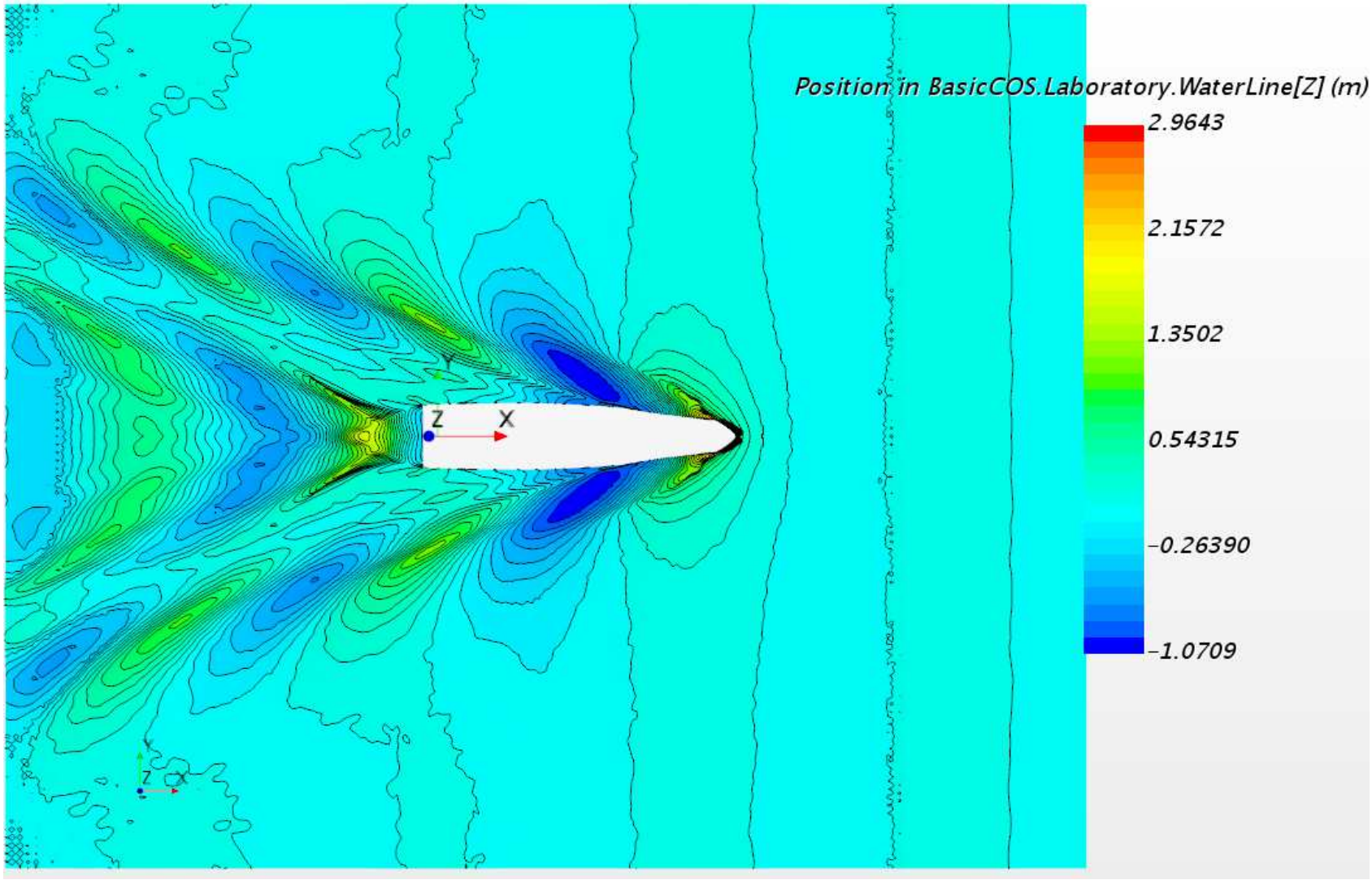

Fig.7.3.6. 17 knots

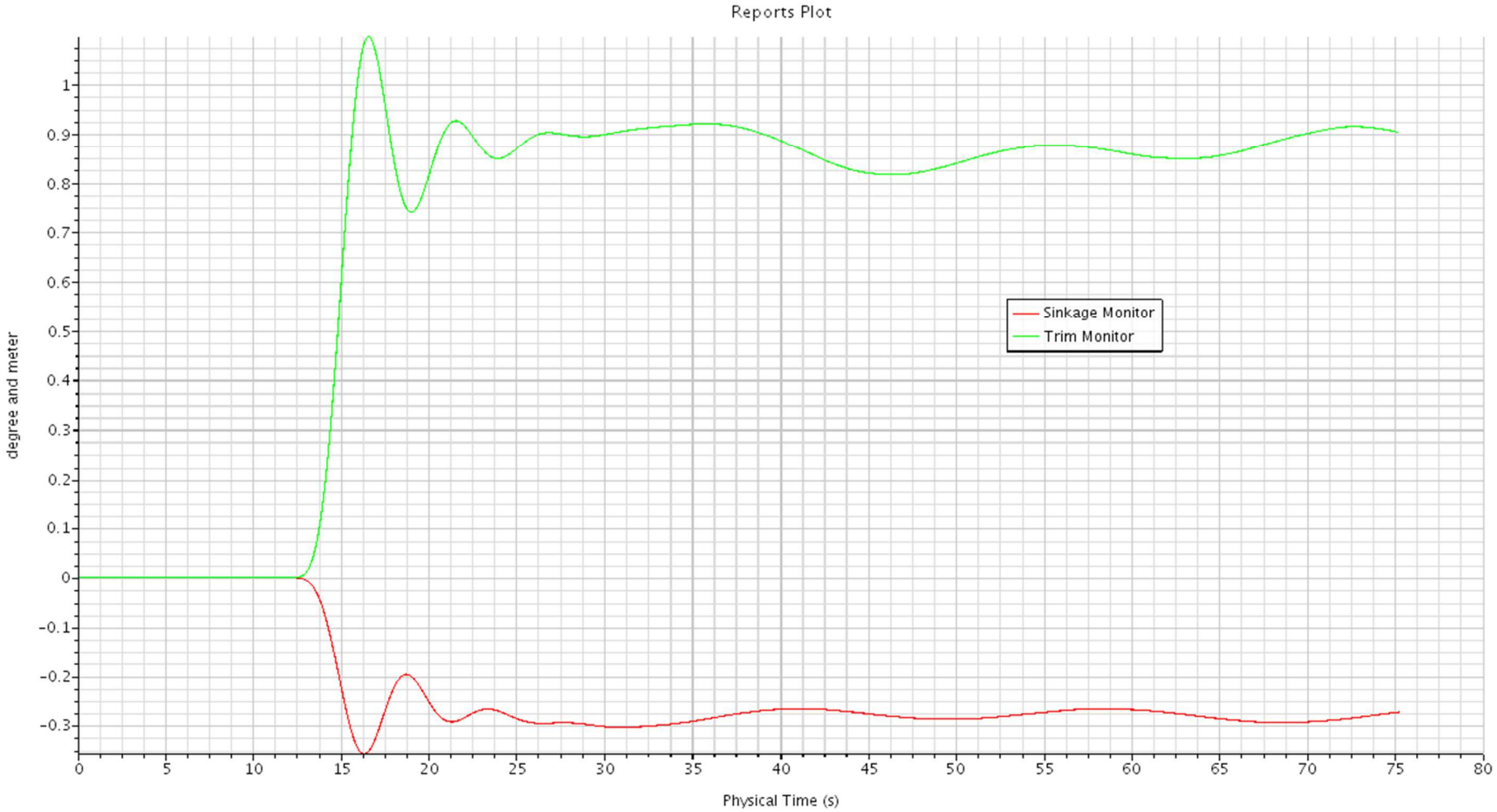

Fig.7.3.7. Motions plot, 15 knots

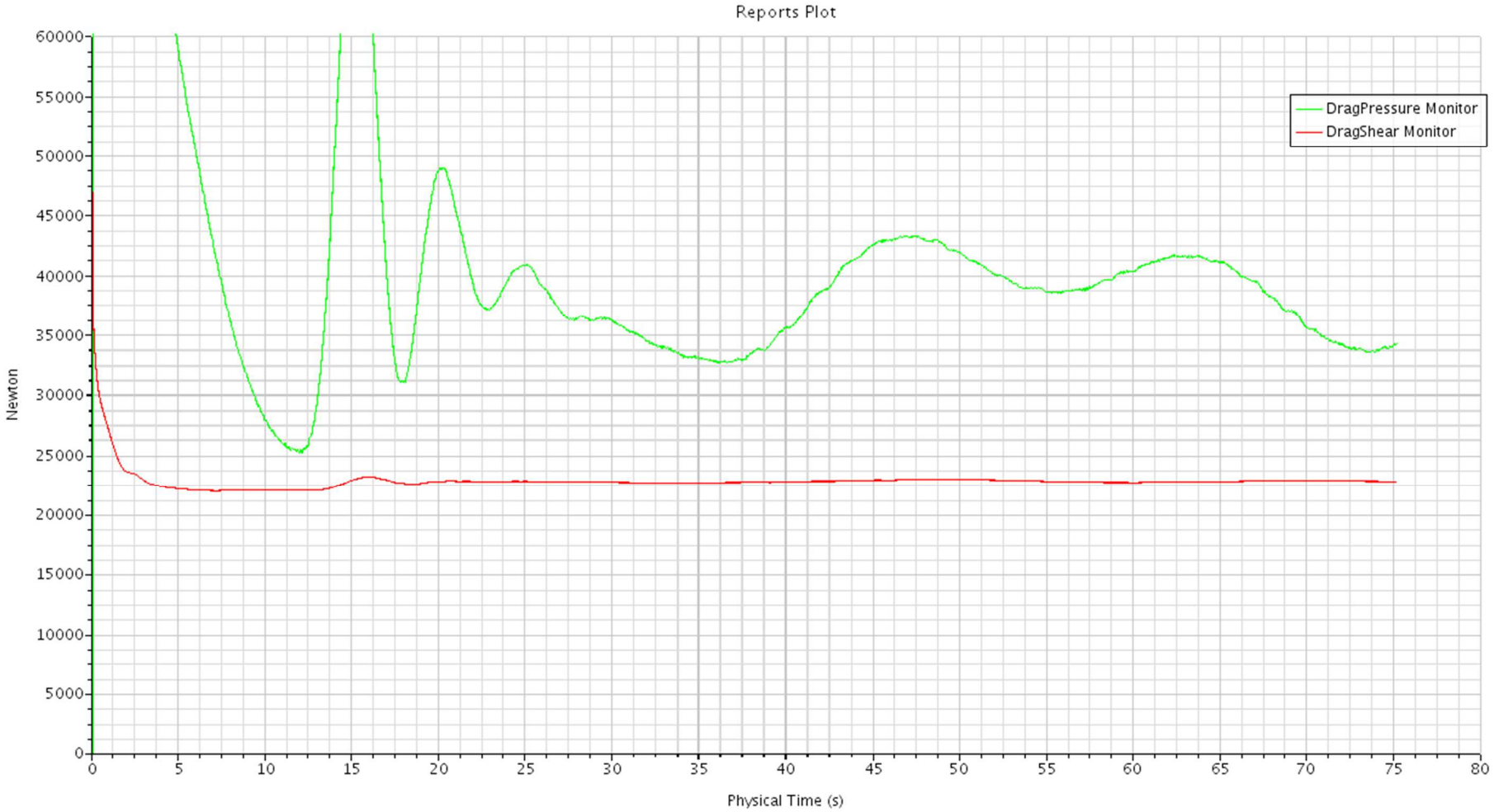

Fig.7.3.8. Pressure and friction drag plot, 15 knots

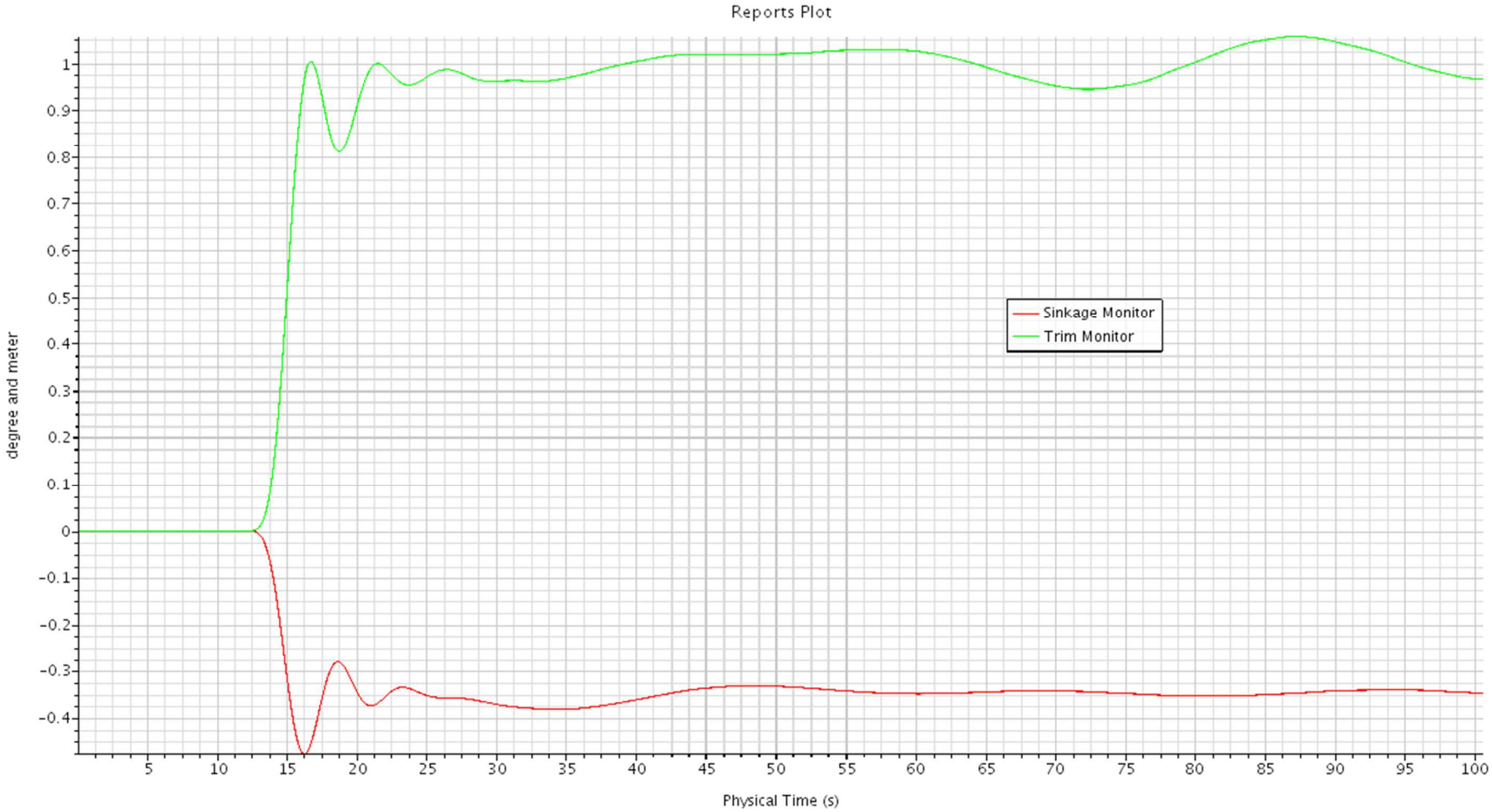

Fig.7.3.9. Motions plot, 17 knots

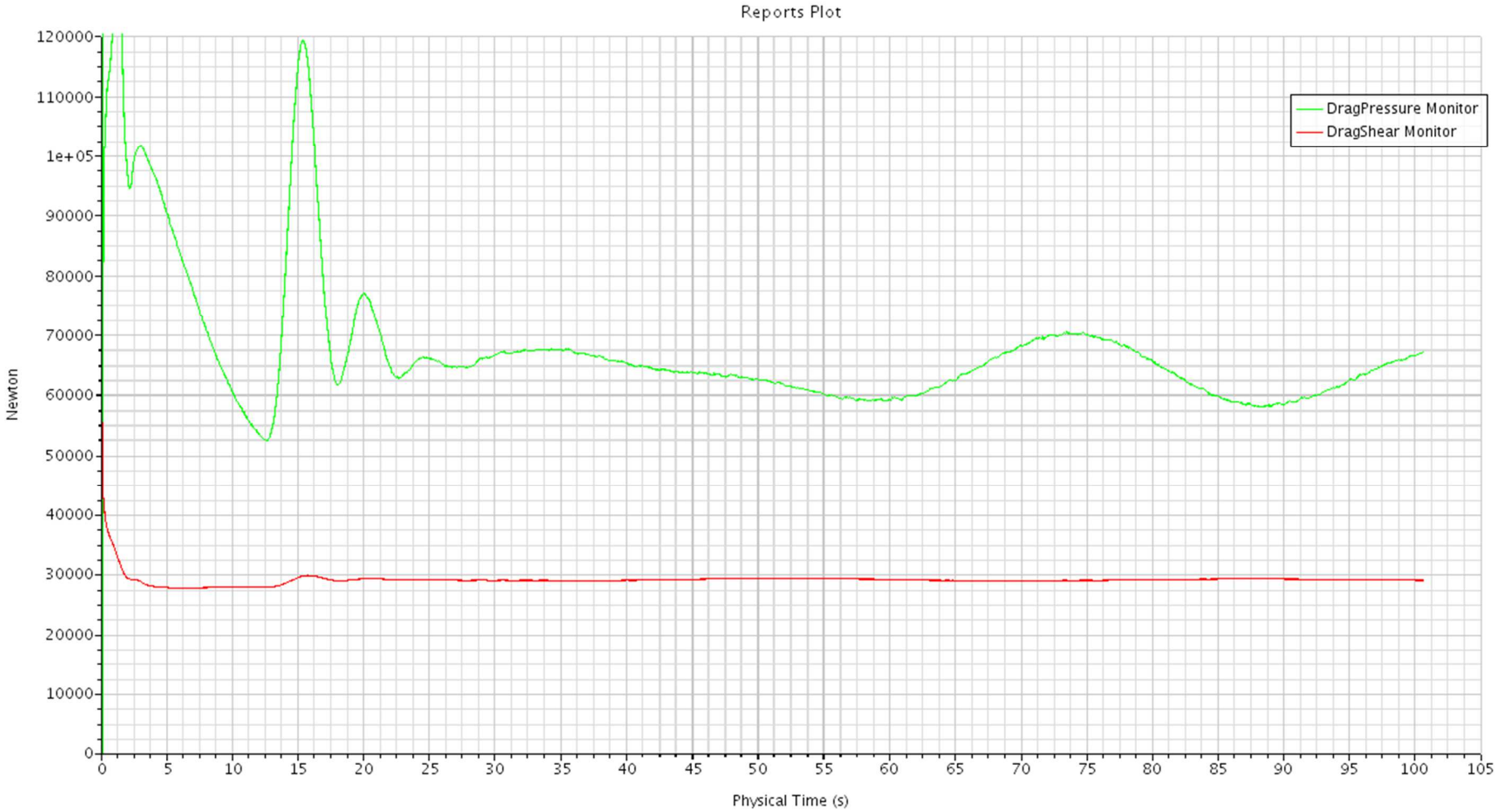

Fig.7.3.10. Pressure and friction drag plot, 17 knots

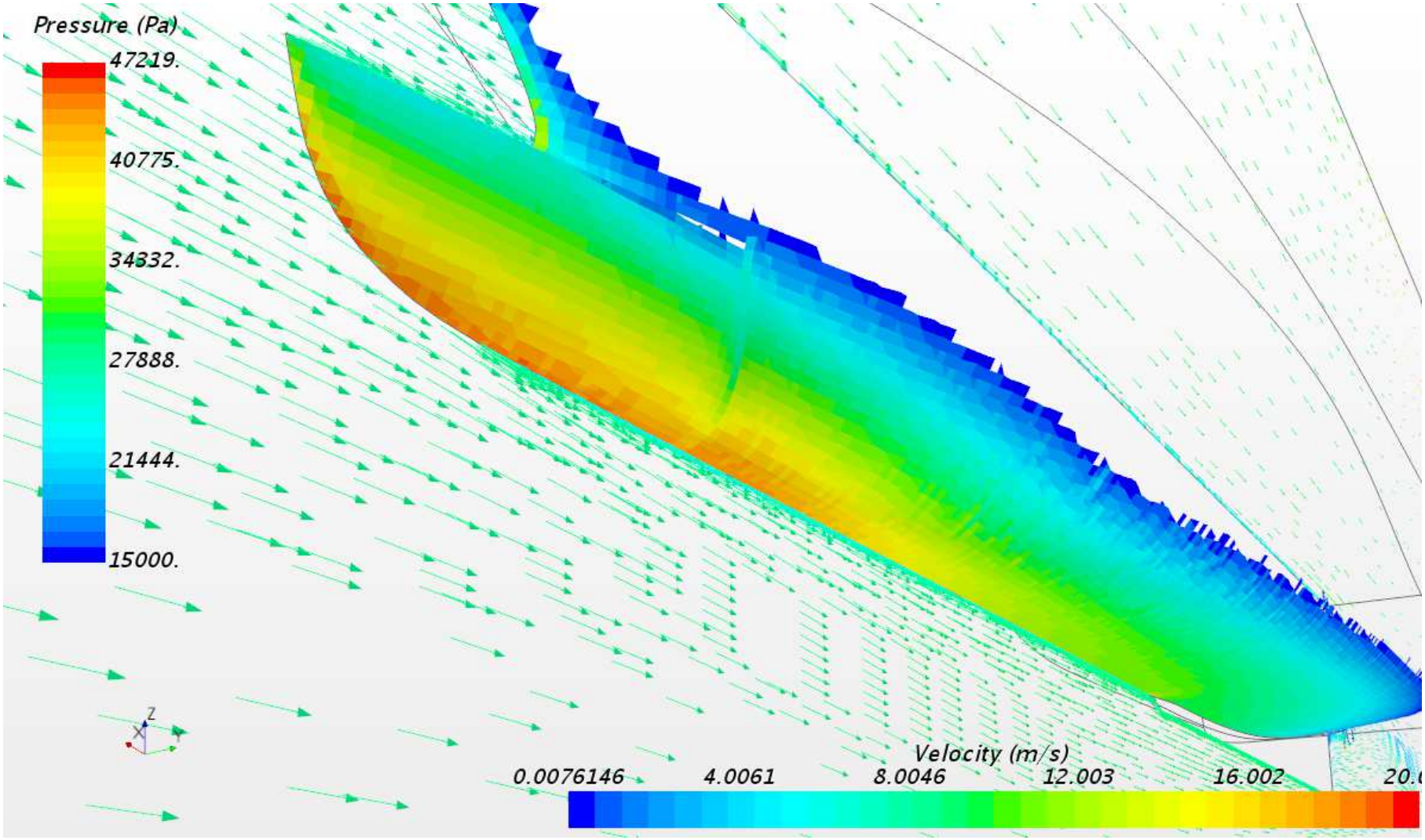

Fig.7.3.11. Pressure and velocity vector scene, 17 knots

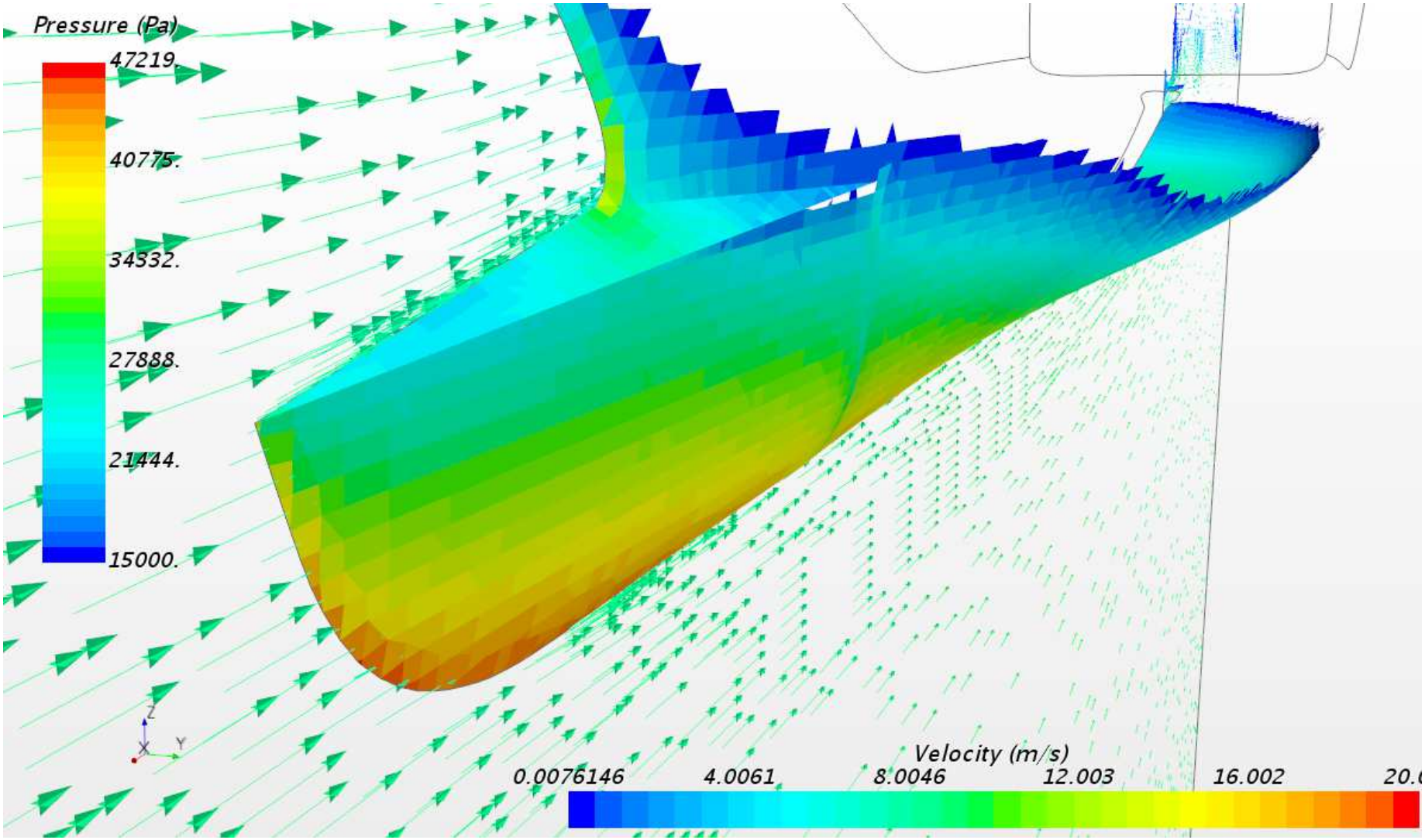

Fig.7.3.11. Pressure and velocity vector scene, 17 knots

CONCLUSION

The results for the new bows shows that the question of application of the blade bow's concept must be researched deeply, since the change of the only one feature – blade's top surface inclination – may sensibly change the values of the resistance and seakeeping behavior of the ship.

The pressure drag increases much when switching from convenient bow to the blade one. But it was noticed, that the value of the pressure drag excess percentage decreases by 7-8% if the yacht's velocity increases. This fact must be noted.

Paying attention on the wave height produced by yacht in fore-part: the height has been increased by almost 30-40%. The blade bows did not function like the bulbous one crushing the incoming wave. In the test cases the initial water surface was flat, even having a velocity directed in oppositely to the ship, however, wave producing aspect should be noticed as well. Important changes to be noted:

1) Pressure drag decreases with speed increasing;
2) Friction drag does not changes much;
3) Trim and sinkage already may be much enough dependent of bow's only one feature has been modified.

The author suggests this problem to be referred to the problem of shape optimization for the first stage of future research. There are some more ideas for the new bow forms ready to be checked on the presented yacht hull without deforming the rest part of it different from the already changed bow part areas. The very first significant factor influencing the way of bow shape modification refers to production issues – 60 meters-long fully displacement yacht with convex shape lines is hard to be changed for the same way as it was done for Ilumen 28M and Benetti F-125 without having huge undefined yet effect on the main hull hydrodynamics.

The concept of blade bow is relatively new, a lot of potential benefits may be found after digging the subject deeper. Some of them already has shown themselves: for example, the trim and sinkage changing patterns depend on some particular features of the bow – good starting point for the parametrical design study.

Hence, the future research might be initiated should include, at least, parametrical design study and bow shape optimization works in order to clarify:

a) what minimum number of geometrical parameters of the blade bow may be modified in order to affect seakeeping patterns in a way needed;
b) optimization of the bow for different types of vessels using already defined parameters from the parametrical design study.

The work is recommended to be continued.

REFERENCES

1. Gemma Fottles, “Dominator Ilumen 28M taking shape in Italy”, web-article, 11th April 2016, electronic magazine “Superyacht”, link to the article: https://www.superyachttimes.com/yacht-news/dominator-ilumen-28m-taking-shape-in-italy
2. Michael Verdon, “Dominator’s Ilumen Is Now More Spacious and Preparing for Launch”, web-article, 13th April 2016, electronic magazine “Robb Report”, link to the article: http://robbreport.com/motors/marine/dominators-ilumen-now-more-spacious-and-preparing-launch-231479/
3. “Benetti NEWS from the yard November – December 2013”, web-article, 16th December 2013, electronic magazine “Sand People Communication”, link to the article: https://sandpeoplecommunication.wordpress.com/2013/12/16/benetti-news-from-the-yard-november-december-2013
4. Marco Ferrando, Lecture notes in Motor Yacht Design, Master of Science course in Yacht Design,
5. Ilumen 28M brochure from Web-site of the Derani Yachts Co. Ltd. (https://www.derani-yachts.com/yachts/dominator-ilumen-28-metre/#)
6. Giuliano Sargentini, http://www.sargentinifoto.it/
7. http://benettiyachts.it/fast-125/
8. https://www.pressreader.com/italy/superyacht/20170109/282428463876372
9. https://www.pressreader.com/italy/superyacht/20170109/282398399105300
10. “Semicustom with a Sporty Spirit”, web-article, 16th September 2013, electronic magazine “Yachting”, link to the article: https://www.yachtingmagazine.com/semicustom-sporty-spirit
11. STAR-CCM+ ver.11, User manual
12. Benetti F-125 page in brochure, http://www.navis-yachts.be/files/65381/Brochure%20Class%20Fast%20Displacement%20Web.pdf
13. “The curious incisive “nose” on new high-speed superyachts”, 9th January 2017, electronic magazine “Superyacht”
14. Joe Banks, A.B. Phillips, Stephen R. Turnock, Southampton University. Free-surface CFD Prediction of Components of Ship Resistance for KCS
15. C.A. Perez G, M. Tan, P.A. Wilson. VALIDATION AND VERIFICATION OF HULL RESISTANCE COMPONENTS USING A COMMERCIAL CFD CODE